Identifying intracellular cisplatin interaction partners and assessing their contribution to cisplatin resistance

Dissertation

zur

Erlangung des Doktorgrades (Dr. rer. nat.)

der

Mathematisch-Naturwissenschaftlichen Fakultät

der

Rheinischen Friedrich-Wilhelms-Universität Bonn

vorgelegt von

MAXIMILIAN KULLMANN

aus

Bonn

Bonn 2016

Angefertigt mit Genehmigung der Mathematisch-Naturwissenschaftlichen Fakultät

der Rheinischen Friedrich-Wilhelms-Universität Bonn

Erstgutachter: Prof. Dr. U. Jaehde

Zweitgutachter: Prof. Dr. G. Bendas

Tag der Promotion: 20. Juli 2016

Erscheinungsjahr: 2016

Diese Dissertation ist auf dem Hochschulschriftenserver der ULB Bonn

http://hss.ulb.uni-bonn.de/diss_online elektronisch publiziert.

Für meinen Vater

A wise man proportions his belief to the evidence.

David Hume

Abbreviations

A2780	Human ovarian carcinoma cell line
A2780cis	Cisplatin-resistant human ovarian carcinoma cell line
Akt	RAC-alpha serine/threonine-protein kinase
ANOVA	Analysis of variance
Ap_4A	Diadenosine tetraphosphate
ATF6	Activating transcription factor 6
Atox1	Antioxidant protein 1
ATP	Adenosine triphosphate
ATP7A	Copper-transporting P-type adenosine triphosphatase 7A
ATP7B	Copper-transporting P-type adenosine triphosphatase 7B
au	Arbitrary units
Bax	Apoptosis regulator BAX
BCA	Bicinchoninic acid
Bcl2	Apoptosis regulator Bcl-2
BCRP	Breast cancer resistance protein
Bim	Bcl-2-like protein 11
BSA	Bovine serum albumin
CFDA	Carboxyfluorescein diacetate
CFDA-NHS	Carboxyfluorescein diacetate N-hydroxysuccinimid ester
CE	Capillary electrophoresis
CE-LIF	Capillary electrophoresis – laser-induced fluorescence
CE-MS	Capillary electrophoresis – mass spectrometry
CHOP	DNA damage-inducible transcript 3 protein
CTR1	Copper transporter 1
DAPI	2-(4-Amidinophenyl)-1H-indole-6-carboxamidine-dihydrochloride

DMF	Dimethylformamide
DMSO	Dimethyl sulfoxide
DNA	Deoxyribonucleic acid
DTT	Dithiothreitol
EDTA	Ethylenediaminetetraacetic acid
EGCG	Epigallocatechin gallate
ER	Endoplasmic reticulum
ERCC1	DNA excision repair protein
ESI	Electrospray ionization
FCS	Fetal calf serum
FITC	Fluorescein isothiocyanate
γGCS	γ-Glutamylcysteine synthetase
GRP78	78-kDa glucose-regulated protein
GSH	Glutathione
GSSG	Oxidized glutathione (glutathione disulfide)
HEPES	4-(2-hydroxyethyl)-1-piperazineethanesulfonic acid
HPLC	High-performance liquid chromatography
HRP	Horseradish peroxidase
HSP	Heat shock protein
HT	5-hydroxtryptamine or serotonin
ICP-MS	Inductively coupled plasma mass spectrometry
IRE1	Inositol-requiring enzyme 1
LC	Liquid chromatography resonance
MALDI	Matrix-assisted laser desorption/ionization
MAPK	Mitogen-activated protein kinase
MMR	Mismatch repair
MRP	Multidrug resistance-associated protein

MS	Mass spectrometry
Msh2	DNA mismatch repair protein Msh2
MSKCC	Memorial Sloan Kettering Cancer Center
MT	Metallothionein
MTT	3-(4,5-Dimethylthiazol-2-yl)-2,5-diphenyltetrazolium bromide
m/z	Mass-to-charge ratio (mass spectrometry)
n	Technical replicates
N	Biological replicates
n. a.	Not active
NER	Nucleotide excision repair
NK1	Neurokinin 1
NMR	Nuclear magnetic resonance
Nrf2	Nuclear factor erythroid 2-related factor 2
n. s.	Not significant
NSCLC	Non-small cell lung cancer
OCT	Organic cation transporter
OS	Overall survival
PACMA31	Propynoic acid carbamoyl methyl amide 31
PAGE	Polyacrylamide gel electrophoresis
PBS	Phosphate buffered saline
PDI	Protein disulfide-isomerase
PDIA1	Protein disulfide-isomerase A1
PDIA3	Protein disulfide-isomerase A3
PERK	PKR-like ER kinase
Pol δ	Polymerase delta
Pol ε	Polymerase epsilon
PVDF	Polyvinylidene fluoride

QC   Quality control

RE   Relative error

RIDD   Regulated IRE1-dependent decay

RIPA   Radioimmunoprecipitation assay buffer

RNA   Ribonucleic acid

RPA   Replication protein A

RSD   Relative standard deviation

S   Standard solution

SD   Standard deviation

SDS   Sodium dodecyl sulfate

SDS-PAGE   Sodium dodecyl sulfate polyacrylamide gel electrophoresis

SEM   Standard error of the mean

siRNA   Small-interfering RNA

SCLC   Small cell lung cancer

TBS   Tris-buffered saline

TBS-T   Tris-buffered saline with Tween®-20

TEMED   Tetramethylethylenediamine

TMZ   Temozolomide

TP53   Tumor suppressor 53

TRAF2   Tumor necrosis factor receptor (TNFR)-associated factor-2

Tris   Tris(hydroxymethyl)aminomethane

UPR   Unfolded protein response

WS   Working solution

XBP-1   X-box binding protein 1

1   INTRODUCTION

1.1   Chemotherapy of solid cancers

Since the first successful application of nitrogen mustard chemotherapy to control non-Hodgkin lymphoma in the 1940s, researchers around the world are on a hunt for new, improved treatment options to cure cancer patients. In the following years several fruitful discoveries of effective treatments were made [1]. In 1951, methotrexate was introduced as the first solid cancer chemotherapy for the treatment of breast carcinoma. Seven years later the first cure of a solid tumor by drug therapy was achieved by a methotrexate treatment of choriocarcinoma. After the discovery of the antitumor effect of vinca alkaloids (1950s) such as vincristine (FDA market approval in 1963), researchers screened other natural compounds for cytotoxic potential. This resulted in the discovery of taxanes (1964) and camptothecins (1966) [2]. Another important class of chemotherapeutics was serendipitously discovered by Barnett Rosenberg in the 1970s. During experiments that involved electric field generation using platinum electrodes he discovered, that the division of bacteria cells was ceased. His investigations of the phenomenon revealed, that cis-[Pt(NH$_3$)$_2$Cl$_2$] (cisplatin, Figure 1) was the effective component inhibiting the cell division [3]. During the following clinical investigations in cancer patients it was found that cisplatin was highly effective against testicular cancer. The FDA approved cisplatin in 1978 for the treatment of patients suffering from testicular and ovarian cancer [4]. In 1989 the research on new platinum drugs with an improved side effect profile led to the approval of the second generation platinum drug carboplatin (Figure 1) for the treatment of ovarian cancer. In 2002, the third generation platinum drug oxaliplatin

(Figure 1) gained FDA approval for colorectal cancer [5]. Today, these chemotherapeutics are used as monotherapy or in combination chemotherapy regimens with various other treatment options such as surgery or radiotherapy. This way some cancer entities can be cured effectively by platinum-based chemotherapy, such as testicular cancer. Other entities, like lung cancer, can be effectively controlled.
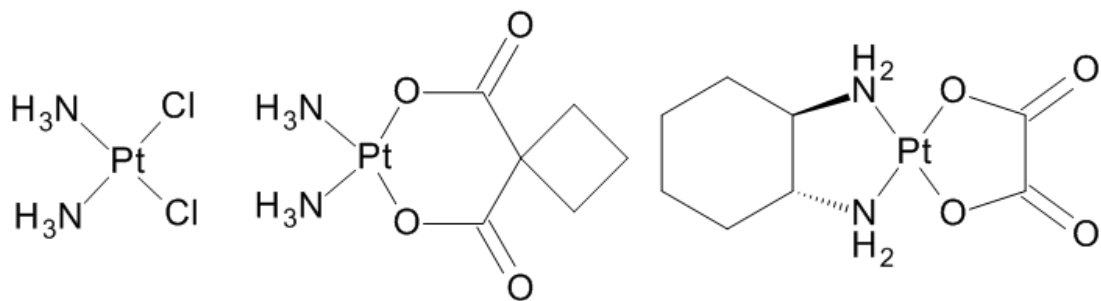
Figure 1   Platinum complexes approved for clinical use: cisplatin, carboplatin and oxaliplatin (left to right).

Over the past twenty years, the introduction of targeted therapies to the treatment arsenal led to the next developmental stage in cancer treatment [6]. The first targeted therapy that achieved FDA market authorization was imatinib in 2001 [7]. Identified drug targets include growth factors, signaling molecules and cell-cycle proteins which may be inhibited or otherwise hindered [8]. Results for the combination of targeted therapies with traditional chemotherapeutics are contradictory depending on cancer entity and therapy, showing either no benefit for the patients or promising improvements of survival [9–11]. A concept followed by some researchers involved the activation of the human immune system to treat cancer [12]. After decades of research, cancer immunotherapy proved its efficacy in the treatment of a variety of tumors and was entitled as 'Breakthrough of the year 2013' by Science [13,14]. More research is needed, as its use is currently limited by the fact that only a minority of

cancer patients benefits from immunotherapy so far [15]. Many scientists believe that the future of chemotherapy lies in personalized medicine. Treating only those patients who will benefit from a drug may stall the financially, scientifically and ethically unacceptable tradition of treating many patients although it is effective only in a few [1,16].

Overall the use of chemotherapy to treat cancer is a success story. From 1990 to 2013, a decrease by around 15% in the age-standardized death rate per 100000 persons for all cancer entities was registered [17]. However, this decline can be attributed not only to the use of improved chemotherapies but also to an increased success of prevention and early diagnosis [18]. Still, cancer is in many cases a life-threatening disease, which needs further research efforts to be better controlled and treated.

1.2   Cisplatin

1.2.1   Mechanism of action

Over the past four decades researchers elucidated the mechanism of action of cisplatin. The most widely accepted hypothesis states that the cytotoxic effect of cisplatin is due to its ability to bind nuclear DNA thus initiating the programmed cell death (apoptosis) [19]. Cisplatin enters a cell by passive diffusion, uptake through gated channels [20], or via active transporters [21]. These mechanisms most probably act simultaneously during cellular uptake [22]. The role of active transport has been elucidated in recent years and differences between the various transporters have been discovered. Evidence suggests, for example, that the active transport of cisplatin over copper transporters (CTR) contributes to the cytotoxic effect [21,23].

As a result of a significantly decreased chloride ion concentration inside the cell (3-20 mM) compared to the extracellular space (100 mM), cisplatin is activated by hydrolysis (Figure 2) [24]. The resulting mono- or diaqua species are highly reactive.
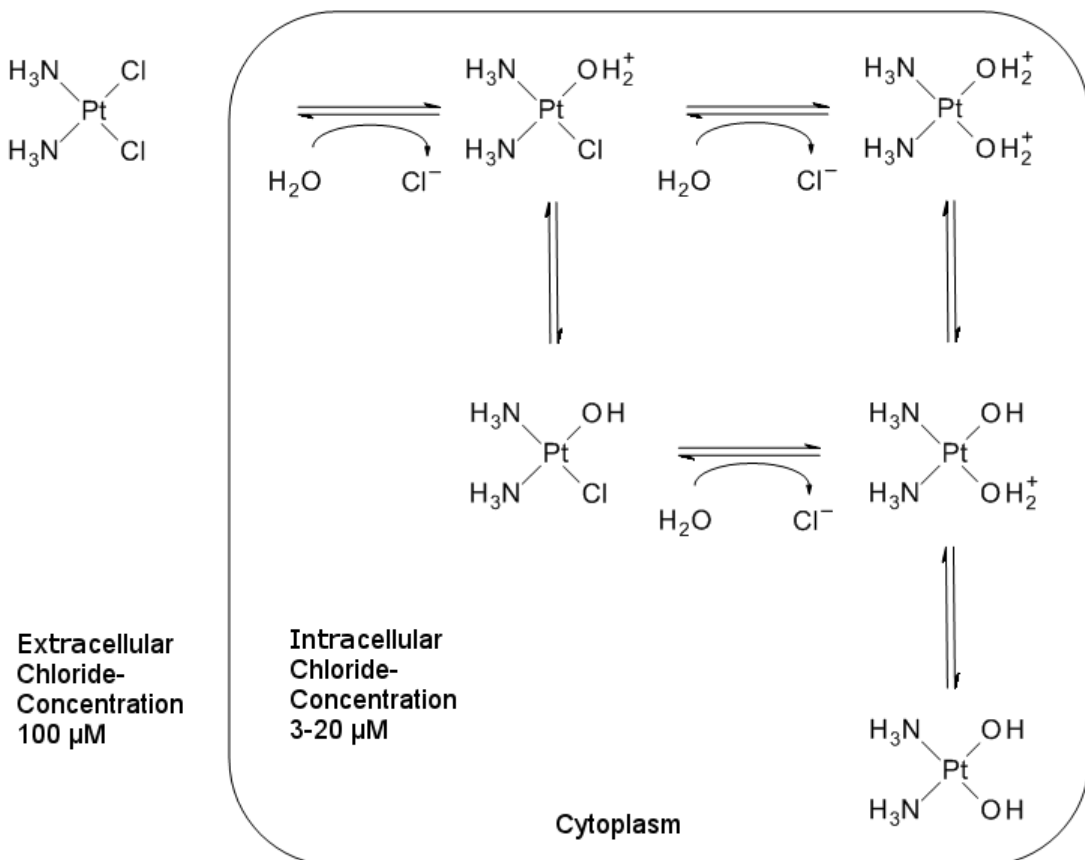
Figure 2   Schematic representation of the stepwise bioactivation of cisplatin in the cytoplasm, modified according to [25].

On its way from the cell membrane to the nucleus, several adduct formation reactions of reactive cisplatin species with small nucleophilic ligands and proteins may potentially occur. A small proportion (around 1%) of the intracellular cisplatin reaches the nucleus where the pharmacologically relevant binding to nuclear DNA takes place. This subsequently activates several cellular processes, which ultimately lead to cell death [26,27]. Early research elucidated that reactive cisplatin species form covalent bonds preferably at the N-7 position of the DNA bases adenine and guanine [28,29]. The resulting bifunctional adducts mainly lead to intrastrand

crosslinks (80 to 90% of all DNA bound platinum). Interstrand crosslinks and monofunctional adducts only account for less than 5% of all adducts (Figure 3) [5]. The cytotoxic effect of cisplatin is mainly attributed to the 1,2-intrastrand crosslinks due to the following: (a) these are the major adducts formed *in vitro* and *in vivo* and (b) the clinically inactive transplatin is unable to form such links [30].
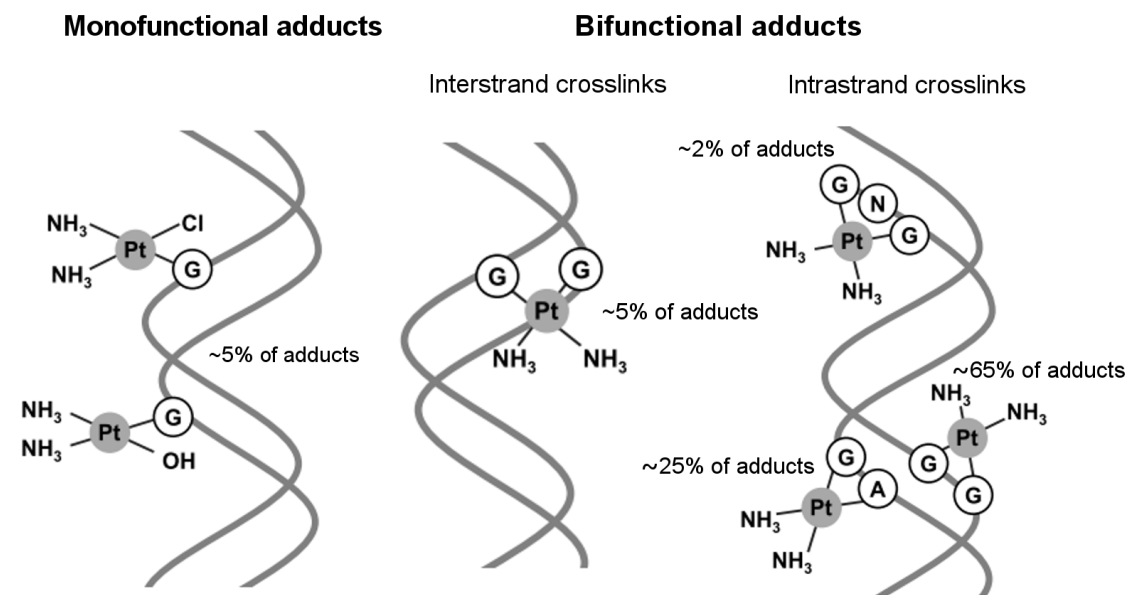
Figure 3   Cisplatin DNA adducts and their respective prevalence (modified after [31]). A = adenine, G = guanine, N = nucleoside

1.2.2 Clinical relevance

Today cisplatin is among the most widely used chemotherapeutic drugs for various cancer entities [24]. It plays a central role in the treatment of testicular cancer and germ cell tumors [32]. More than 90% of testicular cancer patients with 'good risk' disease according to the MSKCC criteria can be cured using chemotherapy regimens, which often include cisplatin [33]. Most patients are treated with the BEP regimen, which consists of a combination of bleomycin, etoposide and cisplatin.

Furthermore, cisplatin is used in the treatment of gastric and esophageal cancer in combination with surgery and radiotherapy [34,35]. For these cancer entities, the

outcome is not as encouraging as for testicular cancer. Single agent chemotherapy with cisplatin showed a response rate of only 10% to 20% for esophageal cancer patients. By addition of fluorouracil and paclitaxel to cisplatin therapy the response rates are improved to around 50% [36].

Small cell lung cancer (SCLC) and non-small cell lung cancer (NSCLC) are the most frequent cause of cancer death worldwide. Besides tumor resection, cisplatin remains a cornerstone of therapy for these tumor entities [37,38]. Treatment guidelines for SCLC recommend a platinum-based chemotherapy in combination with etoposide for patients with extensive disease, reaching response rates ranging from 50 to 90% [39]. In a recent review no benefit of newer cytotoxic agents compared to standard platinum-based therapy for SCLC was reported, emphasizing the importance of the platinum drug in the management of SCLC [40]. In advanced NSCLC, platinum-based therapies were more effective than third-generation regimens including gemcitabine or paclitaxel [41]. Adjuvant chemotherapy with a two-drug, cisplatin-based regimen has been shown to increase the 5-year survival only by 4 to 5% in resected NSCLC patients [42].

Only 20% of all ovarian cancer patients are diagnosed early at stage 1 where the disease is limited to the ovaries. In most cases the disease has metastasized to the pelvic organs (stage 2), the abdomen (stage 3) or beyond the peritoneal cavity (stage 4) [43]. In ovarian cancer patients bearing stage 2-4 tumors, cisplatin is mostly used in therapy regimens in combination with paclitaxel, whereas stage 1 tumors are treated with a combination of carboplatin and paclitaxel [44]. First-line therapy is successful in a majority of patients, but clinical studies showed that more than 70% of patients develop a recurrent disease after a period of time. These patients often obtain some degree of acquired cisplatin resistance [45]. The median survival of

patients with recurrent disease depends on the tumor's platinum sensitivity. Patients with platinum-sensitive disease have a median overall survival of 2 years, whereas patients with platinum-resistant disease have a median overall survival of below one year (9 to 12 months) [46]. In a recent phase I clinical trial, an alternative to the standard intravenous therapy to treat patients with platinum-sensitive, recurrent epithelial ovarian cancer has been evaluated. Cisplatin was administered intraperitoneally after a cytoreductive surgery in an attempt to kill residual cancer cells by an elevated local cisplatin exposition [47]. The procedure is currently under investigation in further clinical trials, hopefully adding another option to the treatment arsenal for ovarian cancer [48,49]. Clinical studies revealed that carboplatin shows an improved side effect profile while exhibiting equal efficacy in some stages of ovarian cancer [50]. Therefore, cisplatin is sometimes replaced by carboplatin in therapy regimens for ovarian cancer [4].

1.2.3 Toxicity

The toxic side effects of cisplatin treatment include but are not limited to emesis and oto-, neuro- and nephrotoxicity. Emesis is probably the most disturbing side effect for patients undergoing cisplatin treatment. More than 90% of patients without an effective antiemetic therapy will suffer from nausea and vomiting, which classifies cisplatin as a highly emetogenic drug [51]. Today anti-emetic therapies including 5-HT_3 antagonists (e.g. ondansetron) in combination with glucocorticoids (dexamethasone) and/or NK_1 receptor antagonists (aprepitant) are available limiting this side effect effectively [52].

Pediatric patients are at high risk for cisplatin-associated ototoxicity, which affects at least 60% of them [53]. Ototoxicity appears to be mainly caused by damage of the

cochlear hair cells by cisplatin in a dose-dependent manner [54]. Options to prevent the ototoxic effect of cisplatin are currently investigated in preclinical and clinical studies. However, a recently published Cochrane review found no evidence for any effective otoprotective treatment [55]. Therefore, new approaches to manage ototoxicity are evaluated. For example, in an animal model in guinea pigs ototoxicity was reduced by intracochlear administration of caspase inhibitors during cisplatin therapy in an attempt to limit the apoptosis-inducing effect of cisplatin [56].

If cisplatin is combined with other potentially neurotoxic agents, such as paclitaxel, development of sensory peripheral neuropathy is a major toxicity [57,58]. As previously described, cisplatin unfolds its activity through DNA platination. This seems to be the cause for the neurotoxic effect as well, as it harms peripheral nerves and dorsal root ganglia neurons, leading to acute and chronic platinum-induced neurotoxicity [59]. Despite the evaluation of many promising approaches, no effective treatment to control the therapy-induced neuropathy has been found yet [60].

For the management of the similarly severe nephrotoxicity some therapeutic approaches are available, such as volume expansion with sodium chloride or the prolongation of infusion time [51]. Importantly, chemotherapeutic efficacy of cisplatin must not be undermined by the measures taken [61]. Involved in the nephrotoxicity of cisplatin are organic cation transporters (OCT), facilitating the uptake of cisplatin into renal tubular cells [62,63]. A high OCT2 expression has been shown at the basolateral side of all three segments of the proximal tubule, giving a possible explanation for this phenomenon [64]. Recently, Sprowl et al. reported that the OCT2 inhibitor cimetidine limits cisplatin-induced nephrotoxicity in an animal model without altering the antitumor efficacy [65].

1.2.4 Mechanisms of acquired resistance

Acquired drug resistance is a major setback to successful therapy especially of ovarian cancer and compromises the effective outcome of chemotherapy. Several mechanisms underlying chemoresistance have been postulated and experimental evidence points to a multifactorial nature (Figure 4). Many of the mechanisms prevent cisplatin from reaching its therapeutic target, the nuclear DNA, in adequate levels to trigger cellular mechanisms leading to cell death (reviewed in [67]). These 'pre-target effects' include but are not limited to a reduced cellular uptake and an increased efflux of cisplatin. Furthermore, an increased inactivation of cisplatin by nucleophilic scavengers prior to DNA binding has been postulated as a mechanism of resistance, which is portrayed in more detail in chapter 1.2.5.

Pre-target resistance	On-target resistance
• Increased efflux • Reduced uptake • Increased inactivation	• Increased NER proficiency • Increased replicative bypass • MMR deficiency
Post-target resistance	Off-target resistance
• Inactivation of TP53 • Inactivation of MAPK • Overexpression of BCL-2	• Autophagy • Heat shock proteins

Figure 4   Proposed mechanisms of acquired cisplatin resistance (modified after [66]).

Intracellular accumulation of cisplatin ultimately results from the interplay between drug influx and drug efflux [24]. As already mentioned the uptake/influx of cisplatin is mediated simultaneously by passive diffusion, gated channels, and active transport. The important contribution of the copper transporter 1 (CTR1) to the regulation of

cisplatin uptake in cancer cells sensitive and, even more crucially, resistant to cisplatin has been shown by several lines of evidence [68]. Cells resistant to cisplatin exhibited cross-resistance to copper, and influx rates for both cisplatin and copper were simultaneously reduced [69]. CTR1-deficient fibroblasts showed a significantly decreased cisplatin uptake compared to wild-type fibroblasts [70]. Cellular accumulation is furthermore influenced by an increased cisplatin efflux, associated with an upregulation of the copper-transporting ATPase 1 and 2 (ATP7A and ATP7B) in resistant cancer cells [69,71]. Other efflux transporters likely to be involved in cisplatin resistance are multidrug resistance-associated proteins (MRP) [72]. MRP2 appears to play a dominant role in cisplatin resistance compared to other members of the family [73]. This manifests for example in the potential of a MRP2 knockdown to increase sensitivity to cisplatin in human ovarian cancer cells [74]. Moreover, in the clinical setting an increased MRP2 expression conferred cisplatin resistance in ovarian cancer [75].

As mentioned, nuclear DNA appears to be the main target for cisplatin's cytotoxic action. On-target mechanisms such as the nucleotide excision repair (NER) and the replicative bypass also contribute to the multifactorial resistance. The NER system enables a cell to remove a majority of platinum adducts from DNA [76]. After the recognition of DNA lesions, they are excised by e.g. DNA excision repair protein (ERCC1). To maintain the genetic integrity, the DNA synthesis is accomplished by the same proteins involved in DNA replication such as replication protein A (RPA), polymerase delta and epsilon (*Pol δ* and *Pol ε*), and others [77]. The replicative bypass, also known as translesion synthesis, enables the cell to synthesize DNA past the site of DNA damage [78]. This function is mediated by different DNA polymerases such as *POLH, POLI* or *POLK* [79]. The mismatch repair system (MMR)

is a further cellular mechanism to detect erroneous insertions or deletions of bases during DNA replication [80]. This system is also able to recognize DNA lesions induced by cisplatin. Mainly the DNA mismatch repair proteins Msh2 (MSH2) and Mlh1 (MLH1) are attributed to the transmission of proapoptotic signals after the detection of cisplatin-DNA adducts [81] and mutation or loss of expression of MSH2 and MLH1 protein in acquired cisplatin resistance has been reported [82–84].

The DNA damage induced by cisplatin leads to activation of proapoptotic cellular signaling. Several genetic and epigenetic alterations of the cell death machinery, which contribute to cellular survival can be classified as 'post-target resistance' (reviewed in [66]). Loss of proapoptotic signaling by inactivation of tumor suppressor 53 (TP53) confers cisplatin resistance to cancer cells [85,86]. This alteration can be found in almost 50% of all human carcinomas that have been investigated [87]. Other genetic alterations, e.g. in proapoptotic mitogen-activated protein kinases (MAPK), are discussed for their possible contribution to acquired cisplatin resistance [88].

Mechanisms of resistance that are independent of DNA platination are termed 'off-target'. This description includes, for example, autophagy as a response to chemotherapy-induced stress. By lysosomal sequestration and degradation of organelles cellular survival is promoted [89]. Other off-target mechanisms contributing to cisplatin resistance need to be further investigated. The discussed mechanisms include induced expression of heat shock proteins (HSP) and induction of other intracellular signaling pathways [66].

In order to identify cellular adaptations on the protein level in resistant cell lines, researchers evaluated the differences in protein expression in sensitive and resistant cancer cells by 2D gel electrophoresis [90–93]. This proteomic approach revealed several differentially expressed proteins, among others stress response proteins,

such as 78 kDa glucose-regulated protein (GRP78) and cell cycle proteins (Annexin, 14-3-3 epsilon). The identified proteins do not necessarily bind cisplatin, but may be involved in cellular mechanisms promoting resistance.

At the moment, the evidence for a multifactorial nature of cisplatin resistance is solidified. Most recent hypotheses proposed, that several of the above described non-overlapping mechanisms occur simultaneously limiting the cytotoxic effect of cisplatin (Figure 4). This partly explains why, despite intensive research, there is still a lack of efficient strategies to overcome or at least manage acquired cisplatin resistance [94].

1.2.5 Intracellular binding as a mechanism of resistance

Inside a tumor cell a plethora of potential binding partners for cisplatin exist. Among the early discovered low molecular weight binding partners of cisplatin was glutathione (GSH) and small, cytoplasmic proteins of the metallothionein family (MT) [95–98]. GSH consists of the three amino acids glutamic acid, cysteine and glycine. MT proteins are rich in the sulfur-containing amino acids cysteine and methionine [99]. Cysteine and methionine are known to avidly bind cisplatin [100]. In 1995 Goto et al. showed that an acquired resistance phenotype of cancer cells may be attributed to increased detoxification of cisplatin by GSH [101]. However, in 2009 Kasherman et al. found that two-thirds of platinum-adducts in whole cell extracts of ovarian cancer cells treated with cisplatin had a molecular mass greater than 3 kDa. This result suggested that GSH plays only a minor role in cisplatin detoxification, whereas other binding partners are of greater importance [102]. More recently, proteins were moved into the focus of research on intracellular binding of cisplatin [103]. The interaction of cisplatin with proteins appears to be an important factor

altering its intracellular distribution, elimination, and ultimately cytotoxicity. Various proteomic approaches identified intracellular cisplatin-interaction partners. Using an agarose pull-down assay several proteins binding to two different platinum-agarose conjugates, among them GRP78 and others were found [104]. The authors suggested that these proteins may play a role in platinum-associated nephro- and ototoxicity. Interesting results were obtained by in-cell NMR spectroscopy, where an intracellular interaction of cisplatin with antioxidant protein 1 (Atox1) was investigated. It was shown, that cisplatin forms an adduct with Atox1, and that the overexpression of Atox1 reduced DNA platination in *E. Coli* [105]. Taken together the knowledge on the contribution of the identified proteins to acquired cisplatin resistance remains limited. Most studies present only a snapshot view of the complex cellular interplay of mechanisms [106].

It has to be noted that all cisplatin interactions with non-DNA targets may contribute to the acquired cisplatin resistance but at the same time may serve as a drug reservoir for cisplatin as postulated by Reedijk. Platinum could be released from its interaction partners after some time and subsequently react with DNA [107]. This would lead to an increase in cytotoxicity of cisplatin and may explain a delayed effect of cisplatin.

1.3   CFDA-cisplatin as model complex for intracellular cisplatin analysis

Due to the currently limited analytical procedures regarding the non-invasive speciation of platinum complexes inside a cell, researchers need to employ model complexes in order to study the intracellular interactions of cisplatin [108]. In 2000 Molenaar et al. introduced a fluorescent cisplatin analogue (CFDA-cisplatin or CFDA-

Pt) by covalently linking a carboxyfluorescein diacetate moiety to cisplatin (Figure 5) as a model substance for research [109]. After cellular uptake, the two acetate groups of the non-fluorescent CFDA moiety are hydrolyzed by cellular esterases, resulting in a fluorescent molecule.
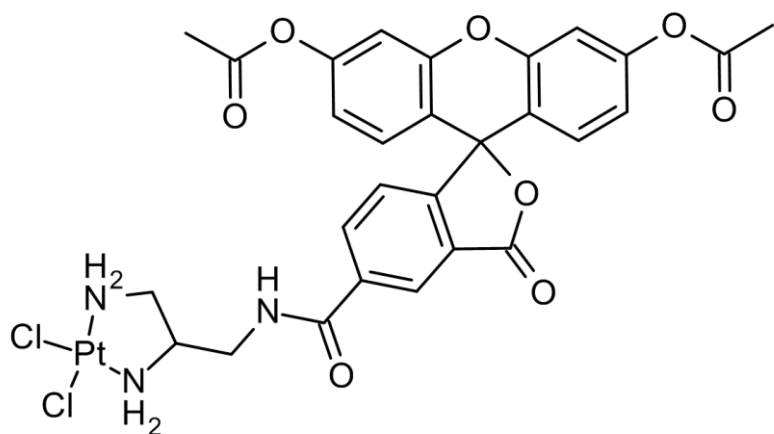
Figure 5   Chemical structure of CFDA-cisplatin.

With the aid of this model complex, the cellular distribution of cisplatin in cancer cells was investigated [109]. Furthermore, it has been shown, that CFDA-cisplatin possesses cytotoxic activity in ovarian cancer cells. Interestingly, the same authors observed that cisplatin-resistant A2780cis cells were cross-resistant to CFDA-cisplatin [110]. Further experiments using CFDA-cisplatin revealed that alterations in the sub-cellular localization of the transporters ATP7A and ATP7B may contribute to the resistant phenotype of A2780cis cells [110]. Intracellular interaction partners of CFDA-cisplatin in A2780 and A2780cis cells have recently been identified after 2D gel electrophoresis and ESI-MS analysis, among them GRP78 and two protein disulfide isomerases (PDIA1, PDIA3) [111].

It has to be noted, that the addition of a large fluorophore to the small molecule cisplatin changes its molecular properties considerably. This limitation needs to be recognized and results have to be interpreted accordingly [108].

1.4   Intracellular interaction partners of cisplatin

1.4.1 78 kDa glucose-regulated protein (GRP78)

GRP78 belongs to the heat shock proteins (HSP70 family) and acts as a chaperone mainly located at the endoplasmic reticulum (ER) [112]. Additionally, expression of GRP78 on the cell surface was described in several malignant cell lines [113].

After ribosomal protein biosynthesis the nascent polypeptides are folded into their native state mostly in the ER [114]. If a cell undergoes stress, such as glucose deprivation or contact with toxic agents, proteins are potentially folded improperly. These 'misfolded' proteins aggregate in the cytoplasm and need to be refolded by chaperones for correct function [115]. Prolonged ER stress, possibly triggered by cisplatin, activates proapoptotic signaling pathways and ultimately leads the cell into apoptotic cell death [116].

GRP78 acts as a master regulator of the unfolded protein response (UPR) either promoting cell survival or cell death depending on the level of ER stress (Figure 6). Under normal conditions, GRP78 is bound by three trans-membrane proteins (PKR-like ER Kinase (PERK), inositol-requiring enzyme 1 (IRE1) and activating transcription factor 6 (ATF6)) [117]. If misfolded proteins cumulate in the cytoplasm, PERK, IRE1 and ATF6 are released from GRP78 and can exert their functions.
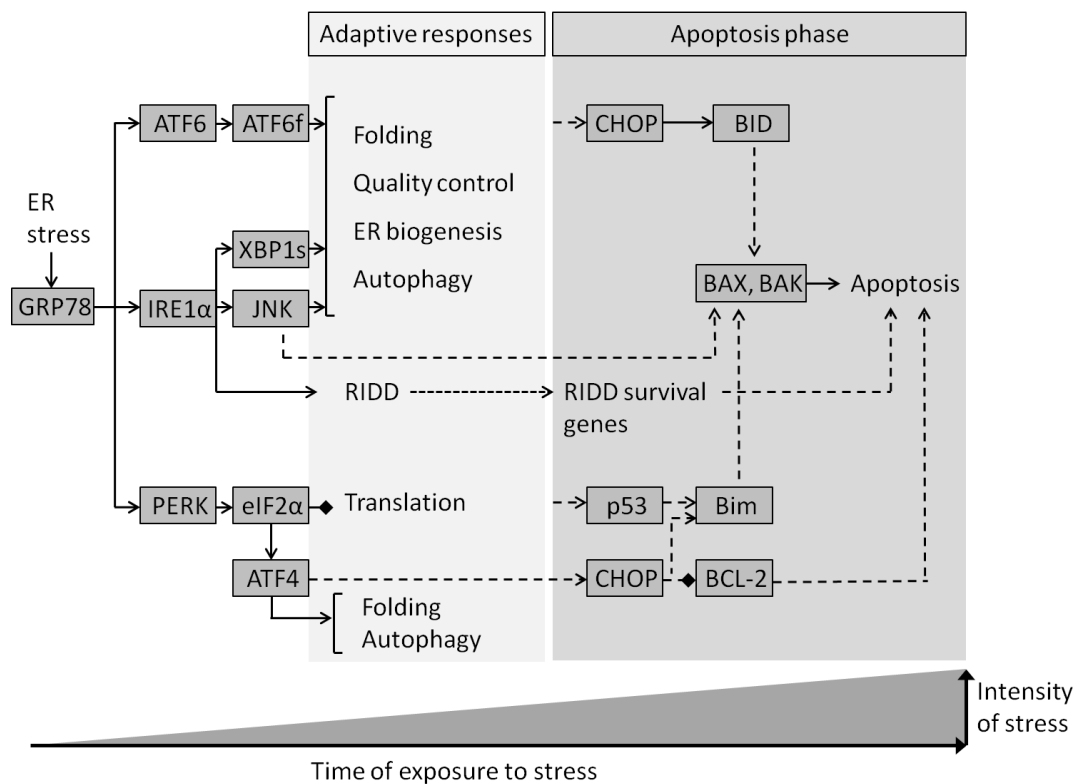
Figure 6   Potential signaling pathways after GRP78-mediated activation of ATF6, IRE1
              and PERK depending on time of exposure and intensity of stress (modified after
              [121]).

The function of PERK is well documented [118]. After release from GRP78, activated

PERK triggers a signal cascade over 'E74-like factor 2' (eIF2) and activating

transcription factor 4 (ATF4), which leads to a decrease of protein influx into the ER

promoting cell survival [119]. If the ER stress intensity further increases PERK leads

to 'DNA damage-inducible transcript 3 protein' (CHOP)-mediated activation of the

proapoptotic proteins 'Bcl-2-like protein 11' (Bim), 'apoptosis regulator BAX' (Bax),

and to suppression of the pro-survival protein 'apoptosis regulator Bcl-2' (Bcl-2)

[116,120]. This shifts the balance towards the proapoptotic way, leading the cell into

apoptosis.

IRE1 can either activate apoptosis or promote survival and again this depends on the

extent of ER stress. Following severe, prolonged ER stress IRE1 activates tumor

necrosis factor receptor (TNFR)-associated factor-2 (TRAF2), which leads to JNK phosphorylation and induction of apoptosis. Another mechanism of IRE1 relies on the activation of regulated IRE1-dependent decay (RIDD) protein, which on the one hand blocks pro-survival protein X-box binding protein 1 (XBP1), and on the other degrades ER-associated mRNA, limiting new protein translation [116]. The inhibition of apoptosis by IRE1, on the other hand, is mediated by splicing of XBP1 to XBP1s, which leads to an induction of chaperone expression. This increase promotes protein folding in the ER, leading to cellular survival [118]. The protease-mediated activation of ATF6 in the Golgi apparatus leads to an induction of the expression of chaperones, which facilitate the refolding of proteins [122]. There is also evidence, that ATF6 is capable of activating CHOP, presenting a possible link between PERK and ATF6 in the induction of apoptosis [116].

GRP78 localized at the cell surface seems to promote cellular survival. In lung carcinoma cells, GRP78 acts as a receptor for the phosphorylation of RAC-alpha serine/threonine-protein kinase (Akt) [123]. Induction of Akt/PI3K (phosphoinositide 3-kinase)-signaling promotes cell proliferation and inhibits apoptosis [124,125].

1.4.2 Protein disulfide isomerases

Protein disulfide isomerases (PDI) are compartmentalized mainly at the endoplasmic reticulum (ER) where they exert an oxidoreductase activity catalyzing the formation, isomerization and reduction of disulfides [126]. Most PDI isoforms contain an amino acid sequence for ER retention, but are also localized in other cellular compartments, e.g. the cytosol [127]. PDIA1 (or PDI, P4HB, p55) and PDIA3 (or GRP58, ERp57, ERp60) are highly homologous sharing similar amino acid sequences (CGHC:

cysteine, glycine, histidine, cysteine) at their active sites [128,129]. Both proteins

consist of four domains (a, a', b and b') (Figure 7).

PDIA1
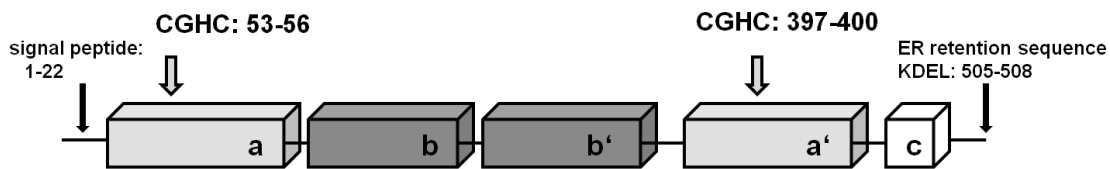
PDIA3
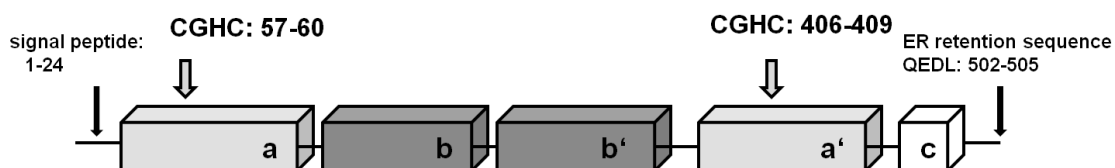
Figure 7   Domain organization of PDIA1 and PDIA3. Active sites are located in the a and
             a' domain (modified after [127]).

The active sites are located in the a and a' domains, whereas the b and b' domains

show some variability between PDIA1 and PDIA3 [127]. The KDEL (lysine, aspartic

acid, glutamic acid, leucine) ER retention sequence can be found in PDIA1. In PDIA3

the ER retention is achieved by a QEDL (glutamine, glutamic acid, aspartic acid,

leucine) sequence [130]. Both PDIA1 and PDIA3 carry seven cysteines, thus

presenting a possible target for irreversible coordination of platinum complexes, as

cisplatin binds preferably to cysteine residues [131].

PDIA1 exerts its chaperone activity mainly depending on its redox status. In order to

oxidize a substrate dithiol to a disulfide, oxidized PDIA1 is reduced [132].

Subsequently, the native state of PDIA1 is reestablished by oxidation of PDIA1 by an

intracellular oxidant such as glutathione disulfide (GSSG) (Figure 8) [129]. In

contrast, to perform a reduction reaction PDIA1 is oxidized. The catalytic cycle is

finished by reduction of PDIA1 by reductants, such as glutathione (GSH), to the native state [133].
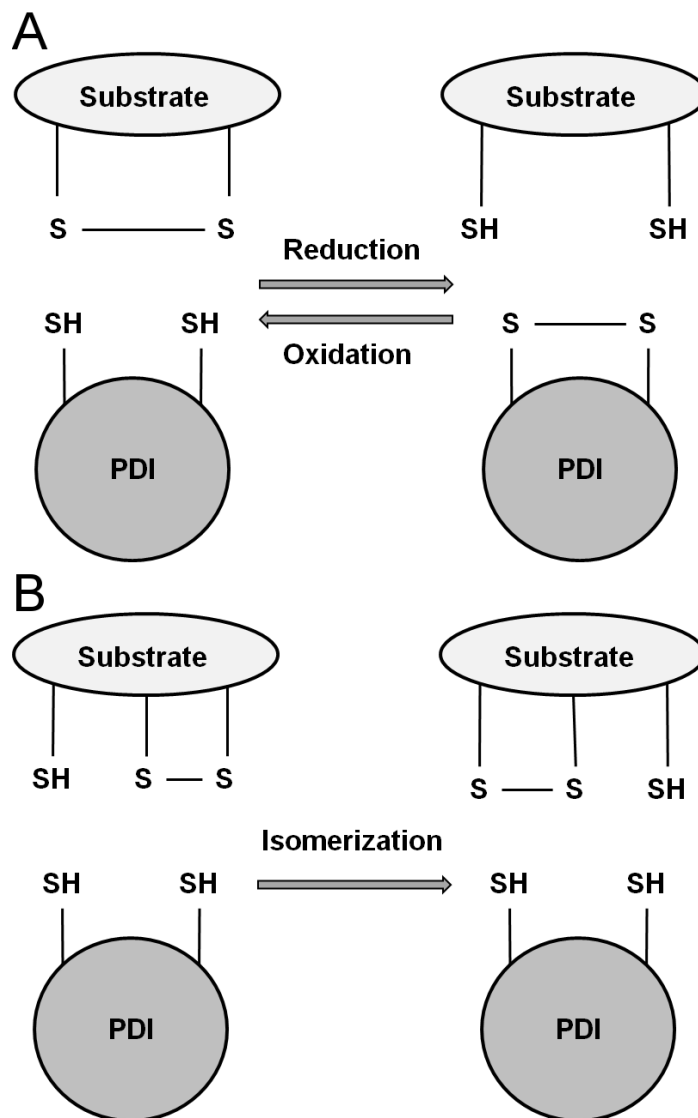
Figure 8   Redox reactions of PDI. (A) Oxidation and reduction. (B) Isomerization [132].

PDIA1 appears to be a promising target for cancer treatment. Diverse tumor entities, such as brain, prostate and ovarian cancer, show a significant upregulation of PDIA1 [134–137]. Also, in female and male breast cancer cells PDIA1 is overexpressed compared to normal tissue [138,139]. Based on these findings the irreversible and selective PDIA1 inhibitor PACMA31 was developed and introduced in 2012 by

Xu et al. (Figure 9). It has been shown to effectively inhibit the growth of ovarian cancer cell lines [140].
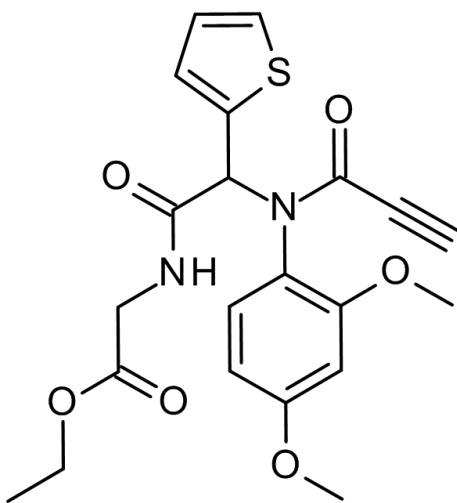
Figure 9   Chemical structure of the irreversible PDIA1 inhibitor PACMA31.

As PDIA1 and PDIA3 are the most homologous of all known protein disulfide isomerases, PDIA3 exerts comparable functions to PDIA1 such as oxidation, reduction and isomerization of disulfide bonds [141]. It also mainly localizes at the ER [130]. The main difference between PDIA3 and PDIA1 lies in PDIA3's ability to bind calnexin or calreticulin with high affinity, which is needed for the folding of glycoproteins [142]. The binding of calnexin and calreticulin occurs at the b and b' domain, which have been shown to be structurally different in PDIA3 compared to PDIA1 [143]. Interestingly, PDIA3 has been postulated to contribute to paclitaxel resistance in ovarian cancer cell lines, as a differential expression of PDIA3 in A2780 and paclitaxel-resistant A2780TC1 cells has been found [144]. Furthermore, PDIA3 is highly expressed in the serous ovarian cancer cell line YDOV-139 and may function as a potential biomarker for this cancer entity [145]. PDIA3 overexpression was associated with low overall survival and recurrence-free survival in cervical cancer patients [146].

As described above, PDIA1 and PDIA3 carry a CGHC-amino acid motif at their active site. Interestingly, it has been shown that cisplatin often binds to a CXXC-motif, for example in the Atox1 protein [147]. Furthermore, the CXXC-motif in the metal-binding domain of ATP7B was necessary for cisplatin binding [148]. By genetic modification of this binding site, resistance against cisplatin in ovarian 2008 cells was reversed [148]. CFDA-cisplatin interacts with PDIA1 and PDIA3 implying the possibility that cisplatin also interacts with the active sites of PDIA1 and PDIA3, abolishing their respective intracellular function and justifying the investigation of these proteins in the context of cisplatin resistance [111]. Furthermore, an interference with PDIA1 or PDIA3, either genetically or pharmacologically, may mitigate the cellular response to ER stress, increasing cisplatin-induced cell death.

2   AIM AND OBJECTIVES

Acquired cisplatin resistance is a major drawback of successful chemotherapy in ovarian cancer. Results of recent research proposed intracellular proteins interacting with cisplatin as mechanism of resistance. One aim of this project was the identification of cytosolic proteins interacting with CFDA-cisplatin, a fluorescent cisplatin analogon, in cisplatin-sensitive A2780 and cisplatin-resistant A2780cis ovarian cancer cells by 2D gel electrophoresis and subsequent mass spectrometric analysis. The following experiments were conducted:

- Purification of CFDA-cisplatin after synthesis using a semi-preparative HPLC for the subsequent determination of proteins interacting with CFDA-cisplatin with a high confidence.

- Sample preparation of A2780 and A2780cis cells treated with CFDA-cisplatin for 2D gel electrophoresis.

- Identification of cytosolic proteins interacting with CFDA-cisplatin by 2D gel electrophoresis and ESI-MS (This task was performed by Sandra Kotz at the University of Cologne).

Among the identified proteins were GRP78, PDIA1 and PDIA3 which may be involved in cisplatin resistance by acting as a molecular sink for cisplatin or by their role in cellular signaling of ER stress response. Another aim of this study was therefore the evaluation of these proteins regarding their contribution to cisplatin resistance by siRNA-mediated knockdown. Several consecutive experiments after knockdown of the mentioned proteins were conducted, such as the MTT assay, an apoptosis assay and measurement of DNA platination. Based on these experimetns the contribution of the proteins to acquired cisplatin resistance was evaluated.

Furthermore, the potential to control cisplatin resistance by a pharmacological inhibition was investigated.

The following objectives were defined:

- Generation of a transient siRNA-mediated knockdown of GRP78, PDIA1 and PDIA3 in A2780 and A2780cis cells.

- Effect of the respective knockdown on cisplatin cytotoxicity, apoptosis induction and DNA platination.

- Effect of pharmacological inhibition of PDIA1 on cisplatin cytotoxicity, apoptosis induction and DNA platination.

3   MATERIAL AND METHODS

3.1   Materials

3.1.1   Chemicals and reagents

Acrylamide (30%)	Roth GmbH & Co., Karlsruhe
Actinomycin	Sigma-Aldrich GmbH, Steinheim
AllStars Negative Control siRNA	Qiagen, Hilden
Annexin V Binding Buffer	BD Bioscience, Franklin Lakes, USA
Ammonium persulfate (APS)	Roth GmbH & Co., Karlsruhe
BCA Protein Assay Kit (Novagen)	Merck KGaA, Darmstadt
Bromophenol blue	AppliChem GmbH, Darmstadt
CASY®-Ton, isotonic diluting solution	Schärfe System, Reutlingen
Cisplatin	Sigma-Aldrich GmbH, Steinheim
2-(4-Amidinophenyl)-1H-indole-6-carboxamidine-dihydrochloride (DAPI)	Sigma-Aldrich GmbH, Steinheim
Dimethylformamide (DMF)	Sigma-Aldrich GmbH, Steinheim
Dimethylsulfoxide (DMSO)	Sigma-Aldrich GmbH, Steinheim
Disodium hydrogenphosphate	Honeywell GmbH, Seelze
Dithiothreitol (DTT)	ThermoFisher Scientific, Rockford, USA
Ethanol 96 – 100 % (V/V)	VWR International, Radnor, USA
FACS Flow	BD Bioscience, Franklin Lakes, USA
Fetal calf serum (FCS)	PAN-Biotech GmbH, Aidenbach
FITC Annexin V Apoptosis Detection Kit with PI	BioLegend, San Diego, USA

FlexiTube siRNA	Qiagen, Hilden
Glycerol	AppliChem GmbH, Darmstadt
Glycerolphosphat	AppliChem GmbH, Darmstadt
Glycine	AppliChem GmbH, Darmstadt
Isopropanol 100 % (V/V)	Merck KGaA, Darmstadt
K2$^{®}$ Transfectionsystem	Biontex Laboratories GmbH, Munich
Leupeptin hemisulfate	Sigma-Aldrich GmbH, Steinheim
Milk powder	Roth GmbH & Co., Karlsruhe
Methanol	Avantor, Deventer, The Netherlands
MTT	AppliChem GmbH, Darmstadt
Nitric acid 65% (V/V). suprapur	Merck KGaA, Darmstadt
Nuclease	ThermoFisher Scientific, Rockford, USA
Penicillin streptomycin solution	PAN-Biotech GmbH, Aidenbach
Pepstatin A	Sigma-Aldrich GmbH, Steinheim
PeqGOLD Protein Marker V	PEQLAB GmbH, Erlangen
Pierce™ ECL Substrate	ThermoFisher Scientific, Rockford, USA
Potassium chloride	Sigma-Aldrich GmbH, Steinheim
Potassium dihydrogen phosphate	AppliChem GmbH, Darmstadt
Propynoic acid carbamoyl methyl amide 31 (PACMA31)	Merck Millipore, Darmstadt
RNAse-free water	Qiagen, Hilden
RPMI 1640 medium	PAN-Biotech GmbH, Aidenbach
Sodium azide	Merck KGaA, Darmstadt
Sodium chloride	Th. Geyer GmbH, Renningen

Sodium dodecyl phsphate (SDS)	Roth GmbH & Co., Karlsruhe
Sodium deoxycholate	AppliChem GmbH, Darmstadt
Sodium hydroxide (NaOH)	Sigma-Aldrich GmbH, Steinheim
Tetramethylethylendiamine (TEMED)	AppliChem GmbH, Darmstadt
Tergitol solution	Sigma-Aldrich GmbH, Steinheim
Tris(hydroxymethyl)aminomethane	AppliChem GmbH, Darmstadt
Triton®X-100	AppliChem GmbH, Darmstadt
Trypsin-EDTA solution	Sigma-Aldrich GmbH, Steinheim
Tween®-20	AppliChem GmbH, Darmstadt
Ultrapure water	Obtained by Purelab Plus™ system, Elga Labwater, Celle

3.1.2 Buffers and solutions

Phosphate buffered saline (PBS)

NaCl	8.0 g
KCl	0.2 g
Na_2HPO_4 x 2 H_2O	1.4 g
Potassium dihydrogen phosphate	0.2 g
Ultrapure water	ad 1000.0 mL
pH adjusted to 7.4 using sodium hydroxide or hydrochloric acid	

Cisplatin stock solution [5 mM]

Cisplatin	1.5 mg
Sodium chloride solution 0.9%	1.0 mL

CFDA-cisplatin stock solution [50 mM]

CFDA-cisplatin	39.88 mg
DMF	1.0 mL

PACMA31 stock solution [58 mM]

PACMA31	25 mg
DMSO	1.0 mL

3-(4,5-Dimethylthiazol-2-yl)-2,5-diphenyltetrazolium bromide (MTT) solution
[5 mg/mL]

MTT	10 mg
PBS	2.0 mL

Radioimmunoprecipitation assay buffer (RIPA)

Tris-HCl	394 mg
NaCl	880 mg
Triton X100	1 mL
Sodium deoxycholate	1 g
EDTA	29.2 mg
Ultrapure water	ad 100 mL
pH adjusted to 7.4 using sodium hydroxide	

Cell lysis buffer (CLB IV)

HEPES	0.238 g
KCl	0.298 g
MgCl$_2$	0.029 g
Glycerine	5 mL
NP-40	0.5 mL
Ultrapure water	ad 100 mL
pH adjusted to 7.4 using sodium hydroxide	

DAPI stock solution [1 mg/mL]

DAPI	1 mg
Methanol	1000 µL

DAPI working solution [5 µg/mL]

DAPI stock solution	5 µL
Ultrapure water	ad 1000 µL

siRNA solution [10 µM]

siRNA (against GRP78, PDIA1, PDIA3 or negative control)	5 nmol
RNAse free water	500 µL

Transfection solution for 2 wells of a 6 well plate

RPMI 1640 medium	125 µL
K2$^®$ reagent	13.5 µL
RPMI 1640 medium	125 µL
siRNA [10 µM]	10 µL
Mix both solutions	

SDS page and protein immunoblotting

Ammonium persulfate (APS) solution [10%]

APS	100 mg
Ultrapure water	ad 1000.0 µL

Dithiothreitol (DTT) solution [3.2 M]

DTT	49.4 mg
Ultrapure water	ad 1000.0 µL

Loading buffer

Stacking gel buffer	1.75 mL
Glycerol	1.5 mL
Sodium dodecyl sulfate solution (see below)	5 mL
Bromophenol blue solution*	1.25 mL

* Saturated bromophenol blue solution in ultrapure water containing 0.1% ethanol.

Sodium dodecyl sulfate (SDS) solution [10%]

SDS	1.0 g
Ultrapure water	ad 10.0 mL

Stacking gel buffer (pH 6.8)

Tris base	12.11 g
Ultrapure water	ad 100.0 mL
pH adjusted to 6.8	

Separating gel buffer (pH 8.8)

Tris base	12.11 g
Ultrapure water	ad 100.0 mL
pH adjusted to 8.8 using hydrochloric acid	

Western Blot

Tris-buffered saline (TBS)

Sodium chloride	4 g
Tris base	0.6 g
Ultrapure water	ad 500.0 mL
pH adjusted to 7.3 using hydrochloric acid	

Tris-buffered saline with Tween®-20 (TBS-T) solution

Tween®-20	1.6 mL
TBS	ad 800.0 mL

Blocking solution

Milk powder	5 g
TBS-T solution	ad 100.0 mL

Transfer buffer

Glycine	14.4 g
Tris base	3 g
Ultrapure water	ad 800.0 mL
pH adjusted to 8.2 to 8.4	

Primary antibody dilution

Sodium azide	10 mg
BSA	500 mg
antibody (goat polyclonal IgG)	as required
TBS-T solution 10.0 mL	

Secondary anti-rabbit antibody solution

Milk powder	0.5 g
Anti-goat IgG horseradish peroxidase-conjugated antibody	as required
TBS-T solution	10.0 mL

3.1.3 Equipment

Axiovert[®] 25 inverted microscope	Carl Zeiss AG, Oberkochen
Beckman Microfuge[®] Lite	Beckman-Coulter, Fullerton, USA
Casy[®]1 cell counter, Modell TT	Schärfe System, Reutlingen
Centrifuge Universal 32R	Hettich GmbH & Co. KG, Tuttlingen
Centrifuge Mikro 200R	Hettich GmbH & Co. KG, Tuttlingen
Colibri[®] microvolume spectrometer	Titertek-Berthold, Pforzheim
Degasser, Degasys[®] Ultimate	Sanwa Tshusho Co., Japan
Gel electrophoresis	Cleaver Scientific Ltd., Warwickshire, UK
FACSCalibur[®], Flow cytometer	BD Bioscience, Franklin Lakes, USA

Fluoroskan Ascent® microplate reader	Thermo Fisher Scientific, Langenselbold
ICP-MS Varian 820	Varian, Darmstadt
Incubator Thermo	Thermo Electron GmbH, Dreieich
InoLab® pH level 2 pH Meter	WTW GmbH, Weilheim
Kern 770 analytical balance	Kern & Sohn GmbH, Balingen-Frommern
Kern EW analytical balance	Kern & Sohn GmbH, Balingen-Frommern
Laminar air flow work bench	Heraeus Holding GmbH, Hanau
MT Classic AB135-S analytical balance	Mettler-Toledo GmbH, Giessen
Multiskan Ascent® microplate reader	Thermo Electron GmbH, Dreieich
Multiskan EX® microplate reader	Thermo Electron GmbH, Dreieich
Nikon A1 Eclipse Ti® confocal microscope	Nikon, Kingston, UK
Purelab Plus™ system	ELGA LabWater, Celle
Shaker KS 15 control	Edmund Bühler GmbH, Hechingen
Sonicator Bandelin HD2070/UW2070	Bandelin electronic GmbH, Berlin
System Gold® Autosampler 507	Beckman Coulter, Krefeld
System Gold® Detector 168	Beckman Coulter, Krefeld
System Gold® Pump 126	Beckman Coulter, Krefeld
Ultrasonic bath Sonorex® Super RK 103 H	Bandelin electronic GmbH, Berlin
Versa Doc™ Imaging System 5000	Bio-Rad Laboratories GmbH, Munich

3.1.4 Consumables

Blotting paper, 7 x 10 cm	Sigma-Aldrich GmbH, Steinheim
Casy$^®$ tubes	Schärfe System, Reutlingen
Cell culture flasks 25, 75, 175 cm2	Sarstedt AG & Co., Nümbrecht
Cell scraper	Sarstedt AG & Co., Nümbrecht
Conical centrifuge tubes 15, 50 mL	Sarstedt AG & Co., Nümbrecht
Cover slips (round, square)	Carl Roth GmbH & Co., Karlsruhe
Cryovials	Sarstedt AG & Co., Nümbrecht
Disposable syringe (10 mL)	B. Braun Melsungen AG, Melsungen
Glass pipettes	Labomedic GmbH, Bonn
Microscope slides	Carl Roth GmbH & Co., Karlsruhe
Pasteur pipettes	Brand GmbH & Co., Wertheim
Petri dishes	Greiner Labortechnik, Frickenhausen
Pipette tips	Mettler-Toledo GmbH, Giessen
Polyvinylidene fluoride membrane	Carl Roth GmbH & Co.KG, Karlsruhe
peqGold Tissue DNA Mini Kit	peqlab Biotechnologie GmbH, Erlangen
Reaction tubes (0.5, 1.5, 2 mL)	Greiner Labortechnik, Frickenhausen
Sample vials (2 mL, conical)	Varian GmbH, Darmstadt
Tissue culture plates, 96 wells	Sarstedt AG & Co., Nümbrecht
Tissue culture plates, 6 wells	Sarstedt AG & Co., Nümbrecht

3.1.5 Software

Ascent Software (Multiskan Ex$^®$)	Thermo Electron GmbH, Dreieich
FlowJo$^®$ V10	Tree Star Inc., Ashland, USA
GraphPad Prism$^®$ 6.0	GraphPad Software, San Diego, USA

Image Lab® 5.1   Bio-Rad Laboratorien, Munich

Microsoft Excel® 2007   Microsoft Corporation, Redmond, USA

System Gold®   Beckman Coulter, Krefeld

3.2   HPLC purification of CFDA-cisplatin

Reversed-phase high-performance liquid chromatography (RP-HPLC) allows the separation of different chemical entities according to their hydrophobicity/polarity. Semi-preparative RP-HPLC can be used to purify compounds of interest after synthesis of small scale batches. A gradient method was optimized on a Beckman Coulter System Gold® HPLC in order to achieve a high purity for CFDA-cisplatin after the chemical synthesis. As solvent A ultrapure water was used without further additives. Solvent B was HPLC grade acetonitrile without any further additives as well. The final gradient method used is shown in Table 1. The method was established on an analytical column (Nucleodur® C_{18} HTec, 5 µM, 250x4 mm) and then transferred to a semi-preparative column (Varioprep Nucleodur® C_{18} HTec, 5 µM, 250x10 mm).

Table 1   RP-HPLC time program for the purification of CFDA-cisplatin.

% B	Duration [min]	Time [min]
20	5	0
30	5	5
60	20	10
95	2	30
95	5	32
20	2	37
20	5	39

The mobile phase flow rate was 1.0 mL/min for the analytical column and 2.7 mL/min for the semi-preparative column. The mobile phases were degassed by sparging with helium followed by an in-line degasser (Degasys®) during the HPLC runs. The injection volume was 40 µL in 'microlitre pickup mode', in order to minimize the sample loss. The chromatograms were recorded with a diode array detector from 220 to 680 nm wavelength. The fraction of interest was collected and dried in vacuum.

3.3 Cell culture

3.3.1 Cell lines and cultivation

The ovarian carcinoma cell line A2780 and the cisplatin-resistant variant A2780cis (European Collection of Cell Cultures, United Kingdom) were cultivated as monolayers in RPMI-1640® medium supplemented with 10% fetal calf serum (FCS), 100 U/mL penicillin and 0.1 mg/mL streptomycin (37 °C, 5% CO_2). Cells were cultivated to about 90% confluence and then sub-cultivated or used in experiments. Backups of each cell line suspended in FCS containing 10% DMSO were stored in liquid nitrogen. After using cells over a period of at most 12 passages they were discarded and a new backup was thawed. The level of resistance of the resistant variants was monitored by the MTT-based cytotoxicity assay (see 3.5). If a distinct number of cells was needed for an experiment, cells in a cell suspension were counted by electronic pulse area analysis using a Casy®1 cell counter. Distribution of cell volume and cell aggregation were assessed at the same time.

3.3.2 Mycoplasma test

A challenge in cell culture is a possible contamination of cells with mycoplasma bacteria that may influence research results. Mycoplasma can grow on cultivated

mammalian cells and are resistant to common antibiotics. Cells were regularly screened for mycoplasma infections using 2-(4-amidinophenyl)-1H-indole-6-carboxamidine-dihydrochloride (DAPI). DAPI binds to cellular DNA and can be detected by fluorescence microscopy.

Cells were seeded on microscope slides in a petri dish. After two to three days the medium was removed and the slide washed with 5 mL of cold PBS. Then, cells were incubated with 80 µL of DAPI working solution in 2 mL methanol for 5 min. Subsequently, the slide was washed with 2 mL methanol and dried in the dark. Cover slips were fixed on the slides using mounting medium. Cells were analyzed using a Nikon Eclipse Ti® fluorescence microscope. Positively stained cells show a blue shade surrounding cells, accounting for stained mycoplasma DNA. No mycoplasma contaminations were detected.

3.4   Sample preparation and cell fractionation

Two-dimensional gel electrophoresis (2DE) is a powerful tool for the separation of complex protein mixtures enabling the separation and visualisation of hundreds to thousands of proteins. In order to reduce the sample complexity for the analysis cell lysates were fractioned into three main fractions (nuclear, mitochondrial, cytosolic). The cytosolic fraction was used for the 2DE experiments performed by Sandra Kotz (University of Cologne).

All steps of the fractionation were performed on ice and all centrifugation steps were done at 4°C if not stated otherwise.

After washing with PBS, cells were harvested in 1 mL PBS using a cell scraper. After centrifugation at 160 g for 4 min, the PBS was discarded and the pellet was dissolved in lysis buffer supplemented with pepstatin A (2 µM) and leupeptin (1 µM). After

swelling on ice for 5 min, the cell suspension was sonicated three times at 25% power with intermittent 30 sec breaks using an ultrasonic homogenizer (Sonicator Bandelin HD2070/UW2070). The lysate was transferred to 1.5 mL reaction tubes and centrifuged at 700 g for 15 min. The pellet was labeled 'nuclear fraction' (N). The supernatant was transferred to a new reaction tube and centrifuged at 15000 g for 20 min. The pellet was labeled 'mitochondrial fraction' (M). The final supernatant was transferred to a new reaction tube and labeled 'cytosolic fraction' (C).

The efficiency of fractionation was analyzed by detection of marker proteins using Western Blot (see 3.8). For the nuclear fraction, an antibody against the nuclear matrix protein lamin B1 (GTX103292) was used. The mitochondrial fraction was analyzed with an antibody against cytochrome c oxidase subunit IV isoform 1 (COX IV) (GTX101499). Cytochrome c oxidase (COX) is the terminal enzyme of the mitochondrial respiratory chain. GAPDH (GTX100118) was used as an indicator for the purity of the cytosolic fraction. Cross-contamination of the fractions was assumed in case that a marker protein was detected in the wrong fraction.

3.5   Cytotoxicity assay

Cytotoxic properties of compounds and in consequence the sensitivity of cells towards these compounds were assessed using an MTT assay. The assay is based on the reduction of 3-(4,5-dimethylthiazol-2-yl)-2,5-diphenyltetrazolium bromide (MTT), a yellow tetrazole, to a purple formazan by mitochondrial dehydrogenases of living cells (see Figure 10).

Cells were seeded in 96-well plates at a density of 1×10^4 cells per well (A2780, A2780cis) in 90 µL cell culture medium and allowed to attach overnight (37 °C, 5% CO_2). As protection against evaporation the outer wells were filled with PBS only.

The following day 10 µL of cisplatin in increasing concentrations were added to each

well. Each concentration was tested in triplicate. The plates were incubated for 71 h.

Then 20 µL of MTT in PBS (5 mg/mL) were added and the plates were placed in the

incubator again for 1 h. The supernatant was discarded. Cells and formed formazan

crystals were lysed by addition of 100 µL DMSO. The plates were shaken and UV

absorbance at 570 nm with background subtraction at 690 nm was measured using a

Multiskan Ascent® microtiter plate reader.
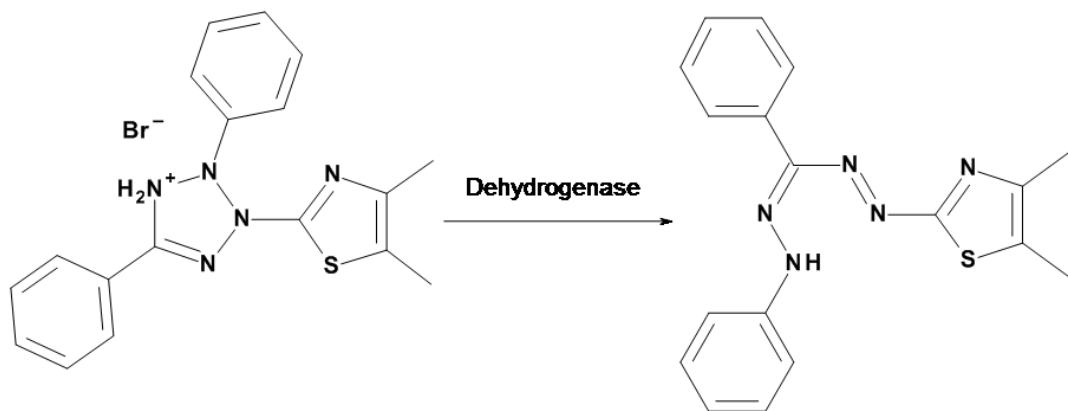
Figure 10   Reduction of MTT by dehydrogenases.

The procedure described was adapted from Mueller et al. [149] but slightly modified

(cell and formazan lysis with DMSO instead of 1:1 isopropanol and 1 M HCl as

described by Alley et al. [150]). Dose-effect curves were calculated by non-linear

regression using the software GraphPad Prism® with a variable slope model

(settings: no comparison, constraint: 'BOTTOM must be greater than 0.0', no

weighting, consider each replicate Y value as an individual point). Effective

concentrations (EC_{50} , EC_{10}: concentrations that provoke 50% or 10% of the maximal

response, respectively) were calculated based on the following equation:

Equation 1 $$Y = \text{Bottom} + \frac{\text{Top-Bottom}}{1+10^{((\text{LogEC}_{50}\text{-x}) \times \text{HillSlope})}}$$

X	concentration
Y	absorption
Bottom	value for Y for the minimal curve asymptote
Top	value for Y for the maximal curve asymptote
LogEC$_{50}$	logarithm of drug concentration producing half maximal response
HillSlope	steepness of concentration response curve

The resistance factor (RF) was calculated by division of the EC$_{50}$ of resistant cells by the EC$_{50}$ value of sensitive cells:

Equation 2
$$RF = \frac{EC_{50}\ resistant}{EC_{50}\ sensitive}$$

EC$_{50}$ resistant	EC$_{50}$ value determined for A2780cis cells
EC$_{50}$ sensitive	EC$_{50}$ value determined for A2780 cells

3.6 Protein quantification

In order to load equal amounts of protein for the Western Blot analysis, the protein concentration of the samples was assessed using the bicinchoninic assay. The assay is based on the reduction of Cu^{2+} to Cu^{+} by proteins under alkaline conditions. Two molecules of bicinchoninic acid (BCA) react with one molecule of Cu^{+} forming a purple chelate complex. The absorbance of the purple chelate complex at 562 nm was determined using a UV microtiter plate reader. Protein concentration was calculated using a calibration curve.

3.6.1 Standard solutions and quality control samples

Standard solutions and quality control (QC) samples were prepared by diluting a 2 mg/mL stock solution of bovine serum albumin (BSA) provided by the manufacturer according to Table 2.

Table 2   Standard solutions and quality controls for protein quantification.

	Volume BSA stock solution [µL]	Volume water [µL]	Protein concentration [µg/mL]
Standard solutions			
S1	50	1950	50
S2	75	1925	75
S3	100	1900	100
S4	200	1800	200
S5	300	1700	300
S6	400	1600	400
Quality control samples			
Q1	150	1850	150
Q2	250	1750	250
Q3	350	1650	350

3.6.2 Sample preparation

Samples were analyzed according to the manufacturer's protocol. After dilution of samples to fit into the calibration range, 25 µL of standard solution, quality control, and sample were transferred to a 96-well plate. Then a mixture of 50 parts BCA working reagent A (containing BCA) and 1 part BCA working reagent B (containing $CuSO_4$) was prepared. 200 µL of the mixture was added to each well and the plate was incubated for 15 min at 60 °C. After 5 min of cooling to room temperature the UV absorbance at 570 nm was determined using a Multiskan Ascent® microtiter plate reader. Linear regression of standard solutions was performed using Microsoft Excel® 2007 and sample concentrations were calculated from the calibration curve. The calibration was considered valid if at least four of the standard solutions did not deviate more than 15% from the nominal value (20% at the lower limit of

quantification) and two of three QC samples did not deviate more than 15% of the nominal value.

3.7 RNA interference

3.7.1 Background

In order to transiently reduce the expression of a target protein, one possibility is silencing the gene of interest by RNA interference (RNAi). A small interference RNA (siRNA) molecule (double-stranded RNA with a length of 21 to 25 base pairs) is introduced into the cell via lipofection. Here, cationic polymers form complexes with the negatively charged siRNA, which then can penetrate into the cell via endocytosis. Endosomes inside the cell release the siRNA. After integration in the RNA-induced silencing complex (RISC) the siRNA hybridizes with the corresponding mRNA. This activates a degradation process of the mRNA by nucleases, which ultimately inhibits translation of the respective protein.

3.7.2 Optimization of siRNA conditions

The transfection conditions were evaluated and optimized using fluorescent siRNA (siGLO®). A2780 and A2780cis cells were seeded in 96-well plates at 1×10^4, 2×10^4 and 3×10^4 cells per well in 100 µL medium without antibiotics. After the attachment of cells overnight, 0.25, 0.5, and 1.0 µL of the K2® and 0.1, 0.2, and 0.3 µL of the Jetprime® transfection reagent were used to transfect 50 nM of siGLO® siRNA. After 24 h, the medium was discarded and the wells were washed with PBS twice. Then, the fluorescence was measured on a Flouroskan® at 485 nm and 538 nm. Afterwards, cell viability was assessed by the MTT assay (Chapter 3.5). In control

experiments, cells were incubated with the transfection reagent without siRNA. For the evaluation of results, the fluorescence of the control cells was defined as 100%.

3.7.3 SiRNA-mediated transient knockdown

A2780 and A2780cis cells were seeded in 6-well plates at 0.5×10^6 cells per well in 1 mL medium without antibiotics and incubated for 24 h. The siRNA directed against the respective protein was introduced into the cell via lipofection (see Table 3). In order to evaluate the influence of the transfection procedure on protein expression, a negative knockdown with a scrambled siRNA (not coding for any protein) was performed. For 2 wells of a 6-well plate 10 µL of the respective siRNA (10 µM) were diluted with 125 µL of medium. At the same time 13.5 µL of K2® transfection reagent were mixed with 125 µL of medium. Both solutions were mixed by gentle pipetting and incubated for 15 min at room temperature. Then, 125 µL of the mixture were added to each well and plates were gently swayed. After 24 h the medium was changed for full medium and cells were incubated for another 48 h. Efficiency of knockdown was assessed by Western Blot (see 3.8).

Table 3   Base sequences of the siRNA used.

Protein	Target Sequence	Sense sequence	Antisense sequence
GRP78	5'-TAGGGTGTGTGTTCACCTTCA-3'	5'-GGGUGUGUGUUCACCUUCATT-3'	5'-UGAAGGUGAACACACACCCTA-3'
PDIA3	5'-AAGGAATAGTCCCATTAGCAA-3'	5'-GGAAUAGUCCCAUUAGCAATT-3'	5'-UUGCUAAUGGGACUAUUCCTT-3'
PDIA1	5'-CAGGACGGTCATTGATTACAA-3'	5'-GGACGGUCAUUGAUUACAATT-3'	5'-UUGUAAUCAAUGACCGUCCTG-3'
Negative control	scrambled sequence		

3.8   SDS Page and Western Blot

Protein expression was analyzed by Western Blot. After the separation of proteins by SDS gel electrophoresis they were transferred to a polyvinylidene fluoride (PVDF) membrane. The detection of proteins was performed by incubation of membranes with antibodies against specific proteins (primary antibodies) followed by incubation with antibodies conjugated with horseradish peroxidase (HRP) (secondary antibody). Proteins were detected after incubation of the membrane with luminol. HRP oxidizes luminol which then shows a chemiluminescent signal. Protein expression in experiments was normalized to the expression of GAPDH as a housekeeping protein.

3.8.1   Sample preparation

Cells were seeded in 6-well plates at densities of $2.5 \times 10^5 - 5 \times 10^5$ cells per well, depending on the incubation time (24 to 48 h). After treatment cells were washed with ice-cold PBS once. Radioimmunoprecipitation (RIPA) buffer was added leading to cell lysis and cells were additionally scraped of the surface with a cell scraper. The lysates were transferred to reaction tubes and incubated on ice for 15 min. After centrifugation (15000 g, 4 °C, 5 min) the supernatant was used for protein quantification and Western Blot analysis.

3.8.2   Gel electrophoresis and Western Blot

Separation of proteins according to size was performed by sodium dodecyl sulfate polyacrylamide gel electrophoresis (SDS-PAGE). Separating and stacking polyacrylamide gels were prepared according to Table 4. The separating gel with fix acrylamide percentages of 10 or 12% was poured into the cassette and overlayed

with isopropyl alcohol. After 15 min isopropyl alcohol was removed, the stacking gel was added on top and wells for sample application were prepared using a comb. After 30 min the fixture containing the gels was placed in the electrophoresis chamber. Electrophoresis buffer was added until the gels were completely covered. The comb was removed and the wells rinsed with buffer. Samples were diluted to a concentration of 10 to 20 µg protein per 20 µL with the loading buffer, which was supplemented with 5% dithiothreitol (DTT) solution. After denaturation of the samples for 15 min at 60 °C, samples as well as a protein marker were pipetted into the wells of the gel. Afterwards the proteins were separated at 200 V for approximately 50 min or until the sample front reached the end of the gel. PVDF membranes were activated with methanol for 20 sec and shaken for 5 min in transfer buffer for equilibration. Afterwards the gel and the membrane were clamped tightly in a fixture. By applying an electric current (100 V, 350 mA, 60 min) the proteins were transferred to the PVDF membrane. In order to visualize more than one protein band on a single blot, the membrane was cut according to protein size in reference to the protein marker. The membranes were subsequently treated with the respective antibodies.

Table 4   Preparation of separating and stacking gel for Western Blot.

	Separating gel 10%	Separating gel 12%	Stacking gel
Acrylamide [30%]	3.30 mL	3.97 mL	833 µL
Separating gel buffer	3.75 mL	3.75 mL	-
Stacking gel buffer	-	-	625 µL
Ultrapure water	2.76 mL	2.10 mL	3.445 mL
SDS [10%]	100 µL	100 µL	50 µL
TEMED*	18 µL	18 µL	5 µL
Ammonium peroxodisulfate [10%]*	70 µL	70 µL	20.8 µL

*Addition shortly before casting the gel in order to initiate polymerization

3.8.3 Visualization of proteins

To minimize unspecific binding of antibodies, membranes were blocked with 5% skim milk solution for 1 h. Subsequently, the membrane was washed three times for 10 min with TBS-T solution. The primary antibody against the respective protein was added and the membrane was incubated overnight at 4 °C. The following morning the antibody solution was removed from the membrane. By conservation with 0.1% sodium azide, the primary antibody solution was reused several times. The membrane was washed three times for 10 min with TBS-T solution. Subsequently, it was incubated for 90 min with the respective secondary antibody conjugated to HRP. The solution was removed and discarded. The last washing step consisted of two times washing for 10 min with TBS-T solution. For visualization Pierce™ ECL Western Blotting Substrate was used according to the manufacturer's protocol and 1000 µL of the substrate were evenly distributed onto the membrane. After 2 min of incubation, the chemiluminescent signal was detected with the ChemiDoc™ XRS Imaging System producing a digital image, which was densitometrically quantified with the Image Lab® software.

3.9   Apoptosis analysis

Apoptosis, or programmed cell death, is a regulated cellular process intended for the maintenance of tissue homeostasis by removal of unwanted cells. It is initiated following cellular stress, which may be inflicted e.g. by DNA damage following a cisplatin treatment. An intracellular proteolytic cascade of procaspases and caspases leads to the cleavage of key proteins in the cell. This enforces the complete disassembly of the cell.

The cell membrane phospholipid phosphatidylserine is under normal cellular circumstances located on the cytoplasmic side of the membrane. At the onset of apoptosis phosphatidylserine translocates to the external leaflet of the membrane. Here, the phospholipid-binding protein Annexin V can specifically recognize and bind to phosphatidylserine with a high affinity. By labeling Annexin V with a fluorochrome such as fluorescein isothiocyanate (FITC) it is possible to identify early apoptotic cells using flow cytometry. An additional DNA dye, which is not cell membrane permeable, such as propidium iodide, permits the differentiation of early and late apoptotic cells. Early apoptotic cells still exhibit cell membrane integrity thus hindering the binding of propidium iodide to the DNA. In late stages of apoptosis, propidium iodide can penetrate the cell and a positive staining can be monitored.

Apoptosis was analyzed using the FITC Annexin V Apoptosis Detection Kit with PI[®] (BioLegend, San Diego, USA) according to the procedure suggested by the manufacturer. Cells were seeded in 6-well plates at a density of 0.5×10^{6} cells per well. After 24 h the knockdown was performed as described in section 3.7. The next day, cells were treated with 10 µM cisplatin for 24 h. Finally, the medium was collected and cells were harvested by addition of 200 µL trypsin. Cells were washed with cold PBS twice and centrifuged at 1000 g for 5 min. The cell pellet was resuspended in Annexin V binding buffer[®] at a concentration of 1×10^{6} cells/mL. After addition of 5 µL FITC Annexin V solution and 10 µL propidium iodide (PI) solution cells were gently vortexed and stained for 15 min at room temperature in the dark. Cells were diluted by addition of 400 µL of Annexin V binding buffer[®] and finally analyzed by flow cytometry within 1 h (FACScalibur[®], BD Biosciences, San Jose, USA). Intact cells were gated with FlowJo[®] v10 (TreeStar, Ashland, USA) in the forward/side scatter to exclude small debris. Annexin V FITC-positive and propidium

iodide-negative (Annexin FITC-V (+)/PI (-)) cells were gated to identify the early apoptotic (EA) population, Annexin FITC-V (+)/PI (+) cells to identify the late apoptotic (LA) population.

3.10 DNA platination

Binding of cisplatin to nuclear DNA is discussed as crucial step in the mechanism of action of cisplatin. DNA platination can be used as a surrogate measure for the therapeutic effect of cisplatin. In order to analyze the DNA platination cells were treated with cisplatin and the nuclear DNA was isolated. After quantification and digestion of DNA in nitric acid, platinum concentration was measured by inductively coupled plasma mass spectrometry (ICP-MS).

Cells were seeded in 6 well plates at a density of 0.5×10^6 cells per well and allowed to attach overnight. After knockdown of the respective protein (see 3.7) cells were treated for 4 h with 100 µM or for 24 h with 5 µM cisplatin. After washing with PBS, nuclear DNA was extracted using the peqGOLD Tissue DNA Mini Kit (PEQlab, Erlangen). The procedure is based on a solid phase extraction of DNA after cell lysis. After medium aspiration, cells were washed with PBS. Then, 400 µL of DNA lysis buffer T, supplemented with 20 µL proteinase K and 15 µL RNAse A were added to the wells. Cells were additionally detached with a cell scraper. Samples were vortexed for 10 sec and then incubated for 15 min at 50 °C with three intermittent vortexing steps for 30 sec. DNA binding buffer was added to the samples and thoroughly mixed. Samples were loaded on the PerfectBind DNA column and centrifuged for 1 min at 10000 g. The supernatant was discarded. Samples were washed twice with 650 µL DNA washing buffer, followed by subsequent centrifugation at 10000 g for 1 min. After a 2 min drying phase of the column at

10000 g, samples were incubated with 100 µL elution buffer for 3 min. Next, samples were eluted by centrifugation at 6.000 g for 1 min. The final DNA concentration was determined in 1 µL sample on a Colibri® microvolume spectrometer (Titertek-Berthold, Pforzheim) based on UV wavelength. The purity of DNA was assessed by the absorption ratio at 260 and 280 nm ($A_{260/280}$).

Samples were digested with 300 µL of 1% nitric acid at 70 °C for 24 h. Platinum content was determined on a Varian 820 ICP-MS as previously described [151]. In brief, for determination by ICP-MS samples are ionized in inductively-coupled plasma. The ions of interest are separated and quantified by a mass spectrometer.

Table 5   Accuracy and precision of DNA platination measurements.

	Concentration [ng/L]			
	50	500	1000	2000
Day 1	49.6	507.6	1031.5	2002.7
	45.9	513.0	991.3	2139.1
Day 2	54.6	559.0	916.6	1880.4
	42.3	470.5	927.9	1877.5
Day 3	49.0	512.3	1030.8	1944.4
	47.4	561.1	1008.6	1758.2
Mean	48.2	520.6	984.4	1933.7
SD	4.1	34.4	50.6	129.5
RSD [%]	8.53	6.61	5.14	6.70
RE [%]	-3.7	4.1	-1.6	-3.3

Each ICP-MS analysis resulted from five replicate measurements consisting of 20 scans of the relevant platinum isotopes. For platinum quantification the platinum isotope 195 (^{195}Pt) was chosen. Quality control samples and an internal standard were used to ensure the accuracy (by calculation of the relative error, Equation 6), and precision (by calculation of the relative standard deviation, Equation 7) of the

measurements (Table 5) which were below the threshold of <15%. The results were finally expressed as mass of platinum per mass of DNA (Pt/DNA [pg/µg]).

3.11 Combination index

Drug combinations may affect multiple targets of a disease, increasing the efficacy of the therapeutic intervention, decreasing the emergence of resistance or minimizing drug toxicity. In order to evaluate the possible benefit of a combination of cisplatin with PACMA31 (Figure 9), the combination index (CI) was calculated with the CompuSyn® software (ComboSyn, Paragon, NJ, USA) as described by Chou [152]. When two drugs are combined and subjected to serial dilutions, the combined mixture behaves like a third drug for the dose-effect relationship. The calculation is based upon the multiple drug-effect equation introduced by Chou and Talalay in 1984 [153]:

Equation 3 $$\text{CI} = \frac{(D)_1}{(D_x)_1} + \frac{(D)_2}{(D_x)_2}$$

$(D)_1$: Concentration of drug 1 in combination with drug 2 that inhibits a system by x%

$(D)_2$: Concentration of drug 2 in combination with drug 1 that inhibits a system by x%

$(D_x)_1$: Drug 1 alone that inhibits a system by x%

$(D_x)_2$: Drug 2 alone that inhibits a system by x%

CI values of < 1, = 1, or > 1 were considered as synergism, additivity and antagonism, respectively.

The result describes the effect of the substances in regard to synergism or antagonism. How this effect is achieved or on what mechanism it is based, needs to be investigated by other experiments.

Cells were seeded in 96-well plates and treated with 10, 20, 40, 60, 80, 100, 200, 400 and 800% of the previously determined EC_{50} of cisplatin, of PACMA31 or a fix combination of cisplatin and PACMA31 (see Table 6). The ratio of cisplatin to PACMA31 in the combination was 5.7 for A2780 and 21.3 for A2780cis cells. After 72 h, the interaction was assessed by the MTT assay as described in 3.5.

Table 6   Cisplatin and PACMA31 concentrations used for the determination of the combination index in A2780 and A2780cis cells. Substances were tested alone and as a fix combination at the indicated concentrations.

Concentration [% of EC_{50}]	Concentration [µM]			
	A2780 cells		A2780cis cells	
	Cisplatin	PACMA31	Cisplatin	PACMA31
10	0.21	0.037	0.98	0.046
20	0.42	0.074	1.96	0.092
40	0.84	0.148	3.92	0.184
60	1.26	0.222	5.88	0.276
80	1.68	0.296	7.84	0.368
100	2.10	0.370	9.80	0.460
200	4.20	0.740	19.6	0.920
400	8.40	1.48	39.2	1.84
800	16.8	2.96	78.4	3.68

3.12 Statistical analysis

The mean of at least three independent experiments (biological replicates) was calculated and the result presented as mean ($\bar{x}$) and standard deviation (SD).

Equation 4
$$\bar{x} = \frac{\sum_{i=1}^{n} x_i}{n}$$

Equation 5
$$SD = \sqrt{\frac{\sum_{i=1}^{n}(x_i - \bar{x})^2}{n-1}}$$

$\overline{x}$:   arithmetic mean

x_i: individual measured values

SD: standard deviation

n: number of measurements

The accuracy and precision of measurement was described by the relative error (RE, Equation 6) and the relative standard deviaton (RSD, Equation 7)

Equation 6 $$RE[\%] = \frac{(\overline{x} - \mu) \times 100}{\mu}$$

Equation 7 $$RSD[\%] = \frac{SD \times 100}{\overline{x}}$$

$\overline{x}$:   arithmetic mean

μ nominal value

SD: standard deviation

EC_{50} data describing the cytotoxic effect were assumed to be log-normally distributed [154]. Therefore, the negative logarithm of the EC_{50} (pEC_{50}) value was calculated. Afterwards, mean and standard error of the mean (SEM) were determined.

Equation 8 $$SEM = \frac{SD}{\sqrt{n}}$$

Statistical comparisons between groups in siRNA experiments were carried out using a one-way analysis of variance (ANOVA). If a significant difference was found the Holm-Sidak post-test was used to determine which means differed.

Differences were considered statistically significant in the case of $p < 0.05$, otherwise no statistically significance was assumed.

4   RESULTS

4.1   Establishing a method for the purification of CFDA-cisplatin

While performing the first experiments with CFDA-cisplatin (Figure 5) it became obvious, that after the synthesis of CFDA-cisplatin using the published method of Molenaar et al. [109], unreacted CFDA-NHS ester (Figure 11 A) and different other impurities were present in the final product. As these impurities may have led to false positive signals in subsequent experiments, purification of the synthesis product was considered mandatory. As other methods of purification, such as recrystallization, were unsuccessful, a HPLC method for purification of CFDA-cisplatin was established.
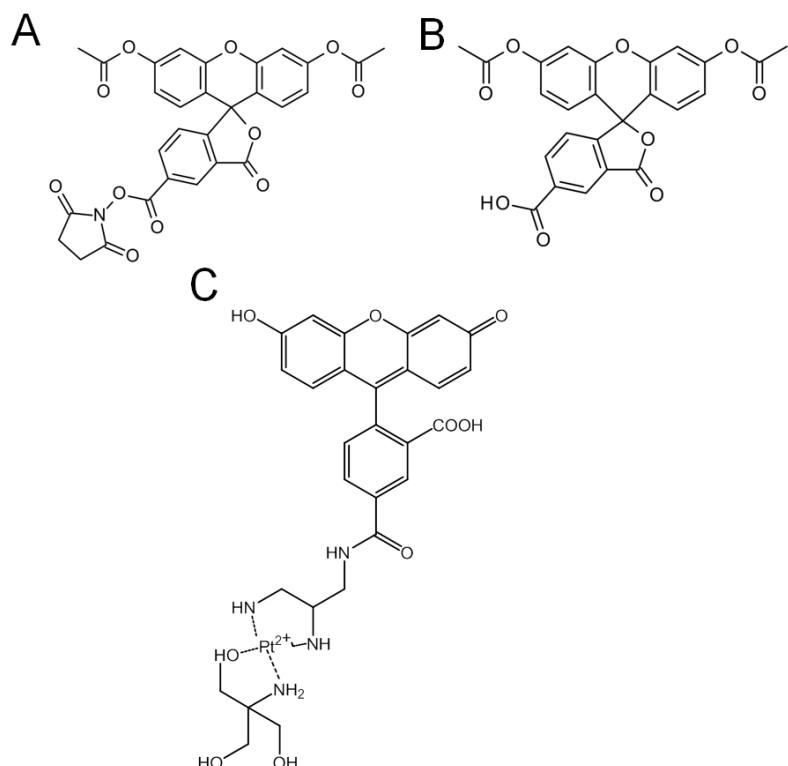

Figure 11   Chemical structure of (A) CFDA-NHS, (B) CFDA-COOH and (C) CFDA-cisplatin-TRIS.

Therefore, several organic solvents (acetonitrile, methanol), an additive to the aqueous solvent (ammonium acetate) and different gradient methods were tested and evaluated regarding their separation performance. In the first tests the best results were gained using water and acetonitrile in a gradient method. Here, an influence of the pH of the solvents on the separation performance was tested by addition of ammonium acetate (CH_3COONH_3) at a concentration of 0.1 mM to the aqueous phase. Subsequently, the pH was adjusted in 0.5 unit steps in the range of 4.5 to 8.0 by CH_3COOH or NaOH (see Appendix A). However, the results showed no improvement of the separation capability over water without additives in the order of pH 7. In the pH range < 6 CFDA-cisplatin decomposed and the chromatographic results deteriorated, showing increasing peaks of byproducts (Appendix A). Hence, the addition of a pH modifier was omitted. After the optimization of the gradient method (see 3.2) using water and acetonitrile without any additives, CFDA-cisplatin purity could be raised to more than 95% and the compound was regarded suitable for cell culture experiments. The final gradient showed a baseline separation of CFDA-cisplatin and its impurities, which was needed for the reliable collection of CFDA-cisplatin (Figure 12). The fractions were analyzed by subsequent LC-MS analysis. The double peak at 28 to 30 min showed the mass of CFDA-cisplatin in both spikes. This may be explained by the mixture of two isomers of CFDA (5-carboxy-fluorescein diacetate and 6-carboxyfluorescein diacetate) that has been used in the synthesis.
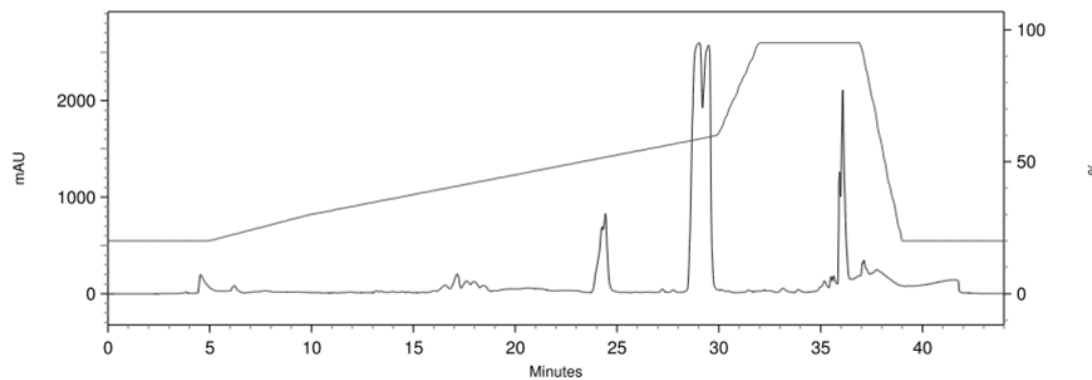
Figure 12   Chromatogram of a semi-preparative HPLC purification run of CFDA-cisplatin. The double-peak at 28 to 30 min contains CFDA-cisplatin.

The differences between the CFDA-cisplatin batches after synthesis and after purification as measured by CE-LIF by Robert Zabel at the ISAS Institute in Dortmund, are shown in Figure 13. As explained above, the crude product of CFDA-cisplatin after synthesis still contained byproducts (Figure 13 a), which were identified using CE-MS as CFDA-TRIS (structure in Figure 11 B), which resulted of the reaction of CFDA-NHS ester with TRIS, and CFDA-COOH, which resulted of the reaction of CFDA-NHS with water. By increasing the amount of precursor in the last step of the synthesis procedure a product with favorable byproduct profile could be produced, but it still contained impurities (Figure 13b). After the HPLC purification procedure a peak of highly purified CFDA-cisplatin (in a complex with TRIS, Figure 11 C) with only negligible peaks of the impurities was detectable by CE-LIF and CE-MS (Figure 13d) [155].
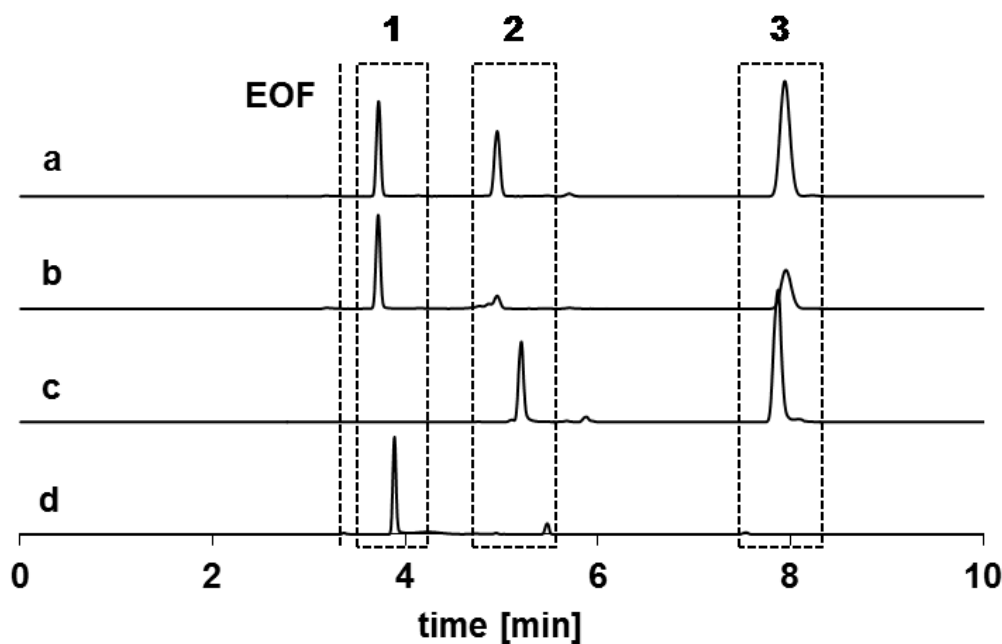
Figure 13   Electropherograms after incubation in TBS overnight at 37 °C of (a) CFDA-cisplatin prepared according to Molenaar et al. [109], (b) CFDA-cisplatin prepared using an excess of platinum precursor Boc-Pt as described in [155], (c) CFDA-NHS and (d) purified CFDA-cisplatin. Identified peaks: (1) CFDA-cisplatin-TRIS, (2) CFDA-TRIS, (3) CFDA-COOH [155].

4.2 Identification of proteins interacting with CFDA-cisplatin

For the identification of proteins interacting with cisplatin by 2D gel electrophoresis the sample complexity was reduced by fractionation of the whole cell lysate into three fractions using differential centrifugation (see 3.4). The efficiency of the fractionation procedure was verified by Western Blot. The nuclear marker protein lamin B1, the mitochondrial marker protein COX IV and the cytosolic marker protein GAPDH were analyzed. After differential centrifugation of the lysate, the cytosolic fraction was almost completely cleared of nuclear and mitochondrial remnants and suitable for the subsequent experiments (Figure 14). There were only slightly visible bands for the respective marker proteins lamin B1 and COX IV detectable, whereas the nuclear and mitochondrial fraction showed strong bands.
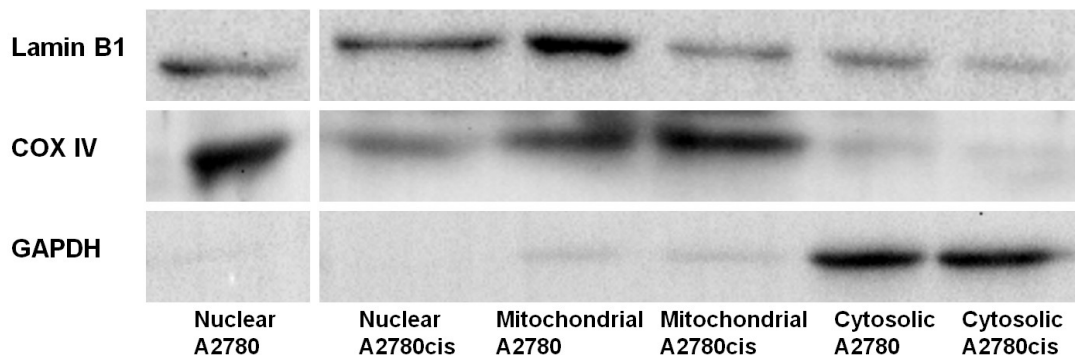
Figure 14   Representative Western Blot after fractionation of A2780 and A2780cis cells. Nuclear marker protein lamin B1, mitochondrial marker protein COX IV and cytosolic marker protein GAPDH were detected in the three fractions.

After incubation of cells with 25 µM CFDA-cisplatin for 2 h, cells were fractionated as described in section 3.4. The following experiments were performed by Sandra Kotz from the University of Cologne with the cytosolic fractions that were prepared in Bonn. The cytosolic fraction was further analyzed by 2D gel electrophoresis. The

simultaneous introduction of an on-gel reference protein marker grid during 2D gel electrophoresis increased the validity of the subsequent analysis [111,156].
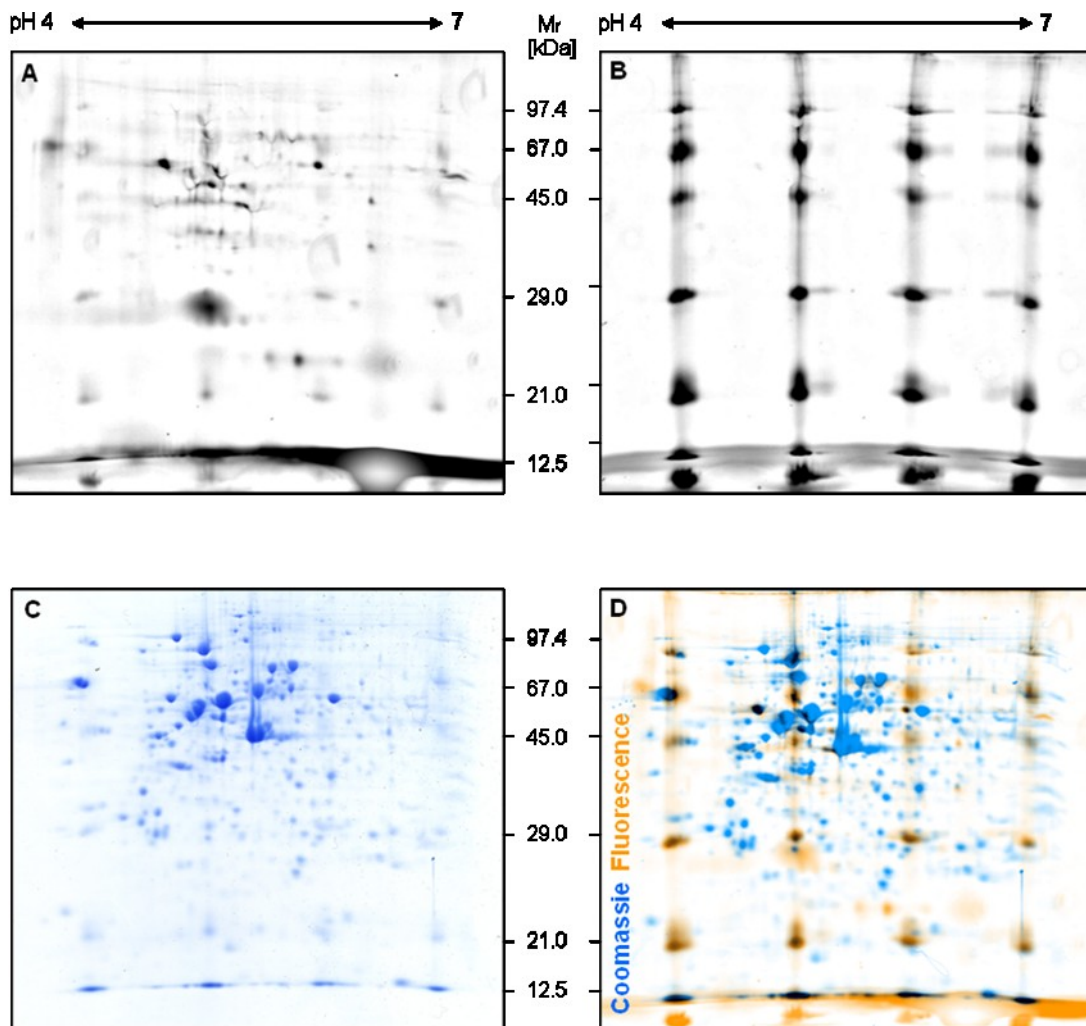
Figure 15   Visualisation of CFDA-cisplatin-protein adducts by 2D gel electrophoresis. A2780cis cells were treated with 25 µM CFDA-cisplatin for 2h (A). The generation of a reference protein spot grid (B) allowed the separation in parallel with 150 µg cytosolic proteins through 2DE. A fluorescence scan was recorded (CFDA-cisplatin: excitation/emission: 488 nm/532 nm (A); SERVA Lightning Red for 1D SDS-PAGE: excitation/emission: 532 nm/580 nm (B)) and the proteins were visualised with Coomassie staining (C). For the image analysis the fluorescence scans from CFDA-cisplatin-protein adducts (A) as well as from protein marker grid (B) and the Coomassie staining image (C) were fused to a master image (D) [111].

As shown in Figure 15, after the 2D gel electrophoresis it was possible to assign fluorescent signals (colored in orange) to distinct protein spots (Coomassie stained in blue). Subsequently, these protein spots were excised from the gel. After enzymatic digestion, the proteins showing fluorescence were identified by ESI-MS analysis. In the pH range 4 to 7 the protein disulfide isomerases PDIA1 and PDIA3 as well as 78 kDa glucose-regulated protein (GRP78) were identified among others (Table 7) [111]. The contribution of these proteins was assessed in the following screening approach.

Table 7   Identified proteins after 2D gel electrophoresis and ESI-MS analysis of CFDA-cisplatin treated A2780 and A2780cis cytosolic fractions.

Protein name	Gene name	Accession number
Protein disulfide isomerase A1	PDIA1	P07237
Protein disulfide isomerase A3	PDIA3	P30101
Protein disulfide isomerase A6	PDIA6	Q15084
78 kDa glucose-regulated protein	HSPA5	P11021
ß-Actin	ACTB	P60709
Vimentin	VIM	P08670

4.3 Optimization of siRNA experiments

The transient siRNA-mediated knockdown of a target protein plays a central role in the following experiments evaluating the contribution of the respective protein to cisplatin resistance. With the aid of a fluorescent siRNA (siGLO® siRNA) the conditions for an optimal transfection were assessed. Experience from previous studies in the workgroup showed that the selection of a potent transfection reagent was crucial for transfection efficiency, therefore two different reagents were tested (K2® transfection system, Biontex Laboratories GmbH; jetprime®, Polyplus Transfection). As confirmed by fluorometric analysis after transfection, the K2®

reagent showed the more efficient transfection of siGLO® siRNA in the cell lines used (A2780, A2780cis) (Figure 16) with at least a doubling in fluorescence compared to control cells transfected without siRNA. Therefore, it was chosen for further experiments.
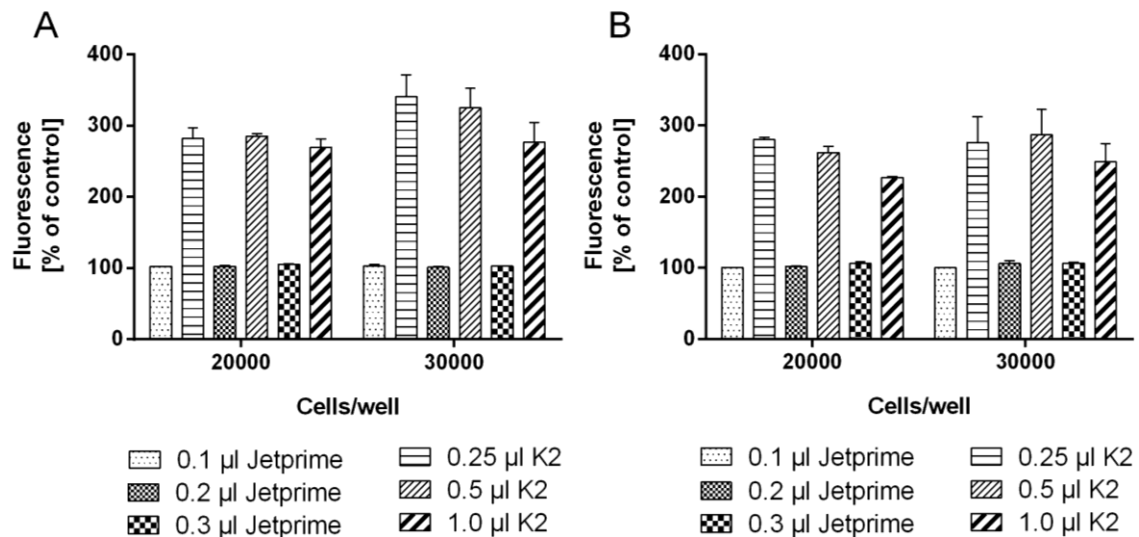
Figure 16   siGLO® transfection efficiency in A2780 (A) and A2780cis (B) cells. Different concentrations of transfection reagent were used with 50 nM of siGLO siRNA for 20.000 or 30.000 cells/well. Fluorescence was compared to control cells transfected without siRNA (mean ± SD, N = 3).

The final concentration of K2® reagent for an efficient transfection was determined in a similar fashion as before (Figure 17). At the same time the impact of the transfection on cell viability was assessed by the MTT assay (Figure 18). All results were recorded for three different cell densities between 10000 and 30000 cells per well. Combining both factors, the optimal conditions for transfection were determined (highest transfection efficiency with lowest impact on viability of cells).

In A2780 cells, the efficiency of transfection for 10000 cells per well was best with 0.75 µL K2® per well, whereas for 20000 and 30000 cells per well it was best for 0.5 µL K2® per well. For A2780cis cells, 0.5 µL K2® per well resulted in the highest

transfection efficiency for a number of 10000 and 20000 cells per well. The most favorable transfection profile for 30000 cells per well was observed with a higher volume of 0.75 µL K2® per well.
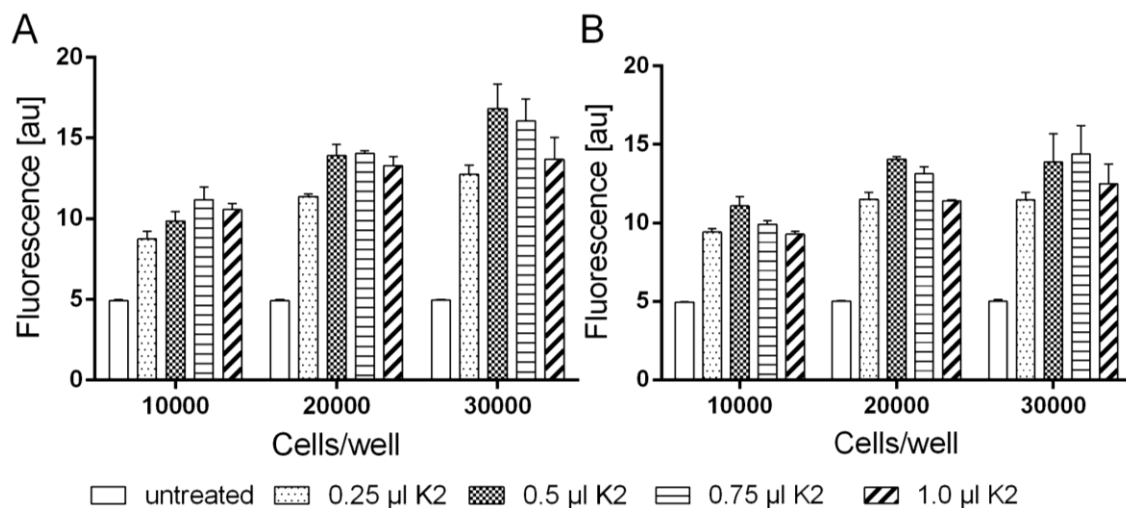
Figure 17   Fluorescence of siGLO® siRNA after transfection in (A) A2780 and (B) A2780cis cells using different volumes of K2® transfection reagent and 50 nM of siGLO® siRNA (mean ± SD, N = 3).
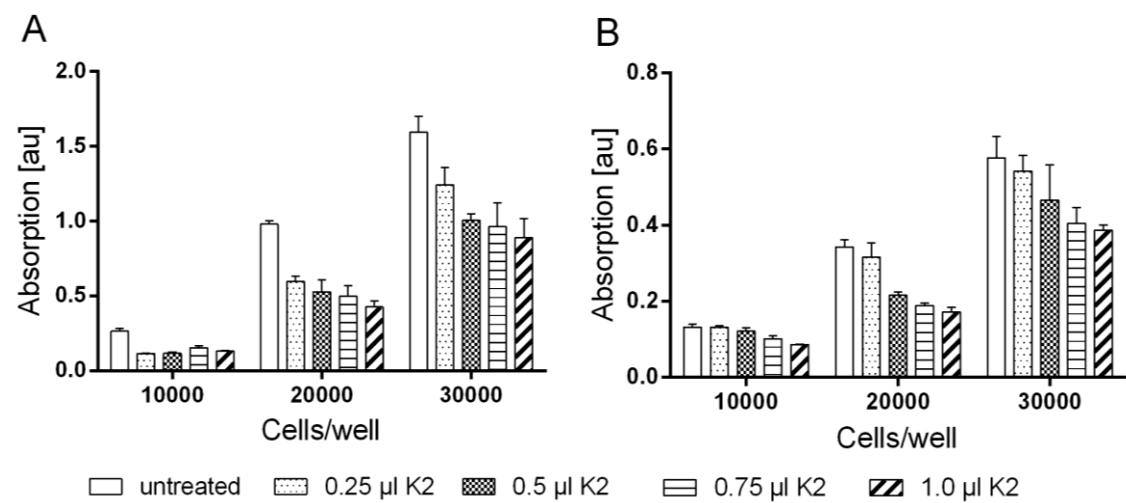
Figure 18   Viability of (A) A2780 and (B) A2780cis cells after transfection of siGLO® siRNA using different volumes of K2® transfection reagent and 50 nM of siGLO® siRNA (mean ± SD, N = 3).

The transfection reagent had a dose-dependent influence on cell viability, with the transfection with the highest volume of 1 µL per well being the most cytotoxic. The resistant cell line A2780cis was more robust against the toxic effect of the transfection reagent than A2780 cells.

Based on these results, a volume of 0.5 µL K2$^®$ transfection reagent per well was chosen for all further experiments as it showed good to very good transfection results (Figure 17) with an acceptable influence on cell viability in both cell lines (Figure 18). The volume was scaled to a 6-well plate for further experiments according to the recommendations of the manufacturer.

4.4 GRP78

4.4.1 siRNA knockdown

The contribution of GRP78 to cisplatin detoxification in the cytoplasm and to apoptosis induction after cisplatin treatment was analyzed after a transient siRNA-mediated silencing of GRP78 in A2780 and A2780cis cells. Using Western Blot analysis, the expression of GRP78 in cells without knockdown was compared to negative knockdown and GRP78 knockdown cells. All results are related to the expression of GAPDH as a housekeeper protein.
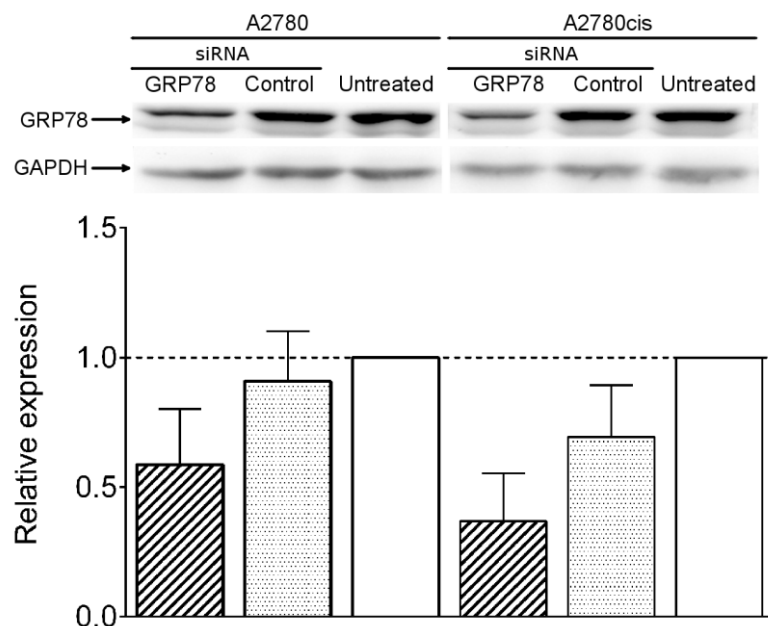
Figure 19   Representative Western Blot and corresponding densitometric quantification of the expression (bar graph) of GRP78 in A2780 and A2780cis cells either without knockdown (untreated) or treated with the respective siRNA (negative control or GRP78). Results of untransfected cells were set to 100%. GAPDH was used as housekeeping protein (mean ± SD, N = 3).

The knockdown with a negative siRNA (non-coding base sequence, see 3.7) showed a small influence on GRP78 expression in A2780cis cells, reducing the expression to 70 ± 10%. In A2780 cells the negative knockdown led to comparable levels of GRP78 in comparison to cells without knockdown (91 ± 10%). If transfected with GRP78-specific siRNA [40 nM], the expression of GRP78 was reduced to 59 ± 9% and 37 ± 8% in A2780 and A2780cis cells, respectively (Figure 19). The concentration of 40 nM was considered suitable, as lower concentrations (< 40 nM) exhibited a decrease in knockdown efficiency, whereas higher concentrations (> 40 nM) produced a decrease in cell viability, particularly in A2780 cells. All results are detailed in Appendix B1.

4.4.2 Cisplatin cytotoxicity

Cisplatin cytotoxicity after GRP78 knockdown was assessed using the MTT assay.
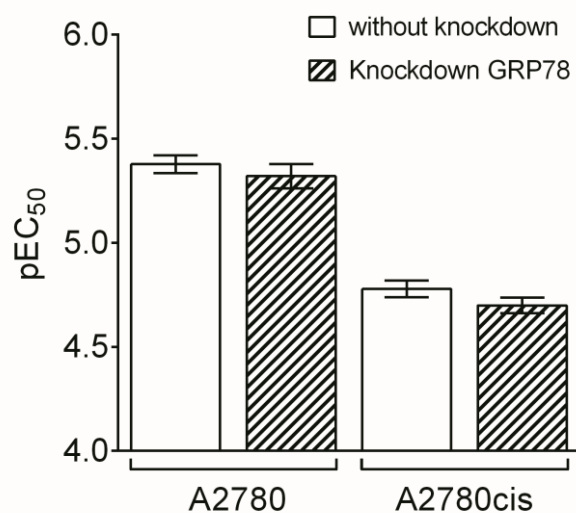
Figure 20   Cisplatin cytotoxicity in A2780 and A2780cis cells assessed without knockdown, and GRP78 knockdown (mean ± SEM, N = 6 - 9).

Results for A2780 cells show a slight tendency for decreased pEC_{50} values between cells without knockdown (5.38 ± 0.04, mean ± SEM) and with GRP78 knockdown (5.32 ± 0.06, mean ± SEM) with no significant difference (p = 0.379) (Figure 20). A2780cis cells exhibited also a non-significant (p = 0.337) decrease of the pEC_{50} value from 4.78 ± 0.04 to 4.70 ± 0.04 (mean ± SEM) after knockdown, rather suggesting an increase in resistance after knockdown. All results are detailed in Appendix B2.

4.4.3 Apoptosis induction

The induction of apoptosis is regarded as one of the final steps in the mechanism of action of cisplatin. The transfection itself had an impact on the cell viability. Hence, in order to compensate for the apoptosis-inducing effect of the knockdown procedure, the ratio of the percentage of apoptotic cells after knockdown and subsequent cisplatin incubation to the percentage of apoptotic cells in corresponding control experiments without cisplatin was calculated. As internal control, simultaneously cells without knockdown were tested using the same procedure. In order to investigate the cisplatin effect on both stages of apoptosis, the early apoptotic (EA) and late apoptotic (LA) cell population was analyzed separately.

Cisplatin exposure strongly induced early and late apoptosis in A2780 cells (fold change: EA 2.6 ± 1.0, LA: 4.3 ± 0.7, mean ± SD). As expected in resistant cells, cisplatin induced apoptosis to a lesser extent, for EA the fold change was 1.3 ± 0.4 and for LA 1.4 ± 0.4. As mentioned above, the knockdown procedure alone was cytotoxic and induced apoptosis, possibly caused by its influence on cellular functions. Thus, results for negative knockdown and GRP78 knockdown have to be interpreted accordingly. In A2780 cells the knockdown procedure influenced the

induction of apoptosis even stronger than in A2780cis cells. Compared to cells without knockdown an increase of early apoptotic A2780 cells after the negative knockdown was noted. After GRP78 knockdown, A2780 cells present a far lower fold change of apoptotic cells (EA: 1.4 ± 0.5, LA: 1.3 ± 0.3, mean ± SD) than after negative knockdown cells (EA: 3.3 ± 2.5, LA: 1.9 ± 0.3, mean ± SD) (Figure 21). In resistant cells, early apoptosis after GRP78 knockdown was induced to a slightly greater extent (EA: 1.9 ± 0.5, mean ± SD), compared to cells with negative knockdown (EA: 1.3 ± 0.8, mean ± SD) and without knockdown (EA: 1.3 ± 0.4, mean ± SD). However, late apoptosis remained on the same level after GRP78 knockdown (LA: 1.5 ± 0.4, mean ± SD) as after negative knockdown (LA: 1.5 ± 1.1, mean ± SD) or without knockdown (LA: 1.4 ± 0.4, mean ± SD). All results are detailed in Appendix B3.
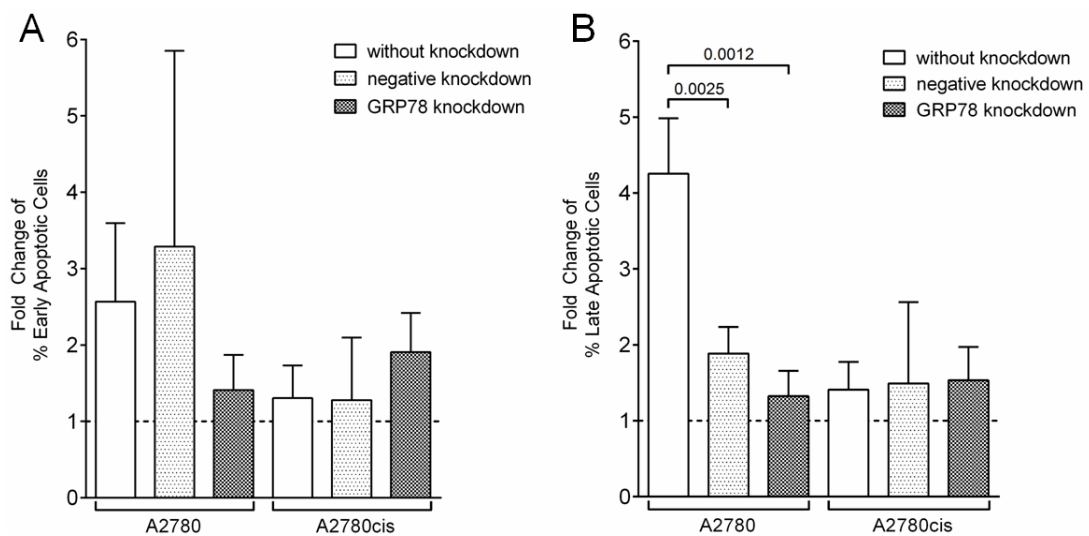
Figure 21   Cisplatin-associated apoptosis induction in A2780 and A2780cis cells assessed without knockdown, after negative or GRP78 knockdown. Fold change of the percentage of (A) early apoptotic (EA) and (B) late apoptotic (LA) cells after a 24 h incubation with 10 µM cisplatin related to a corresponding control experiment without cisplatin treatment (mean ± SD, N = 3 - 6).

4.5   PDIA1

4.5.1   siRNA knockdown

In A2780 and A2780cis cells a negative knockdown showed no influence on PDIA1 expression with PDIA1 levels comparable to cells without knockdown (Figure 22). After transfection of PDIA1-specific siRNA the expression was reduced to 44.9 ± 3.4% and 47.4 ± 4.1 % of its basal level in A2780 and A2780cis cells, respectively (Figure 22). All results are detailed in Appendix C1.
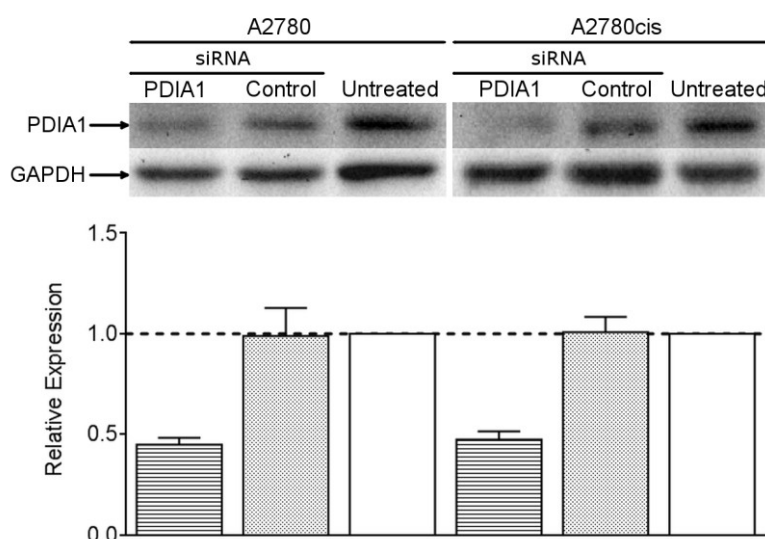
Figure 22   Representative Western Blot and corresponding densitometric quantification of the expression (bar graph) of PDIA1 in A2780 and A2780cis cells either without knockdown (untreated) or treated with the respective siRNA (negative control or PDIA1). Results of untreated cells were set to 100%. GAPDH was used as housekeeping protein (mean ± SD, N = 3).

4.5.2 Cisplatin cytotoxicity

After PDIA1 knockdown, the MTT assay revealed a slight and not significant sensitization to cisplatin treatment (p = 0.06) for A2780 cells. However, cisplatin-resistant A2780cis cells were significantly sensitized to cisplatin after PDIA1 knockdown compared to either negative knockdown controls (p = 0.019) or controls without knockdown (p = 0.046) (Figure 23). All results are detailed in Appendix C2.
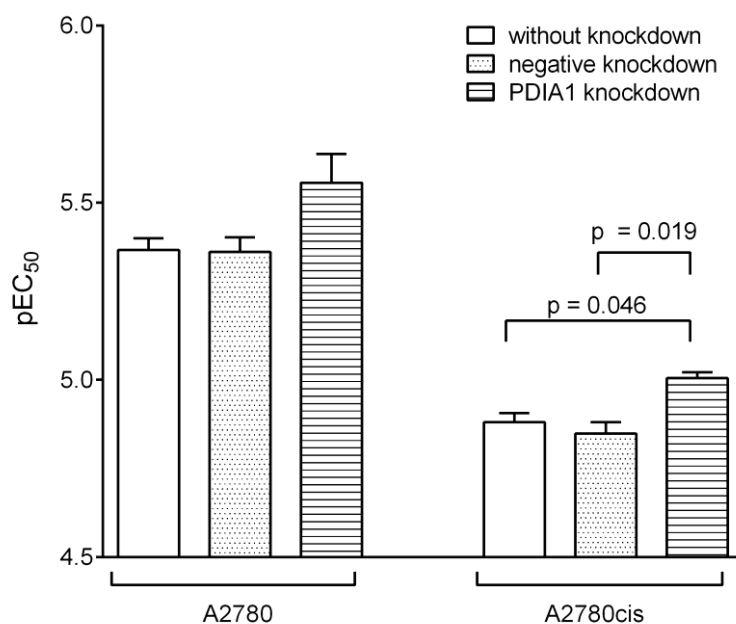
Figure 23   Cisplatin cytotoxicity in A2780 and A2780cis cells without knockdown, negative knockdown and PDIA1 knockdown (mean ± SEM, N = 3 - 6).

4.5.3 Apoptosis induction

As expected, cisplatin exposure generally induced early and late apoptosis in A2780 cells (fold change: EA: 3.5 ± 0.8; LA: 3.9 ± 1.3, mean ± SD) and to a lower extent in A2780cis cells (EA: 2.1 ± 1.2; LA: 2.4 ± 0.6, mean ± SD). Within the same cell line no significant differences in early and late apoptosis induced by cisplatin were found between the different knockdown experiments. However, some trends were observed. In sensitive A2780 cells, apoptosis induction by cisplatin was not affected

by PDIA1 knockdown exhibiting EA and LA ratios comparable to negative knockdown cells (Figure 24). In resistant A2780cis cells, PDIA1 knockdown led to higher ratios of EA and LA cells (EA: 3.5 ± 2.1; LA: 2.2 ± 1.0, mean ± SD) compared to negative knockdown cells (EA: 1.4 ± 0.9; LA: 1.4 ± 0.9, mean ± SD), indicating a cisplatin-sensitizing effect of PDIA1 knockdown in these cells. All results are detailed in Appendix C3.
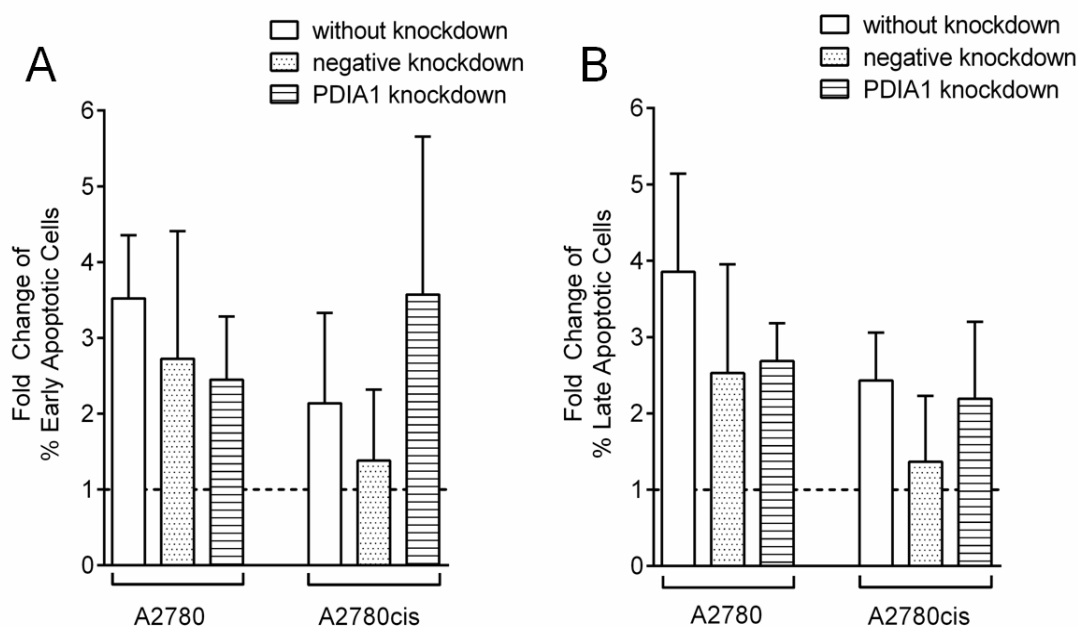

Figure 24   Cisplatin-associated apoptosis induction in A2780 and A2780cis cells assessed without knockdown, after negative or PDIA1 knockdown. Fold change of the percentage of (A) early apoptotic (EA) and (B) late apoptotic (LA) cells after a 24 h incubation with 10 µM cisplatin related to a corresponding control experiment without cisplatin treatment (mean ± SD, N = 3 - 6).

4.5.4 DNA platination

The platination of nuclear DNA is regarded as the main cornerstone of the cytotoxic mechanism of action of cisplatin [157]. Thus, the DNA platination after knockdown of PDIA1 was investigated under two different conditions (high cisplatin concentration, short incubation time (HS) [100 µM cisplatin, 4 h] and low cisplatin concentration,

long incubation time (LL) [5 µM cisplatin, 24 h]). Control experiments were performed using cells without knockdown and negative knockdown cells. HS incubation of A2780 cells after PDIA1 knockdown showed no difference in the DNA platination compared to the control cells without knockdown and negative knockdown cells (without knockdown: 220.3 ± 16.0 pg Pt/µg DNA; neg. knockdown: 205.9 ± 29.8 pg Pt/µg DNA; PDIA1 knockdown: 198.4 ± 19.8 pg Pt/µg DNA, mean ± SD) (Figure 25). In contrast, LL incubation led to slightly higher DNA platination after PDIA1 knockdown, especially compared to cells without knockdown (without knockdown: 17.5 ± 4.4 pg Pt/µg DNA; neg. knockdown: 20.2 ± 3.2 pg Pt/µg DNA; PDIA1 knockdown: 21.9 ± 2.3 pg Pt/µg DNA, mean ± SD) (Figure 26). The resistant cells showed a different pattern. Here, HS incubation after PDIA1 knockdown led to an increased DNA platination (without knockdown: 75.7 ± 33.4 pg Pt/µg DNA; neg. knockdown: 113.4 ± 20.8 pg Pt/µg DNA; PDIA1 knockdown: 127.4 ± 38.9 pg Pt/µg DNA, mean ± SD) (Figure 25).
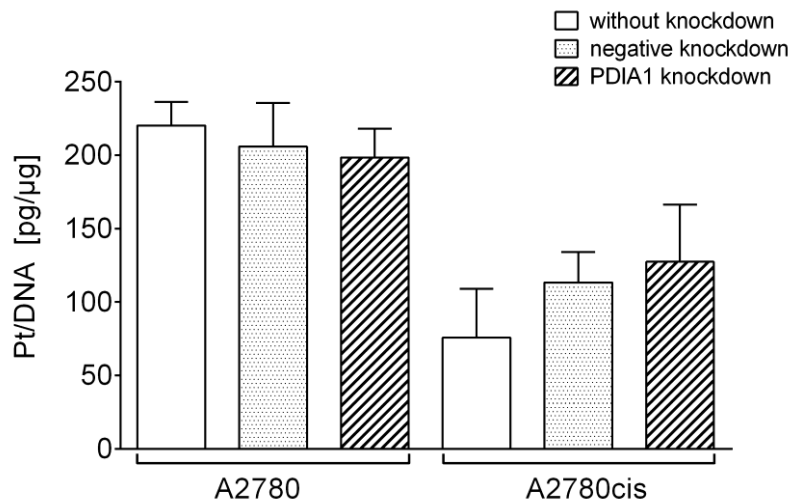
Figure 25   DNA platination after incubation with 100 µM cisplatin for 4 h in A2780 and A2780cis cells assessed without knockdown, after negative or PDIA1 knockdown (mean ± SD, N = 3).

The LL incubation showed mixed results, as the negative knockdown had the highest influence on DNA platination and PDIA1 knockdown led to platinum levels comparable to cells without knockdown (without knockdown: 12.8 ± 7.1 pg Pt/µg DNA; neg. knockdown: 22.8 ± 4.5 pg Pt/µg DNA; PDIA1 knockdown: 14.5 ± 5.7 pg Pt/µg DNA, mean ± SD) (Figure 26). After LL incubation the ratio of DNA platination between sensitive and resistant cells without knockdown, with negative knockdown and with PDIA1 knockdown was reduced to a factor of 1.37, 0.89 and 1.33, respectively. After HS incubation this ratio was 3.71, 1.82 and 1.56, respectively. All results are detailed in Appendix C4
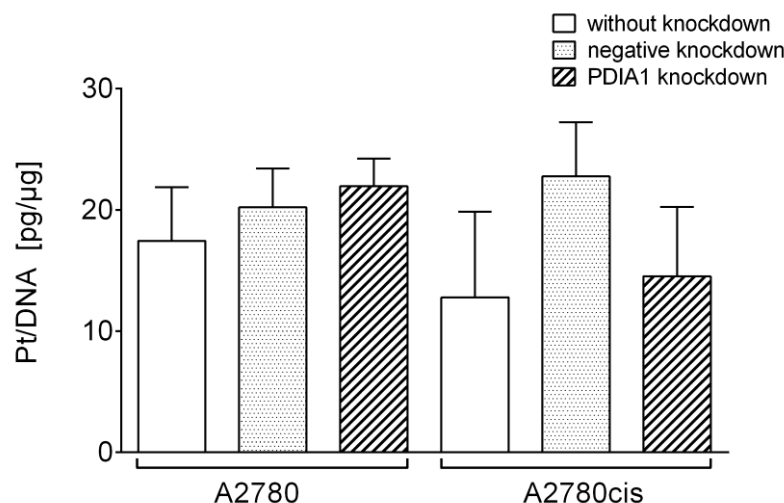
Figure 26   DNA platination after incubation with 5 µM cisplatin for 24 h in A2780 and A2780cis cells assessed without knockdown, after negative or PDIA1 knockdown (mean ± SD, N = 3).

4.5.5 Pharmacological inhibition of PDIA1 by PACMA31

To better understand the role of PDIA1 for acquired cisplatin resistance the effect of the recently described irreversible PDI inhibitor PACMA31 on cisplatin cytotoxicity was investigated [140]. PACMA31 has been reported to be selective for PDIA1 over other protein families, but its selectivity over other PDI isoforms is not yet known.

First, the cytotoxic effect of PACMA31 on A2780 and A2780cis cells alone and then in combination with cisplatin was analyzed.

Table 8   Cytotoxicity of PACMA31 in A2780 and A2780cis cells (mean ± SEM, N = 9).

	A2780	A2780cis
pEC_{50}	6.47 ± 0.05	6.40 ± 0.06
EC_{50} [µM]	0.37	0.46
pEC_{10}	6.62 ± 0.07	6.50 ± 0.05
EC_{10} [µM]	0.29	0.35

The EC_{50} and EC_{10} of PACMA31 were determined (Table 8). The results show that PACMA31 is highly cytotoxic in A2780 and A2780cis cells with markedly lower EC_{50} values than cisplatin. The resistance factor for PACMA31 was 1.2.
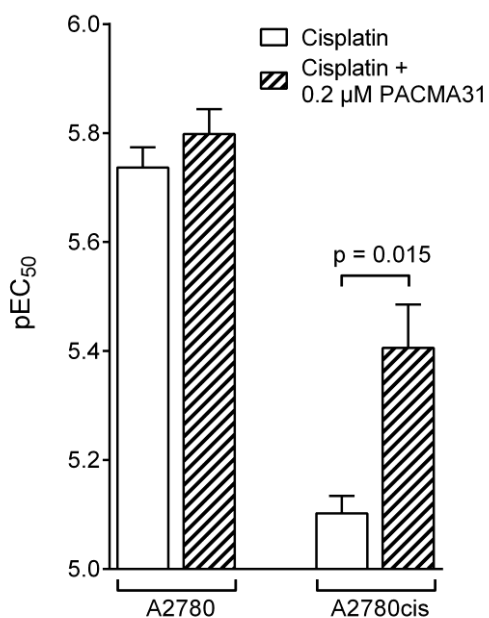
Figure 27   Cisplatin cytotoxicity in A2780 and A2780cis cells without and with co-incubation with 0.2 µM PACMA31 (mean ± SEM, N = 3 - 6).

In a second experiment, the cytotoxicity of a combination of PACMA31 at a concentration of 0.2 µM (which is lower than its EC_{10} concentration) together with cisplatin was investigated. Whereas sensitivity of A2780 cells did not significantly change, A2780cis cells were significantly sensitized to cisplatin treatment (p = 0.015) (Figure 27). The resistance factor decreased from 4.3 ± 0.06 to 2.5 ± 0.27 (mean ± SEM, N = 3-6, p = 0.0032) upon addition of PACMA31 at the concentration of 0.2 µM. All results are detailed in Appendix D1.

In a further step it was investigated if a pharmacological inhibition of PDIA1 had any influence on DNA platination. Similar conditions as in the previous experiments were applied, such as HS with 100 µM cisplatin for 4 h and LL with 5 µM cisplatin for 24 h. Co-incubation with 0.2 µM or 0.4 µM PACMA31 at the HS conditions caused a slightly and not significantly reduced DNA platination in A2780 and A2780cis cells (Figure 28).
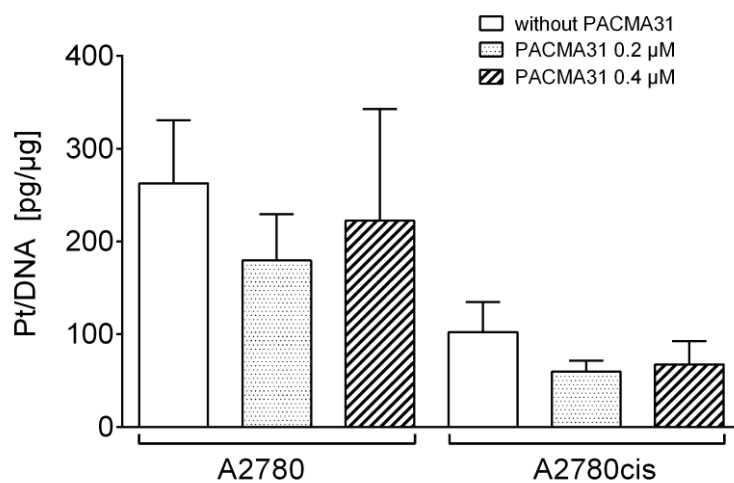
Figure 28   DNA platination after incubation with 100 µM cisplatin for 4 h in A2780 and A2780cis cells and co-incubation with 0.2 µM or 0.4 µM PACMA31 (mean ± SD, N = 3 - 6).

At the LL conditions, a tendency for reduced DNA platination upon 0.2 µM PACMA31 co-incubation was observed whereas the tendency was smaller in the case of 0.4 µM

PACMA31. In A2780cis cells, a co-incubation with 0.2 µM PACMA31 showed no influence and 0.4 µM PACMA31 led to a slight increase of platinated DNA (Figure 29).
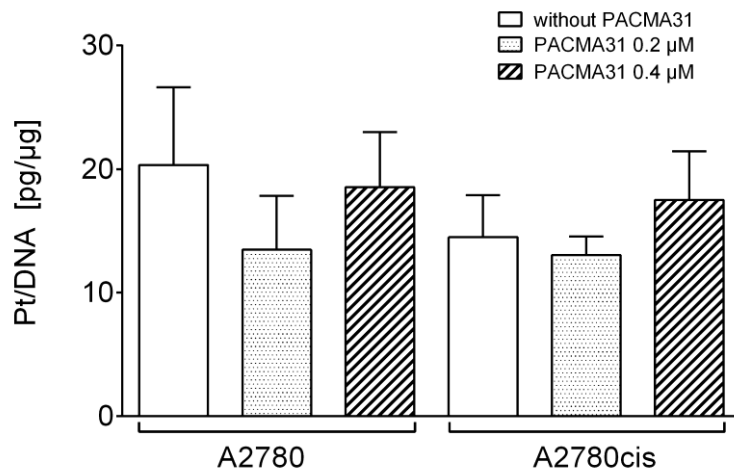
Figure 29   DNA platination after incubation with 5 µM cisplatin for 24 h in A2780 and A2780cis cells and co-incubated with 0.2 µM or 0.4 µM PACMA31 (mean ± SD, N = 3 - 6).

In order to further assess the potential of PACMA31 to overcome cisplatin resistance, the combination index according to Chou was determined [152]. Combination of increasing concentrations of cisplatin and PACMA31 were tested in an MTT assay. For the combination of PACMA31 with cisplatin in sensitive A2780 cells a synergistic effect at effective concentration combinations higher than EC_{90} with the strongest synergism at EC_{95} was found. At the EC_{50} and EC_{75} concentration both drugs act as antagonists in A2780 cells, reducing the expected cytotoxic effect. In resistant A2780cis cells the synergistic effect was much more pronounced. Here, a CI value lower than 1 was already determined at the EC_{75} concentration (Figure 30). Again, the strongest effect was found at EC_{95} concentration. At the EC_{50} concentration both drugs showed an additive effect in A2780cis cells (CI = 1). All results are detailed in Appendix D3.
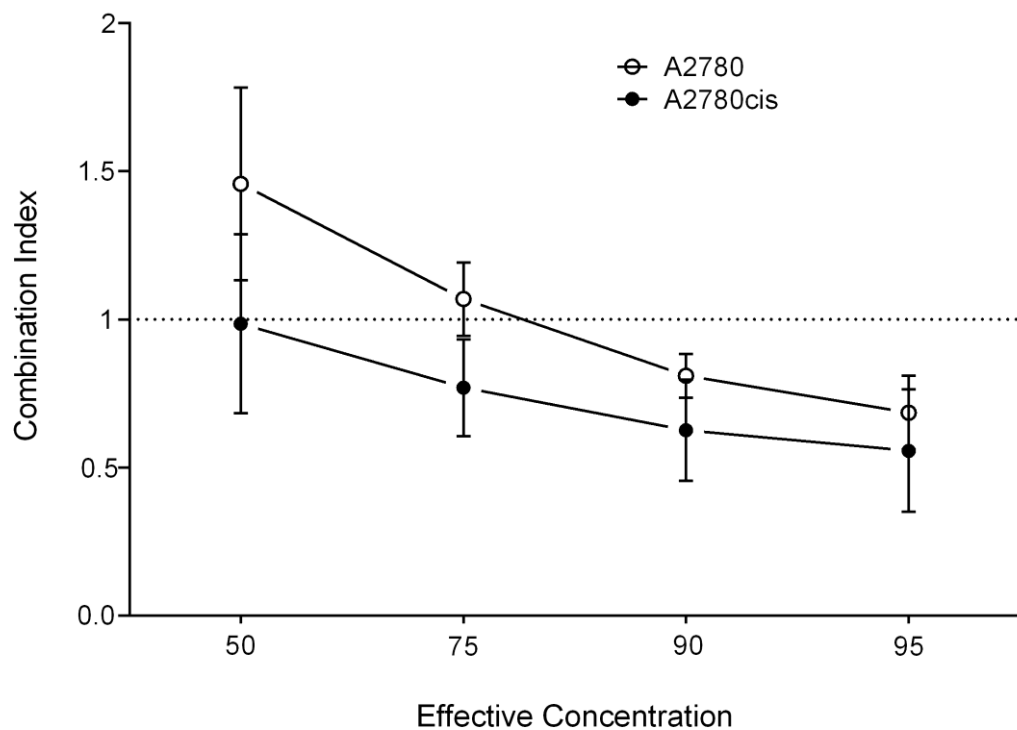
Figure 30   Combination index (CI) for PACMA31 and cisplatin in A2780 and A2780cis cells. CI was determined for EC_{50} to EC_{95} (mean ± SD, N = 9).

4.6 PDIA3

4.6.1 siRNA knockdown

After PDIA3 knockdown, the expression of PDIA3 in A2780 and A2780cis cells was reduced to 40.4 ± 9.9% and to 16.5 ± 9.8% of its basal level in untreated cells, respectively (Figure 31). The negative knockdown did not affect PDIA3 expression in A2780 (107.2 ± 6.5%) and A2780cis cells (91.5 ± 16.7%). All results are detailed in Appendix E1.
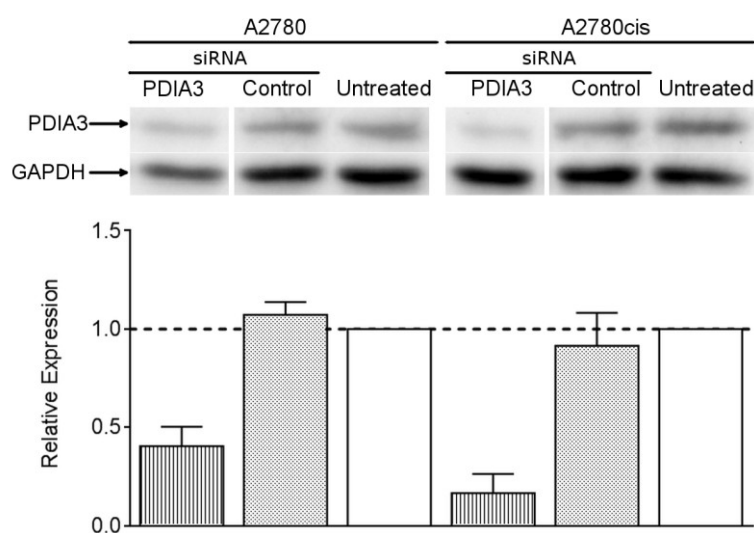
Figure 31   Representative Western Blot and corresponding densitometric quantification of the expression (bar graph) of PDIA3 in A2780 and A2780cis cells either without knockdown (untreated) or treated with the respective siRNA (negative control or PDIA3). Results of untreated cells were set to 100%. GAPDH was used as housekeeping protein (mean ± SD, N = 3).

4.6.2 Cisplatin cytotoxicity

In A2780 cells a knockdown of PDIA3 had no influence on cisplatin cytotoxicity. The pEC_{50} values are comparable for the three conditions investigated (without knockdown: 5.37 ± 0.03; negative knockdown: 5.36 ± 0.04; PDIA3 knockdown:

5.39 ± 0.03. mean ± SEM) (Figure 32). In A2780cis cells, a slight but not significant desensitizing tendency of PDIA3 knockdown was observed (without knockdown: 4.88 ± 0.03; negative knockdown: 4.85 ± 0.03; PDIA3 knockdown: 4.80 ± 0.02, mean ± SEM). All results are detailed in Appendix E2.
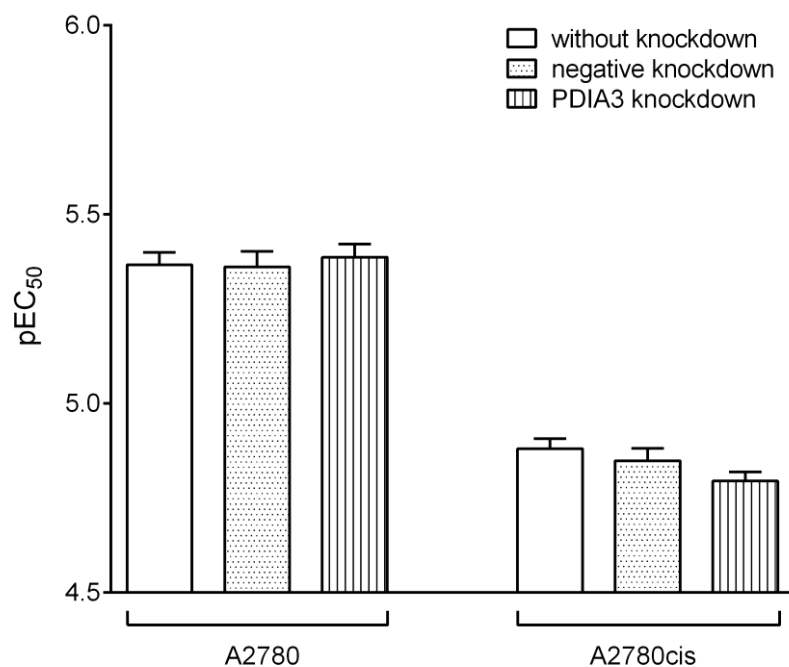
Figure 32   Cisplatin cytotoxicity in A2780 and A2780cis cells assessed without knockdown, negative knockdown and PDIA3 knockdown (mean ± SEM, N = 5 - 7).

4.6.3 Apoptosis induction

After PDIA3 knockdown in A2780 cells, cisplatin treatment showed a decreased apoptosis-inducing effect (EA: 1.4 ± 0.3; LA: 1.3 ± 0.1, mean ± SD) (Figure 33). This may be explained by a stronger apoptosis-inducing effect of the PDIA3 knockdown alone. Still, some apoptosis-inducing effect of cisplatin was detectable as the ratio after PDIA3 knockdown with cisplatin and without cisplatin was greater than 1. In A2780cis cells PDIA3 knockdown showed comparable ratios as negative knockdown for EA (1.2 ± 0.3 vs. 1.4 ± 0.9, mean ± SD) and LA (1.2 ± 0.3 vs. 1.4 ± 0.9,

mean ± SD) indicating no cisplatin-sensitizing effect of PDIA3 knockdown. All results are detailed in Appendix E3.
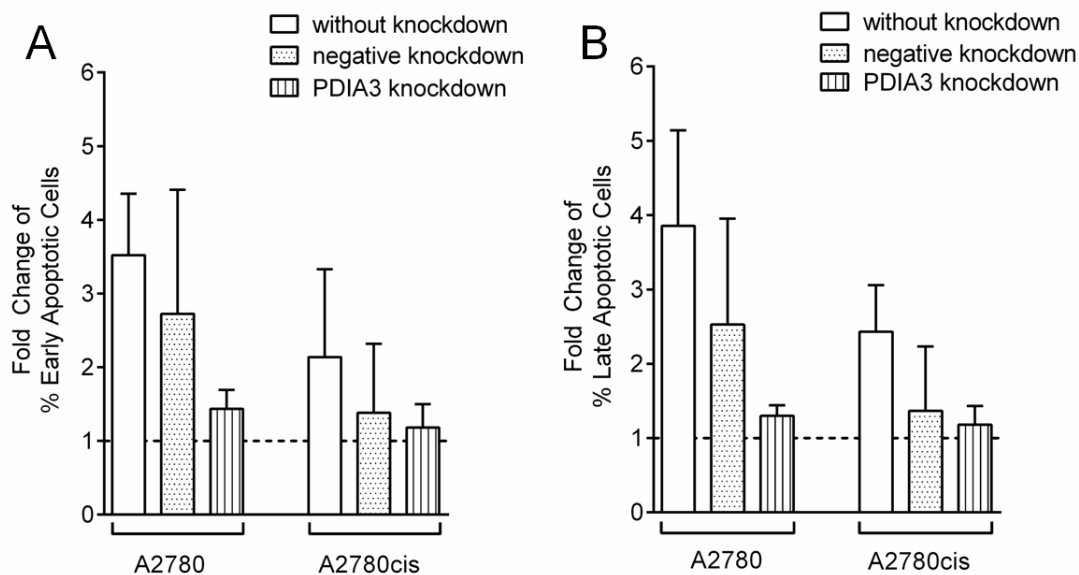
Figure 33   Cisplatin-associated apoptosis induction in A2780 and A2780cis cells assessed without knockdown, after negative or PDIA3 knockdown. Fold change of the percentage of (A) early apoptotic (EA) and (B) late apoptotic (LA) cells after a 24 h incubation with 10 µM cisplatin related to a corresponding control experiment without cisplatin treatment (mean ± SD, N = 3 - 6).

4.6.4 DNA platination

Interestingly, HS incubation of A2780 cells after PDIA3 knockdown significantly increased the DNA platination compared to cells with a negative knockdown (without knockdown: 318.9 ± 44.2 pg Pt/µg DNA; neg. knockdown: 324.1 ± 20.8 pg Pt/µg DNA, PDIA3 knockdown: 383.6 ± 30.4 pg Pt/µg DNA, mean ± SD) (Figure 34). A comparable but not significant increase in A2780 cells was detectable after LL incubation (without knockdown: 21.1 ± 7.5 pg Pt/µg DNA; negative knockdown: 59.9 ± 15.6 pg Pt/µg DNA;   PDIA3   knockdown: 68.7 ± 35.6   pg Pt/µg DNA, mean ± SD) (Figure 35). Again, the resistant cells showed a different pattern. HS incubation after PDIA3 knockdown led to a similar DNA platination compared to

negative knockdown (without knockdown: 102.3 ± 32.3 pg Pt/µg DNA; negative knockdown: 155.0 ± 56.8 pg Pt/µg DNA, PDIA3 knockdown: 136.1 ± 68.7 pg Pt/µg DNA, mean ± SD).
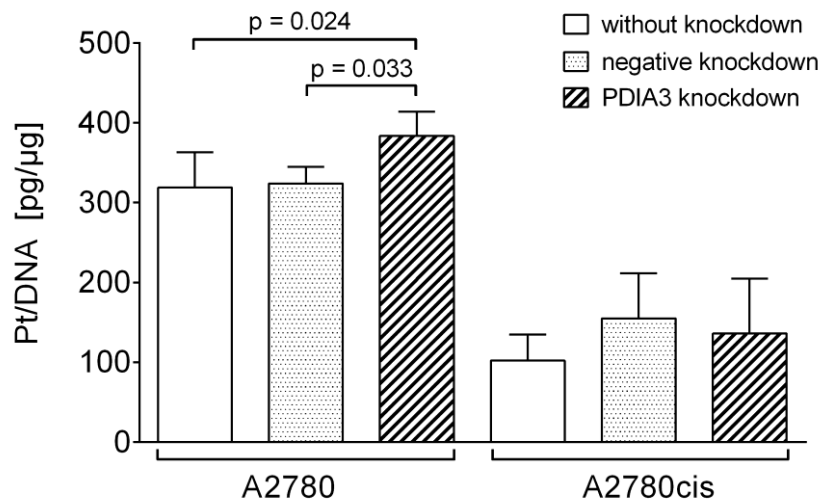
Figure 34   DNA platination after incubation with 100 µM cisplatin for 4 h in A2780 and A2780cis cells assessed without knockdown, after negative or PDIA3 knockdown (mean ± SD, N = 5).

After LL incubation the negative knockdown showed lower DNA platination than the PDIA3 knockdown in A2780cis cells (without knockdown: 15.3 ± 3.2 pg Pt/µg DNA; negative knockdown: 39.3 ± 36.5 pg Pt/µg DNA; PDIA3 knockdown: 49.9 ± 32.9 pg Pt/µg DNA, mean ± SD). The ratio of DNA platination between sensitive and resistant cells without knockdown, with negative knockdown and with PDIA3 knockdown was 3.12, 2.09 and 2.82 after HS incubation, respectively. After LL incubation the ratio was reduced to factors of 1.38, 2.56 and 1.80, respectively. All results are detailed in Appendix E4.
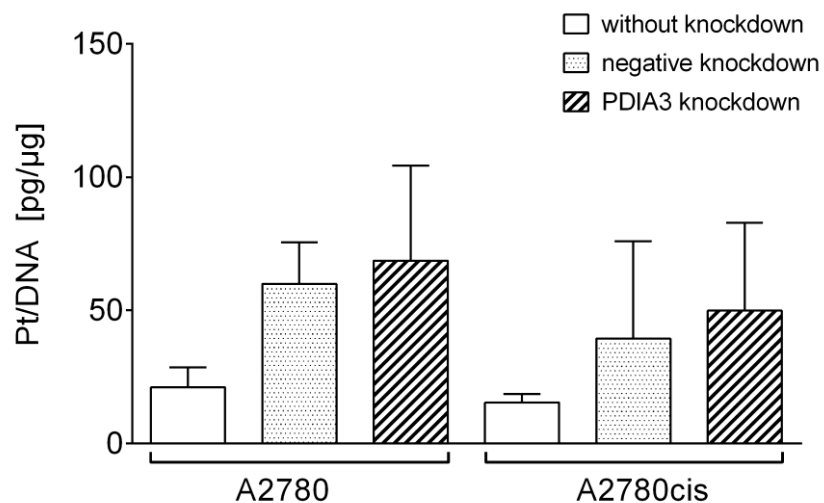
Figure 35   DNA platination after incubation with 5 µM cisplatin for 24 h in A2780 and A2780cis cells assessed without knockdown, after negative or PDIA3 knockdown (mean ± SD, N = 5).

5   DISCUSSION

5.1   Purification of CFDA-cisplatin

CFDA-cisplatin (CFDA-Pt) was introduced in 2000 by Molenaar et al. as a model substance, enabling researchers to follow the distribution and the intracellular protein binding of cisplatin [109]. After the synthesis of CFDA-cisplatin according to the literature procedure, first results of the LC-MS characterization of the final product revealed several major impurities, while the yield of CFDA-cisplatin was only about 40% [109,155]. The original synthesis by Molenaar et al. reported yields of 55-70%, which however was impossible to reproduce [109]. The capillary electrophoresis with laser-induced fluorescence detection (CE-LIF) analysis of the product, with a limit of detection in the low attomolar (picogram) concentration range, detected fluorescent impurities, which were proved to carry a CFDA moiety [155]. By an on-line CE-MS coupling the identification of the main impurities was possible. It became clear that the CFDA-NHS ester, which was one of the educts used in the synthesis, was still present. Furthermore, CFDA-COOH was identified which is formed upon the reaction of CFDA-NHS with water [155]. The impurities could potentially lead to false-positive results by producing signals after binding of CFDA-NHS to proteins. Hence, the purification of the final product was necessary. The most practicable approach was the semi-preparative high performance liquid chromatography (HPLC). Several columns were tested, such as the reversed-phase Nucleodur C18 Gravity® and Nucleodur HTec C18®. The latter revealed a suitable performance for the purification of CFDA-cisplatin. Several methods were tested during the optimization process of the method, such as an isocratic elution with H_2O/acetonitrile 30%/70%. The finally established method used a gradient of H_2O/acetonitrile from 80%/20% to 5%/95%

enabling base-line separation of CFDA-cisplatin and its impurities. The purified product was analyzed by LC-MS and again by CE-LIF. After all, CFDA-cisplatin showed a purity of at least 95% [155]. This was sufficient for the subsequent *in vitro* and other experiments. The crucial purification step greatly improved the reliability as well as the confidence in the screening approach and the following experiments.

A drawback for the purification process was the time-consuming HPLC run, which lasted 44 minutes. As described above, this was necessary to achieve base-line separation. Furthermore, the loss of product upon purification was around 50%, which was higher than expected. This suggests that during the purification some of the substance either decayed or got lost due to the HPLC setup.

5.2   siRNA transfection

Since the discovery and spreading application in life sciences, the methods for siRNA transfection have been steadily improved. Still, the interplay between the most effective siRNA for a target protein in a cell and the transfection reagent has great impact on knockdown efficiency [158]. Thus, the experimental conditions always need to be optimized for each cell line transfected for the first time [159].

The time and costs to design and evaluate an effective siRNA were saved by using siRNA validated by the manufacturer (Qiagen) [160]. As stated in 4.3, the K2[®] transfection reagent was compared with other commercially available products. Results for the A2780 cell line were most encouraging in the case of the K2[®] transfection reagent, which was therefore used in this study.

Various methods to assess transfection efficiency exist. For example, the transfection with a cell death control siRNA leads the cell into apoptosis and transfection efficiency can be simply correlated to cell viability. As a simultaneous measurement

of the transfection efficiency and apoptosis initiation was needed, the transfection of a fluorescent siRNA followed by a MTT assay was regarded as a feasible alternative [161]. Here, the measurement of fluorescence intensity after transfection can be correlated with transfection efficiency [162]. Subsequently, the absorption of formazan after MTT treatment correlates with the cell viability after the transfection procedure. In order to increase the comparability between experiments, the experimental conditions determined by this approach were then used in all following experiments.

The therapeutic application of siRNA to treat diseases in humans is developing with a pace seen never before in the development of an entirely new therapeutic approach. From the first discovery of specific post-translational gene silencing in *C. elegans* in 1998 by Mello and Fire, researchers brought siRNA therapy to the clinics as early as 2010 [163,164]. The potential of siRNA therapy is enormous having the ability to ameliorate basically every human disease that is caused by over-expression of a specific protein [165]. However, remaining obstacles need to be elucidated and are currently being tackled to improve siRNA therapy. The main problem is the safe and efficient delivery of siRNA to the target tissue [166]. Several approaches have already proven their efficacy to deliver siRNA *in vivo*, such as polymers or lipids [166]. Targeting the siRNA to cancer cell-specific receptors can improve its distribution. For example, around 95% of ovarian epithelial carcinomas express the scavenger receptor B1 (SR-B1). Therefore, delivery of siRNA targeted to SR-B1 showed an even distribution of ~80% in a given tumor [167]. A further application for siRNA-based therapeutics is drug resistance in cancer which, as stated earlier, may be caused by over-expression of transporters or signaling pathway proteins [168]. Here, a combined treatment with siRNA and a chemotherapeutic drug may support

the management of drug resistance [169]. In a recent publication, the administration of siRNA and a cisplatin prodrug through nanoparticle-mediated codelivery showed promising results sensitizing cancer cells to therapy and proved to be efficacious in an animal model [170].

5.3   Contribution of GRP78 to acquired cisplatin resistance

GRP78 is part of the heat shock protein family (HSP) and a master regulator of the unfolded protein response (UPR). As described in section 1.4.1, cells activate the UPR in order to cope with ER stress, which may occur after exposition to a chemotherapeutic agent [121]. Furthermore, the basal expression of GRP78 has been shown to be increased in several, mostly rapidly proliferating cancer entities such as melanoma, endometrial, breast, or prostate cancer [171–174]. It appears mandatory for these cancer cells to maintain their protein folding capacity even under stressed conditions for the rapid synthesis of new proteins. Interference with the mechanisms associated with an increased stress tolerance seems to be a reasonable approach to sensitize cells to cytotoxic treatment [175]. This has been shown in cell models of different cancer entities [176]. In melanoma cells (Mel-RM, MM200) cisplatin sensitivity was significantly increased after siRNA inhibition of GRP78 [171]. TuBEC cells, which were derived from blood vessels of malignant glioma tissues, showed highly elevated GRP78 expression and were resistant to etoposide and temozolomide treatment [177]. With a lentiviral construct expressing siRNA against GRP78 TuBEC cells were sensitized to the anticancer drugs [177]. Colorectal cancer cells have been sensitized to paclitaxel by inhibition of GRP78, leading to an increased activation of apoptosis-mediating proteins [178]. Two endometrial cancer cell lines (Ishikawa, AN3CA) could be sensitized to cisplatin

treatment by knockdown of GRP78 [172]. Additionally, Cali et al. showed that cell growth and invasiveness of these cell lines was reduced after silencing GRP78 [179]. Another approach includes administration of small molecules that inhibit the GRP78 function. Epigallocatechin gallate (EGCG) is a major component of green tea and has been shown to exert many beneficial effects such as chemopreventive or anticarcinogenic effects. In TuBEC cells, combination of EGCG with temozolomoide or etoposide caused significantly more cell death than the drugs alone [177]. In breast cancer cells, etoposide resistance could be overcome by treatment with EGCG [180]. Genistein, an isoflavone and phytoestrogen which can be found e.g. in soybeans, has been shown to inhibit the growth of breast cancer cells by blocking the binding of a transcription factor to the GRP78 promoter thus inhibiting translation [181]. Recent results for the plant compound honokiol, a lignan which can be extracted e.g. from the southern magnolia, suggest a mechanism of action comparable to EGCG (binding the unfolded ATPase domain of GRP78), but a higher affinity for GRP78 than EGCG. This may explain the higher sensitivity of different cancer cell lines to honokiol [182]. These studies suggest a relevance of GRP78 for cancer progression and development of chemoresistance.

Other authors report opposing results. Ahmad et al. transiently up-regulated GRP78 in lung cancer cells, which led to a hypersensitization of cells to cisplatin [183]. Colon cancer cells pre-treated with 6-aminonicotinamide or 2-deoxyglucose over-expressed GRP78. The elevated GRP78 levels led to an increase in sensitivity to cisplatin, 1,3-bis(2-chlorethyl)-1-nitrosourea (BCNU or carmustin) and melphalan [184]. This may be caused by the ability of GRP78 to induce apoptosis by activating PERK. The more GRP78 is available the more PERK is activated, enhancing the apoptosis inducing effect of cisplatin.

In order to elucidate the contribution of GRP78 to acquired cisplatin resistance in the ovarian cancer cells A2780 and A2780cis a knockdown was conducted. Investigation of cisplatin cytotoxicity using the MTT assay showed no significant changes. Interestingly, the resistance factor of A2780cis cells increased slightly after a GRP78 knockdown. The results suggest a compensation mechanism in A2780cis cells. GRP78 acts as the master regulator of the UPR and supports the cellular survival after mild ER stress. The resistant cells may be able to deal with the ER stress independently of GRP78 activity, potentially through an upregulation of other ER stress signaling proteins such as ATF6 or IRE1. The results of the apoptosis assay present a slightly different picture than the MTT data. Here, apoptosis induction in sensitive cells was reduced after GRP78 knockdown, which may be due to an increased activation of the pro-survival pathways and a decreased activation of the pro-apoptotic pathways. A2780cis cells show a small increase in early apoptotic cells, but no change in late apoptotic cells. Here, it seems possible that the early pro-apoptotic pathway is increasingly activated after GRP78 knockdown, at least in comparison to A2780cis cells with a negative knockdown. The results of the late apoptosis are in accordance with the MTT assay, as no difference between the investigated conditions could be detected. Interpretation of the results is limited by the influence of the knockdown. The knockdown of GRP78 reduced the protein expression only to around 60% of the basal level in A2780 and to 40% in A2780cis cells. It is possible that in A2780 cells the remaining GRP78 protein was able to fulfill its cellular tasks, supporting the reduction of ER stress levels. After the knockdown of a protein the proliferation of A2780cis cells changed to a lesser extent than that of A2780 cells, which may explain the higher knockdown efficiency in A2780cis cells. As this project concentrated on the functional protein, there was no evaluation of the

efficacy of the siRNA to inhibit mRNA transcription by quantitative real-time polymerase chain reaction. This additional transcriptome analysis should be considered in future projects, in order to increase the understanding of the cellular effects of the knockdown itself. Furthermore, it should be noted that the results are limited to a cisplatin exposure of 24 h. Induction of early apoptosis may be stronger at earlier time points whereas late apoptosis may need even longer exposure times.

In addition, GRP78 expression may be salvaged by cisplatin incubation, which may restore GRP78 levels after cisplatin exposure to basal levels. The circumvention of this problem appears difficult. It may be possible to perform the knockdown simultaneously with cisplatin exposure, but the results would need special interpretation, as the knockdown itself always exhibits a mild cytotoxic effect. Furthermore, various possible reactions of siRNA with cisplatin have been reported. In one study, the platination of the sense-strands in siRNA did not abolish the gene silencing activity *in vitro* [185]. However, the same group showed later that cisplatin did interfere with the siRNA silencing capacity [186]. A permanent knockdown using a shRNA construct may also be considered but may lead to other problems in return such as the comparability of shRNA-transfected cells to wild-type cells. For shRNA-knockdown a compensatory protein upregulation has been described *in vitro* and *in vivo* [187,188]. In summary, the results suggest that in A2780 and A2780cis cells the siRNA-mediated knockdown of GRP78 has no significant effect on cisplatin cytotoxicity after 48 h or on cisplatin-induced apoptosis after 24 h.

5.4   Contribution of PDIA1 to acquired cisplatin resistance

5.4.1   Effects of siRNA knockdown

Protein disulfide isomerases exhibit intracellular functions, which mainly support cellular homeostasis. Depending on the substrate, they form (oxidize), break (reduce) or rearrange (isomerize) disulfide bonds in proteins [126]. Since PDIA1 is able to fulfill various intracellular tasks, the role of PDIA1 comprehensibly appears cell-type specific. In HeLa cells, a PDIA1 knockdown showed no significant effect on viability, whereas in MCF-7 cells the same knockdown was cytotoxic [189]. It has recently been shown that an upregulation of PDIA1 in glioblastoma is associated with resistance against temozolomide (TMZ). Again, the effect of a PDIA1 knockdown on TMZ cytotoxicity was cell-line dependent with the strongest effects of knockdown in TMZ-resistant D54-R cells [190]. The study described here suggests a similar pattern in ovarian cancer cells, as the cisplatin-resistant A2780cis cells are significantly sensitized to cisplatin treatment after PDIA1 knockdown, whereas in sensitive A2780 cells only a tendency for a sensitization to cisplatin treatment after PDIA1 knockdown was observed. Additionally, a tendency to increased apoptosis in the early and late stage upon cisplatin treatment in A2780cis cells after PDIA1 knockdown was observed, which is in agreement with the results of the MTT assay. There was no significant change in the amount of platinated DNA detectable after the PDIA1 knockdown. This implies that the increased cytotoxicity and apoptosis induction may be independent of cisplatin binding to the nuclear DNA. Cisplatin potentially exerts its effect additionally by an extra-nuclear mechanism. An increase in ER stress levels after the PDIA1 knockdown seems possible, which has been associated with cisplatin cytotoxicity in cytoplasts (enucleated cells) [191]. If the chaperone activity of

PDIA1 is lost the cell is not able to reduce the increasing amount of misfolded proteins. Compensation mechanisms by other chaperones may not be sufficient to limit the ER stress to an acceptable level.

It is important to consider that the apoptosis results reported, are limited to a cisplatin exposure of 24 h and 10 µM cisplatin. Therefore, it may be interesting to investigate the time- and concentration-dependence of the cisplatin-sensitizing effect of the PDIA1 knockdown. The results of the DNA platination experiments may be limited due to the complex experimental setting which introduces more variability than the MTT or apoptosis assay. The multiple steps include (I) the knockdown procedure, (II) cisplatin exposure and (III) DNA extraction. This is followed by (IV) DNA quantification and finally (V) platinum determination. All of those experiments carry a liability of an individual error. Nevertheless, the results presented here indicate that PDIA1 may be a worthwhile target to be investigated in the context of acquired cisplatin resistance.

5.4.2 Effects of pharmacologic inhibition of PDIA1

Transient genetic modifications by siRNA treatment of various cellular proteins other than PDIA1, have been investigated in preclinical settings multiple times. The next step would be the *in vivo* treatment with siRNA, which is already under investigation in animals as well as in humans (see section 5.2). However, the most common therapeutic option used clinically to inhibit the function of a target is still the pharmacological inhibition. Thus, the potential of the recently developed PDIA1 inhibitor PACMA31 to reverse cisplatin resistance was investigated. PACMA31 covalently binds to Cys397/Cys400 at the CGHC motif of PDIA1's active site,

abolishing its intracellular function [140]. At the same time, this binding may block a predominant binding site of cisplatin [147].

PACMA31 shows comparable cytotoxicity in A2780/A2780cis cells as in the OVCAR-3 cell line for which an EC_{50} of 0.32 µM was reported [140]. Interestingly, A2780cis cells did not show any resistance to PACMA31 with a resistance factor of only 1.2. The results suggest that PACMA31 overcomes cisplatin resistance in A2780cis cells by its ability to inhibit PDIA1. The stronger effect of a pharmacological inhibition may be a result of the irreversible inhibition of PDIA1 by PACMA31, which blocks the function of the protein to a greater extent than a siRNA knockdown. As the sensitizing effect by PACMA31 was much stronger than that of a PDIA1 knockdown, one may speculate that a knockdown to just below 50% of the basal level may be insufficient to remarkably limit the protein function. Results from DNA platination studies suggest that the synergistic effect of cisplatin and PACMA31 is not mediated by an increased amount of platinum bound to DNA. The effect is potentially induced by the impaired ability of the cell to manage the ER stress imposed by cisplatin. Inactive PDIA1 may be further amplifying the effect of PACMA31. The intact protein may prevent the cell from initiating compensational up-regulation of other chaperone molecules such as other protein disulfide isomerases. This may also explain the difference between the smaller effects found after the siRNA knockdown compared to the pharmacological inhibition. Altogether, the results suggest that beside irreversible PDIA1 inhibition there may be additional or alternative underlying mechanisms, e.g. an elevation of the ER stress level. The assumption of an alternative mechanism is also supported by the fact that PACMA31 is per se highly cytotoxic on these cells.

Nevertheless, this is the first study that manifests a synergistic interaction of PACMA31 and cisplatin in their ability to inhibit the growth of cancer cells. As postulated by Chou, it is of paramount importance for drug combinations in cancer therapy to exhibit synergy especially at high EC concentrations (higher than EC_{90}) [192], in the best case eradicating all cancer cells. Our results show a synergistic effect of PACMA31 and cisplatin for concentrations above the respective EC_{75} in resistant cells. This indicates that a combined treatment of cisplatin and PACMA31 may improve the therapy outcome in resistant ovarian cancer.

In the meantime various other small molecule, irreversible PDIA1 inhibitors have been reported such as 16F16, juniferdin and analogues of P1 [193–195]. First described in 2014, members of the T8 class appear to be interesting candidate molecules for further development [196]. T8 and its derivatives are the first reversible PDIA1 inhibitors and show a high specificity for PDIA1. They have been shown to sensitize tumor cells to chemotherapeutic agents, such as etoposide or doxorubicin [196]. Kaplan et al. recently reported another reversible PDIA1 inhibitor, LOC14, which shows nanomolar potency [197]. This inihibitor binds adjacent to the active site cysteines of PDIA1, thus oxidizing PDIA1. Because of the high similarity of the binding site between PDIA1 and PDIA3 the authors suggest that LOC14 may simultaneously react with PDIA3 [197]. For 16F16, it has also been shown, that it binds both isoforms PDIA1 and PDIA3 investigated here [193]. This may also hold true for PACMA31. Further studies to identify the PACMA31 binding site in PDIA3 and cisplatin binding sites in PDIA1 and PDIA3 are required. It seems reasonable to further improve the existing inhibitors by molecular modeling approaches and lead optimization of these structures to further increase their specificity. The evaluation of these compounds as co-therapy with cisplatin and other platinum analogues in

ovarian cancer but also other entities is warranted based on these first promising results.

5.5   Contribution of PDIA3 to acquired cisplatin resistance

As mentioned in section 1.4.2, PDIA3 is the closest homologue of PDIA1 among the identified protein disulfide isomerases, showing about 50% sequence identity in the catalytical active domains a and a' [198]. Structural differences between the b and b' domains of the proteins may explain the functional differences between the two chaperones. The differing surface charges of the b and b' domains of PDIA3 support the binding of calnexin and calreticulin [198]. This important step in the folding of glycoproteins was only described for PDIA3 and not PDIA1 [199]. Additionally, the binding of calnexin increases the enzymatic activity of PDIA3 remarkably [200].

The knockdown of PDIA3 showed no effect on cisplatin cytotoxicity, implying that the PDIA3 knockdown is not able to sensitize A2780 or A2780cis cells to cisplatin treatment in accordance with the apoptosis results. Here, no additional apoptosis induction was detectable after knockdown and cisplatin treatment. The effects of cisplatin may have been covered by the huge impact of the PDIA3 knockdown itself, which increased the number of apoptotic cells. After compensating for the knockdown influence by calculating the ratio of apoptotic cells after knockdown and cisplatin treatment to knockdown alone, no effect was observed. A toxic effect of complete catalytic inhibition or shRNA inhibition of PDIA1 and PDIA3 has been shown by Hoffstrom et al. in PC12 cells [193]. One explanation may be the slightly more efficient siRNA knockdown of PDIA3 (A2780: ~40% or A2780cis: ~20%) over PDIA1 (A2780: ~45% or A2780cis: ~50%). This may have led to the extended

detrimental cellular responses (increased apoptosis initiation) after PDIA3 knockdown.

DNA platination was significantly increased after 4 h incubation with 100 µM cisplatin in A2780 cells. After 24 h incubation with 5 µM the effect was not detectable. The resistant cells showed no difference in DNA platination after PDIA3 knockdown under both experimental conditions. The results imply that the increased amount of platinum bound to DNA had no effect on the cells. As stated earlier the knockdown had a huge impact on cells which may have led to an increase in membrane permeability in A2780 cells. This would have simplified the uptake of cisplatin via passive diffusion leading to the increased DNA platination after 4 h treatment. The role of this effect diminishes over time, leading to different results for 24 h treatment. Coppari et al. described a nuclear localization of PDIA3 [201]. Furthermore, it was shown that cisplatin induces the binding of PDIA3 to DNA in the nucleus. As it was shown in our project by Sandra Kotz that CFDA-cisplatin interacts with PDIA3, which may be responsible for an increased platinum amount detected at the DNA level. This effect has been described for mitomycin C, which may be shuttled to DNA by PDIA3 [202].

Zhao et al. described the reduction of apoptotic signaling after pharmacological inhibition of PDIA1 and PDIA3 with securinine, thiomuscimol, or bacitracin [203]. These results contradict the results presented here. However, it has to be noted that bacitracin is by far not as specific in inhibiting PDIA1 and PDIA3 as PACMA31 is [204]. One study showed that bacitracin analogues vary in their IC_{50} for PDI inhibition from 20 µM (bacitracin F) to 1050 µM (bacitracin B) questioning the results of Zhao et al. [203,205]. In human endothelial cells the siRNA knockdown of PDIA3 appeared to regulate the tunicamycin-induced apoptosis, protecting the cell from apoptosis and

increasing the unfolded protein response by up-regulation of GRP78 expression [206]. This contradicts the hypothesis that a PDIA3 knockdown itself may be harmful for the cells per se, but as suggested earlier, these results may be cell line-dependent. To investigate the contribution of PDIA1 and PDIA3 further, it may be helpful to perform a simultaneous knockdown of both proteins. However, this approach needs special precautions as the effects of a simultaneous knockdown on cell viability have to be closely monitored.

In contrast to the results presented before, Tufo et al. found no contribution of PDIA1 and PDIA3 to cisplatin resistance in NSCLC, but found some relevance for PDIA4 and PDIA6. Cell death was induced by genetic and pharmacological inhibition of PDIA4 and PDIA6. PDIA4 inhibition acted by restoring the apoptosis pathway, while PDIA6 acted by a non-canonical cell death pathway [207]. Interestingly, PDIA6 has been found to interact with CFDA-cisplatin as well and may be an interesting target for future studies [111]. When comparing the results by Tufo et al. with the results for PDIA1 and PDIA3 presented here, proteins of the PDI family seem to act cell type-specific [207].

5.6 Clinical relevance of intracellular binding partners for cisplatin resistance

Beside the nuclear DNA, intracellular partners interacting with cisplatin have been associated with the impairment of efficacy, emergence of resistance and toxicity of cisplatin [67]. Among these non-DNA targets inside the cell are peptides, proteins, RNA, and phospholipids. At the same time other intracellular molecules interacting with cisplatin have been suggested to support cisplatin cytotoxicity, for example the mitochondrial DNA [208]. Further complexity to this ambivalent problem of the

cisplatin effect inside a cell is added by the cell type-specific action of some proteins, which may exert their functions in various ways in different tissue types. Therefore, the identified molecules that interact with cisplatin need to be thoroughly evaluated to determine their contribution to cisplatin action and to assess the clinical relevance for patients.

Several lines of evidence point to a multifactorial 'symphony' of mechanisms which underlie cisplatin resistance in ovarian cancer patients. One of the mechanisms appears to be the intracellular detoxification of cisplatin by interacting with molecules. Various interacting partners mediate resistance of tumor cells to cisplatin in patients. Some interacting partners identified and their respective relevance are reviewed here.

Diadenosine tetraphosphate (Ap$_4$A), an intracellular dinucleotide, is among the intracellular interacting partners of cisplatin, which has been shown to form a 1:1 complex with cisplatin *in vitro* [209]. As Ap$_4$A is involved in the induction of apoptosis or DNA repair, interaction of cisplatin with Ap$_4$A may facilitate or reduce cell death [210]. Recent research showed that Ap$_4$A levels significantly increased after treatment of different cell lines with non-cytotoxic concentrations of the DNA cross-linking agent mitomycin C. Further experimental evidence suggests that Ap$_4$A aids the cellular survival after DNA damage [211]. In a cell culture model, Ap$_4$A analogues showed an apoptosis-inducing effect on HEK293T cells by acting as a substrate for the proapoptotic fragile histidine triad (FHIT) protein. The proapoptotic activity of FHIT correlated with its substrate binding affinity. Analogues that showed a high affinity for the FHIT protein thus induced apoptosis and may therefore translate into clinical practice as an anticancer therapy [212].

The role of glutathione (GSH) in cisplatin resistance is controversially discussed in the scientific literature. After chronic exposure of cultured cells to increasing cisplatin concentrations to generate resistant sublines, a high intracellular glutathione concentration correlated with a resistant cellular phenotype [213,214]. The correlative nature of the studies limits the generalization of the results. Furthermore, in human tumor xenografts it was impossible to reproduce these observations [215]. Depleting cells of GSH by treatment with buthionine sulfoximine (BSO) resulted in increased sensitivity to platinum drugs [216,217]. On the contrary, others found no correlation between GSH depletion and cisplatin sensitivity in cultured cells [218]. As these results show, it is currently unclear if elevated GSH levels are responsible for resistance or if they are a mere cellular reaction induced by cisplatin. In the clinical setting, a GSH substitution rather than depletion by administration of GSH was investigated, in order to ameliorate cisplatin-induced neurotoxicity, possibly by the ability of GSH to limit the accumulation of cisplatin in the dorsal root ganglia. Results of a systematic review suggested a small neuroprotective effect of GSH, but the studies showed several limitations, such as small sample size and variability in outcome measurements [219].

Metallothioneins (MT) are avid intracellular interacting partners of cisplatin, with their reaction with cisplatin progressing about 20 times faster than with GSH [98]. Cisplatin resistance has been associated with an increased expression of MT both *in vitro* as well as *in vivo* [220,221]. The clinical perspective of an interference with or a depletion of MTs in cancer patients to increase cisplatin efficacy is poor as adverse effects of this approach have already been reported, such as hepatotoxicity and nephrotoxicity [222,223].

Heat shock protein 90 (HSP90) is the most abundant molecular chaperone in the cytosol, exerting several essential functions such as protein aggregation prevention and degradation [224]. Overexpression of HSP90 has been described for myeloma cancers [225]. Furthermore, cisplatin has been shown to bind HSP90 at the carboxyl terminal and the amino terminal domain. This interaction inhibits the aggregation prevention activity of HSP90 towards client proteins [226]. Clinical importance for HSP90 may be introduced by small-molecule inhibitors of HSP90 function, such as geldanamycin or raidicicol [227]. Derivatives of geldanamycin (e.g. 17-allylamino-17-demethoxygeldanamycin (17-AAG)) in combination therapies with paclitaxel are currently in clinical development. Second generation synthetic HSP90 inhibitors are also under investigation and clinical evaluation in combination therapies for different cancer entities [227].

The clinical relevance of the intracellular interacting partners of CFDA-cisplatin found in this study needs to be further evaluated. PDIA1 appears to be the most promising candidate. As stated earlier, several small molecule inhibitors have been recently published (5.4.2). Their efficacy in the treatment of cancer needs to be evaluated in cell models. If they prove to be effective, animal studies need to evaluate the safety of these inhibitors. As the ER stress response and the folding of nascent proteins is conducted, at least in part, by PDIA1, dose-dependent side effects of the inhibitors are conceivable. If safety can be confirmed in animals, it is essential to evaluate the efficacy and safety in clinical studies before the drugs can enter therapy regimens for cancer. Another therapeutic approach that could make use of PDIA1 is the knockdown of this protein in ovarian cancer patients. Some studies already presented promising results for cancer treatment by the siRNA-mediated down-regulation of proteins in animal models [228]. Others reported the improvement of the

therapeutic efficacy of chemotherapies by co-delivery of siRNA directed against specific proteins [170]. The next step in the development of siRNA therapeutics includes the evaluation of these treatments in humans [165]. Another important research focus is the control of drug resistance using siRNA approaches [168]. Knockdown of validated target proteins, shown to play an important role in drug resistance, has the potential to augment the efficacy of anti-cancer drugs.

6   CONCLUSION AND OUTLOOK

This project presents an approach to identify and assess the relevance of intracellular proteins interacting with CFDA-cisplatin. Besides, this study describes the methodology and results of a screening approach applied to previously identified proteins interacting with CFDA-cisplatin, in order to evaluate their contribution to acquired cisplatin resistance in an ovarian carcinoma cell line pair. In conclusion, the results suggest a contribution of PDIA1 to acquired cisplatin resistance in A2780cis cells. A pharmacologic inhibition of PDIA1 by PACMA31 synergistically increases cisplatin cytotoxicity. The results imply no direct contribution of the proteins GRP78 and PDIA3 to acquired cisplatin resistance.

In the simultaneously performed screening study, several other proteins interacting with CFDA-cisplatin have been identified. Some of those appear to be interesting targets for further evaluation, as they have already been associated with resistance to anticancer therapy in the scientific literature, some of them even in the context of acquired cisplatin resistance.

The complexity of intracellular signaling pathways may be limiting the efficacy of a single protein knockdown by compensation mechanisms. Thus, an approach to knockdown several proteins at the same time may provide new possibilities to improve the efficacy of a cytotoxic agent. Results have to be interpreted with caution as the multiple protein knockdown may affect cellular functions in an unexpected extent. For example, protein disulfide isomerases are essential for normal cell growth as they fold newly synthesized proteins. After interference with several of these crucial proteins, it is likely that a critical disturbance of their cellular function in healthy cells would lead to severe side effects.

Pharmacological inhibition, which is still the most common way for chemotherapeutic interventions, needs to be further improved. There are now several small molecule inhibitors for PDIA1 reported (PACMA31, 16F16, P1, and T8), which show efficacy in cancer cell models or even animal models. By rational drug design, these compounds may become suitable for use in humans, further increasing the efficacy and at the same time limiting the side effects. This study suggests that the therapeutic efficacy of cisplatin in ovarian cancer may be synergistically improved in combination therapy with PDIA1 inhibitors. This needs to be investigated in cell models of other cancer entities and, if the efficacy is confirmed, in animal models. Other established chemotherapeutic regimens may also be combined with PDIA1 inhibitors leading to therapeutic benefits for patients.

During this study several new questions arose:

- Why is an effect of PDIA1 interference on cisplatin cytotoxicity not associated with an increased DNA platination?

- Why does a PDIA3 knockdown lead to a markedly increased apoptosis induction level in contrast to a PDIA1 knockdown?

- Why does cisplatin treatment not add to apoptosis induction after PDIA3 knockdown but after PDIA1 knockdown?

These questions need to be addressed in future studies to deepen our understanding of the multifactorial nature of acquired cisplatin resistance and to improve our capability to control resistance in the clinical setting.

7   SUMMARY

Intracellular binding of cisplatin to non-DNA partners, such as proteins, has received increasing attention as an additional mode of action as well as a mechanism of resistance. In this project three cisplatin-interacting proteins, two members of the protein disulfide isomerase family (PDIA1 and PDIA3) and 78 kDA glucose-regulated protein (GRP78), have been identified by means of the fluorescent cisplatin analogue CFDA-cisplatin. These proteins have been investigated regarding their contribution to acquired cisplatin resistance using a sensitive and cisplatin-resistant ovarian cancer cell line pair (A2780/A2780cis).

Cisplatin cytotoxicity after knockdown of PDIA1, PDIA3, or GRP78 was assessed using the MTT assay. Whereas PDIA1 knockdown led to increased cisplatin cytotoxicity in resistant A2780cis cells, PDIA3 and GRP78 knockdown showed no influence. The cisplatin-induced apoptosis after knockdown of the respective proteins was evaluated by flow cytometry with Annexin V and propidium iodide staining. Compared to control cells, PDIA1 knockdown led to an increase of apoptotic A2780cis cells after cisplatin treatment. The knockdown of GRP78 showed no effect. The knockdown of PDIA3 readily displayed a strong apoptosis-inducing effect, even without cisplatin treatment. DNA platination, assessed by ICP-MS analysis, was not altered after PDIA1 knockdown suggesting an alternative mechanism accounting for the increased cisplatin cytotoxicity. Co-incubation with the PDIA1 inhibitor PACMA31 re-sensitized A2780cis cells to cisplatin treatment. PACMA31 co-incubation with cisplatin did not alter the DNA platination in A2780 and A2780cis cells. Combination index analysis revealed that the combination of cisplatin and PACMA31 acts synergistically.

The results warrant further evaluation of PDIA1 as promising target for chemotherapy. The pharmacological inhibition of PDIA1 by PACMA31 in combination with cisplatin may serve as a new therapeutic approach in ovarian cancer treatment.

8 REFERENCES

[1] Chabner BA, Roberts TG. Timeline: Chemotherapy and the war on cancer. Nat Rev Cancer 2005; 5: 65–72.

[2] DeVita VT, Chu E. A history of cancer chemotherapy. Cancer Res 2008; 68: 8643–8653.

[3] Alderden RA, Hall MD, Hambley TW. The discovery and development of cisplatin. J Chem Educ 2006; 83: 728–734.

[4] Muggia F. Platinum compounds 30 years after the introduction of cisplatin: implications for the treatment of ovarian cancer. Gynecol Oncol 2009; 112: 275–281.

[5] Kelland L. The resurgence of platinum-based cancer chemotherapy. Nat Rev Cancer 2007; 7: 573–584.

[6] Sawyers C. Targeted cancer therapy. Nature 2004; 432: 294–297.

[7] Iqbal N, Iqbal N. Imatinib: a breakthrough of targeted therapy in cancer. Chemother Res Pract 2014; 2014: 357027.

[8] Yap TA, Carden CP, Kaye SB. Beyond chemotherapy: targeted therapies in ovarian cancer. Nat Rev Cancer 2009; 9: 167–181.

[9] Johnson DH. Targeted therapies in combination with chemotherapy in non-small cell lung cancer. Clin Cancer Res 2006; 12: 4451–4457.

[10] Slamon DJ, Leyland-Jones B, Shak S, Fuchs H, Paton V, Bajamonde A et al. Use of chemotherapy plus a monoclonal antibody against HER2 for metastatic breast cancer that overexpresses HER2. N Engl J Med 2001; 344: 783–792.

[11] Flaherty KT. Chemotherapy and targeted therapy combinations in advanced melanoma. Clin Cancer Res 2006; 12: 2366s-2370s.

[12] Mellman I, Coukos G, Dranoff G. Cancer immunotherapy comes of age. Nature 2011; 480: 480–489.

[13] Ito F, Chang AE. Cancer immunotherapy: current status and future directions. Surg Oncol Clin N Am 2013; 22: 765–783.

[14] Couzin-Frankel J. Breakthrough of the year 2013. Cancer immunotherapy. Science 2013; 342: 1432–1433.

[15] Wargo JA, Cooper ZA, Flaherty KT. Universes collide: combining immunotherapy with targeted therapy for cancer. Cancer Discov 2014; 4: 1377–1386.

[16] Schilsky RL. Personalized medicine in oncology: the future is now. Nat Rev Drug Discov 2010; 9: 363–366.

[17] Global, regional, and national age-sex specific all-cause and cause-specific mortality for 240 causes of death, 1990-2013: a systematic analysis for the Global Burden of Disease Study 2013. Lancet 2015; 385: 117–171.

[18] Siegel RL, Miller KD, Jemal A. Cancer statistics, 2015. CA Cancer J Clin 2015; 65: 5–29.

[19] Siddik ZH. Cisplatin: mode of cytotoxic action and molecular basis of resistance. Oncogene 2003; 22: 7265–7279.

[20] Gately DP, Howell SB. Cellular accumulation of the anticancer agent cisplatin: a review. Br J Cancer 1993; 67: 1171–1176.

[21] Harrach S, Ciarimboli G. Role of transporters in the distribution of platinum-based drugs. Front Pharmacol 2015; 6: 85.

[22] Burger H, Loos WJ, Eechoute K, Verweij J, Mathijssen RH, Wiemer EA. Drug transporters of platinum-based anticancer agents and their clinical significance. Drug Resist Updat 2011; 14: 22–34.

[23] Howell SB, Safaei R, Larson CA, Sailor MJ. Copper transporters and the cellular pharmacology of the platinum-containing cancer drugs. Mol Pharmacol 2010; 77: 887–894.

[24] Klein AV, Hambley TW. Platinum drug distribution in cancer cells and tumors. Chem Rev 2009; 109: 4911–4920.

[25] Hall MD, Okabe M, Shen D, Liang X, Gottesman MM. The role of cellular accumulation in determining sensitivity to platinum-based chemotherapy. Annu Rev Pharmacol Toxicol 2008; 48: 495–535.

[26] Yu F, Megyesi J, Price PM. Cytoplasmic initiation of cisplatin cytotoxicity. Am J Physiol Renal Physiol 2008; 295: F44-52.

[27] Wang D, Lippard SJ. Cellular processing of platinum anticancer drugs. Nat Rev Drug Discov 2005; 4: 307–320.

[28] Pinto AL, Lippard SJ. Binding of the antitumor drug cis-diamminedichloroplatinum(II) (cisplatin) to DNA. Biochim Biophys Acta 1985; 780: 167–180.

[29] Warnke U, Rappel C, Meier H, Kloft C, Galanski M, Hartinger CG et al. Analysis of platinum adducts with DNA nucleotides and nucleosides by capillary electrophoresis coupled to ESI-MS: indications of guanosine 5'-monophosphate O6-N7 chelation. ChemBioChem 2004; 5: 1543–1549.

[30] Jamieson ER, Lippard SJ. Structure, recognition, and processing of cisplatin-DNA adducts. Chem Rev 1999; 99: 2467–2498.

[31] Mohn C. Relevance of glutathione and MRP-mediated efflux for platinum resistance. PhD thesis, University of Bonn, Bonn, 2013.

[32] NCCN guideline. Testicular cancer, 2015. http://www.nccn.org. Accessed 21 July 2015.

[33] Hanna N, Einhorn LH. Testicular cancer: a reflection on 50 years of discovery. J Clin Oncol 2014; 32: 3085–3092.

[34] NCCN guideline. Gastric cancer, 2015. http://www.nccn.org. Accessed 21 July 2015.

[35] NCCN guideline. Esophageal and esophagogastric junction cancers, 2015. http://www.nccn.org. Accessed 21 July 2015.

[36] Ilson DH. Esophageal cancer chemotherapy: recent advances. Gastrointest Cancer Res 2008; 2: 85–92.

[37] NCCN guideline. Small cell lung cancer, 2015. http://www.nccn.org. Accessed 1 September 2015.

[38] NCCN guideline. Non-small cell lung cancer, 2015. http://www.nccn.org. Accessed 1 September 2015.

[39] Morabito A, Carillio G, Daniele G, Piccirillo MC, Montanino A, Costanzo R et al. Treatment of small cell lung cancer. Crit Rev Oncol Hematol 2014; 91: 257–270.

[40] Kalemkerian GP. Advances in pharmacotherapy of small cell lung cancer. Expert Opin Pharmacother 2014; 15: 2385–2396.

[41] D'Addario G, Pintilie M, Leighl NB, Feld R, Cerny T, Shepherd FA. Platinum-based versus non-platinum-based chemotherapy in advanced non-small-cell lung cancer: a meta-analysis of the published literature. J Clin Oncol 2005; 23: 2926–2936.

[42] Artal Cortés Á, Calera Urquizu L, Hernando Cubero J. Adjuvant chemotherapy in non-small cell lung cancer: state-of-the-art. Transl Lung Cancer Res 2015; 4: 191–197.

[43] Bast RC, Hennessy B, Mills GB. The biology of ovarian cancer: new opportunities for translation. Nat Rev Cancer 2009; 9: 415–428.

[44] NCCN guideline. Ovarian cancer - including fallopian tube cancer and primary peritoneal cancer, 2015. http://www.nccn.org. Accessed 21 July 2015.

[45] Ozols RF, Bundy BN, Greer BE, Fowler JM, Clarke-Pearson D, Burger RA et al. Phase III trial of carboplatin and paclitaxel compared with cisplatin and paclitaxel in patients with optimally resected stage III ovarian cancer: a Gynecologic Oncology Group study. J Clin Oncol 2003; 21: 3194–3200.

[46] Davis A, Tinker AV, Friedlander M. "Platinum resistant" ovarian cancer: what is it, who to treat and how to measure benefit? Gynecol Oncol 2014; 133: 624–631.

[47] Zivanovic O, Abramian A, Kullmann M, Fuhrmann C, Coch C, Hoeller T et al. HIPEC ROC I: a phase I study of cisplatin administered as hyperthermic intraoperative intraperitoneal chemoperfusion followed by postoperative intravenous platinum-based chemotherapy in patients with platinum-sensitive recurrent epithelial ovarian cancer. Int J Cancer 2015; 136: 699–708.

[48] van Driel WJ, Lok CA, Verwaal V, Sonke GS. The role of hyperthermic intraperitoneal intraoperative chemotherapy in ovarian cancer. Curr Treat Options Oncol 2015; 16: 14.

[49] Roviello F, Roviello G, Petrioli R, Marrelli D. Hyperthermic intraperitoneal chemotherapy for the treatment of ovarian cancer: A brief overview of recent results. Crit Rev Oncol Hematol 2015; 95: 297–305.

[50] Högberg T, Glimelius B, Nygren P. A systematic overview of chemotherapy effects in ovarian cancer. Acta Oncol 2001; 40: 340–360.

[51] Markman M. Toxicities of the platinum antineoplastic agents. Expert Opin Drug Saf 2003; 2: 597–607.

[52] Olver IN. Aprepitant in antiemetic combinations to prevent chemotherapy-induced nausea and vomiting. Int J Clin Pract 2004; 58: 201–206.

[53] Langer T, Am Zehnhoff-Dinnesen A, Radtke S, Meitert J, Zolk O. Understanding platinum-induced ototoxicity. Trends Pharmacol Sci 2013; 34: 458–469.

[54] Brock PR, Knight KR, Freyer DR, Campbell KC, Steyger PS, Blakley BW et al. Platinum-induced ototoxicity in children: a consensus review on mechanisms, predisposition, and protection, including a new International Society of Pediatric Oncology Boston ototoxicity scale. J Clin Oncol 2012; 30: 2408–2417.

[55] van As JW, van den Berg, H, van Dalen EC. Medical interventions for the prevention of platinum-induced hearing loss in children with cancer. Cochrane Database Syst Rev 2014; 7: CD009219.

[56] Karasawa T, Steyger PS. An integrated view of cisplatin-induced nephrotoxicity and ototoxicity. Toxicol Lett 2015; 237: 219–227.

[57] Vermorken JB. The integration of paclitaxel and new platinum compounds in the treatment of advanced ovarian cancer. Int J Gynecol Cancer 2001; 11 Suppl 1: 21–30.

[58] Du Bois A, Neijt JP, Thigpen JT. First line chemotherapy with carboplatin plus paclitaxel in advanced ovarian cancer - a new standard of care? Ann Oncol 1999; 10 Suppl 1: 35–41.

[59] Avan A, Postma TJ, Ceresa C, Avan A, Cavaletti G, Giovannetti E et al. Platinum-induced neurotoxicity and preventive strategies: past, present, and future. Oncologist 2015; 20: 411–432.

[60] Amptoulach S, Tsavaris N. Neurotoxicity caused by the treatment with platinum analogues. Chemother Res Pract 2011; 2011: 843019.

[61] Miller RP, Tadagavadi RK, Ramesh G, Reeves WB. Mechanisms of cisplatin nephrotoxicity. Toxins (Basel) 2010; 2: 2490–2518.

[62] Ciarimboli G, Deuster D, Knief A, Sperling M, Holtkamp M, Edemir B et al. Organic cation transporter 2 mediates cisplatin-induced oto- and nephrotoxicity and is a target for protective interventions. Am J Pathol 2010; 176: 1169–1180.

[63] Ciarimboli G, Ludwig T, Lang D, Pavenstädt H, Koepsell H, Piechota H et al. Cisplatin nephrotoxicity is critically mediated via the human organic cation transporter 2. Am J Pathol 2005; 167: 1477–1484.

[64] Motohashi H, Sakurai Y, Saito H, Masuda S, Urakami Y, Goto M et al. Gene expression levels and immunolocalization of organic ion transporters in the human kidney. J Am Soc Nephrol 2002; 13: 866–874.

[65] Sprowl JA, van Doorn L, Hu S, van Gerven L, de_Bruijn P, Li L et al. Conjunctive therapy of cisplatin with the OCT2 inhibitor cimetidine: influence on antitumor efficacy and systemic clearance. Clin Pharmacol Ther 2013; 94: 585–592.

[66] Galluzzi L, Senovilla L, Vitale I, Michels J, Martins I, Kepp O et al. Molecular mechanisms of cisplatin resistance. Oncogene 2012; 31: 1869–1883.

[67] Mezencev R. Interactions of cisplatin with non-DNA targets and their influence on anticancer activity and drug toxicity: the complex world of the platinum complex. Curr Cancer Drug Targets 2015; 14: 794–816.

[68] Safaei R. Role of copper transporters in the uptake and efflux of platinum containing drugs. Cancer Lett 2006; 234: 34–39.

[69] Katano K, Kondo A, Safaei R, Holzer A, Samimi G, Mishima M et al. Acquisition of resistance to cisplatin is accompanied by changes in the cellular pharmacology of copper. Cancer Res 2002; 62: 6559–6565.

[70] Holzer AK, Manorek GH, Howell SB. Contribution of the major copper influx transporter CTR1 to the cellular accumulation of cisplatin, carboplatin, and oxaliplatin. Mol Pharmacol 2006; 70: 1390–1394.

[71] Safaei R, Holzer AK, Katano K, Samimi G, Howell SB. The role of copper transporters in the development of resistance to Pt drugs. J Inorg Biochem 2004; 98: 1607–1613.

[72] Chen Z, Tiwari AK. Multidrug resistance proteins (MRPs/ABCCs) in cancer chemotherapy and genetic diseases. FEBS J 2011; 278: 3226–3245.

[73] Cnubben NH, Wortelboer HM, van Zanden JJ, Rietjens IM, van Bladeren PJ. Metabolism of ATP-binding cassette drug transporter inhibitors: complicating factor for multidrug resistance. Expert Opin Drug Metab Toxicol 2005; 1: 219–232.

[74]   Ma J, Chen B, Xin X. Inhibition of multi-drug resistance of ovarian carcinoma by small interfering RNA targeting to MRP2 gene. Arch Gynecol Obstet 2009; 279: 149–157.

[75]   Surowiak P, Materna V, Kaplenko I, Spaczynski M, Dolinska-Krajewska B, Gebarowska E et al. ABCC2 (MRP2, cMOAT) can be localized in the nuclear membrane of ovarian carcinomas and correlates with resistance to cisplatin and clinical outcome. Clin Cancer Res 2006; 12: 7149–7158.

[76]   Shuck SC, Short EA, Turchi JJ. Eukaryotic nucleotide excision repair: from understanding mechanisms to influencing biology. Cell Res 2008; 18: 64–72.

[77]   Gillet, Ludovic C J, Schärer OD. Molecular mechanisms of mammalian global genome nucleotide excision repair. Chem Rev 2006; 106: 253–276.

[78]   Mamenta EL, Poma EE, Kaufmann WK, Delmastro DA, Grady HL, Chaney SG. Enhanced replicative bypass of platinum-DNA adducts in cisplatin-resistant human ovarian carcinoma cell lines. Cancer Res 1994; 54: 3500–3505.

[79]   Shachar S, Ziv O, Avkin S, Adar S, Wittschieben J, Reissner T et al. Two-polymerase mechanisms dictate error-free and error-prone translesion DNA synthesis in mammals. EMBO J 2009; 28: 383–393.

[80]   Kunkel TA, Erie DA. DNA mismatch repair. Annu Rev Biochem 2005; 74: 681–710.

[81]   Vaisman A, Varchenko M, Umar A, Kunkel TA, Risinger JI, Barrett JC et al. The role of hMLH1, hMSH3, and hMSH6 defects in cisplatin and oxaliplatin resistance: correlation with replicative bypass of platinum-DNA adducts. Cancer Res 1998; 58: 3579–3585.

[82]   Aebi S, Kurdi-Haidar B, Gordon R, Cenni B, Zheng H, Fink D et al. Loss of DNA mismatch repair in acquired resistance to cisplatin. Cancer Res 1996; 56: 3087–3090.

[83]   Massey A, Offman J, Macpherson P, Karran P. DNA mismatch repair and acquired cisplatin resistance in E. coli and human ovarian carcinoma cells. DNA Repair (Amst) 2003; 2: 73–89.

[84]   Brown R, Hirst GL, Gallagher WM, McIlwrath AJ, Margison GP, van der Zee, AG et al. hMLH1 expression and cellular responses of ovarian tumour cells to treatment with cytotoxic anticancer agents. Oncogene 1997; 15: 45–52.

[85]   Vousden KH, Lane DP. p53 in health and disease. Nat Rev Mol Cell Biol 2007; 8: 275–283.

[86]   Branch P, Masson M, Aquilina G, Bignami M, Karran P. Spontaneous development of drug resistance: mismatch repair and p53 defects in resistance to cisplatin in human tumor cells. Oncogene 2000; 19: 3138–3145.

[87]   Kirsch DG, Kastan MB. Tumor-suppressor p53: implications for tumor development and prognosis. J Clin Oncol 1998; 16: 3158–3168.

[88] Brozovic A, Osmak M. Activation of mitogen-activated protein kinases by cisplatin and their role in cisplatin-resistance. Cancer Lett 2007; 251: 1–16.

[89] Kroemer G, Mariño G, Levine B. Autophagy and the integrated stress response. Mol Cell 2010; 40: 280–293.

[90] Castagna A, Antonioli P, Astner H, Hamdan M, Righetti SC, Perego P et al. A proteomic approach to cisplatin resistance in the cervix squamous cell carcinoma cell line A431. Proteomics 2004; 4: 3246–3267.

[91] Zhang J, Liu Y. Use of comparative proteomics to identify potential resistance mechanisms in cancer treatment. Cancer Treat Rev 2007; 33: 741–756.

[92] Yan X, Pan L, Yuan Y, Lang J, Mao N. Identification of platinum-resistance associated proteins through proteomic analysis of human ovarian cancer cells and their platinum-resistant sublines. J Proteome Res 2007; 6: 772–780.

[93] Lincet H, Guével B, Pineau C, Allouche S, Lemoisson E, Poulain L et al. Comparative 2D-DIGE proteomic analysis of ovarian carcinoma cells: toward a reorientation of biosynthesis pathways associated with acquired platinum resistance. J Proteomics 2012; 75: 1157–1169.

[94] Galluzzi L, Vitale I, Michels J, Brenner C, Szabadkai G, Harel-Bellan A et al. Systems biology of cisplatin resistance: past, present and future. Cell Death Dis 2014; 5: e1257.

[95] Ishikawa T, Ali-Osman F. Glutathione-associated cis-diamminedichloroplatinum(II) metabolism and ATP-dependent efflux from leukemia cells. Molecular characterization of glutathione-platinum complex and its biological significance. J Biol Chem 1993; 268: 20116–20125.

[96] Hagrman D, Goodisman J, Souid A. Kinetic study on the reactions of platinum drugs with glutathione. J Pharmacol Exp Ther 2004; 308: 658–666.

[97] Kasahara K, Fujiwara Y, Nishio K, Ohmori T, Sugimoto Y, Komiya K et al. Metallothionein content correlates with the sensitivity of human small cell lung cancer cell lines to cisplatin. Cancer Res 1991; 51: 3237–3242.

[98] Hagrman D, Goodisman J, Dabrowiak JC, Souid A. Kinetic study on the reaction of cisplatin with metallothionein. Drug Metab Dispos 2003; 31: 916–923.

[99] Vasák M. Advances in metallothionein structure and functions. J Trace Elem Med Biol 2005; 19: 13–17.

[100] Zimmermann T, Burda JV. Cisplatin interaction with amino acids cysteine and methionine from gas phase to solutions with constant pH. Interdiscip Sci 2010; 2: 98–114.

[101] Goto S, Yoshida K, Morikawa T, Urata Y, Suzuki K, Kondo T. Augmentation of transport for cisplatin-glutathione adduct in cisplatin-resistant cancer cells. Cancer Res 1995; 55: 4297–4301.

[102] Kasherman Y, Sturup S, Gibson D. Is glutathione the major cellular target of cisplatin? A study of the interactions of cisplatin with cancer cell extracts. J Med Chem 2009; 52: 4319–4328.

[103] Pinato O, Musetti C, Sissi C. Pt-based drugs: the spotlight will be on proteins. Metallomics 2014; 6: 380–395.

[104] Karasawa T, Sibrian-Vazquez M, Strongin RM, Steyger PS. Identification of cisplatin-binding proteins using agarose conjugates of platinum compounds. PLoS ONE 2013; 8: e66220.

[105] Arnesano F, Banci L, Bertini I, Felli IC, Losacco M, Natile G. Probing the interaction of cisplatin with the human copper chaperone Atox1 by solution and in-cell NMR spectroscopy. J Am Chem Soc 2011; 133: 18361–18369.

[106] Chavez JD, Hoopmann MR, Weisbrod CR, Takara K, Bruce JE. Quantitative proteomic and interaction network analysis of cisplatin resistance in HeLa cells. PLoS ONE 2011; 6: e19892.

[107] Reedijk J. Why does Cisplatin reach Guanine-n7 with competing s-donor ligands available in the cell? Chem Rev 1999; 99: 2499–2510.

[108] Wexselblatt E, Yavin E, Gibson D. Cellular interactions of platinum drugs. Inorg Chim Acta 2012; 393: 75–83.

[109] Molenaar C, Teuben JM, Heetebrij RJ, Tanke HJ, Reedijk J. New insights in the cellular processing of platinum antitumor compounds, using fluorophore-labeled platinum complexes and digital fluorescence microscopy. J Biol Inorg Chem 2000; 5: 655–665.

[110] Kalayda GV, Wagner CH, Buss I, Reedijk J, Jaehde U. Altered localisation of the copper efflux transporters ATP7A and ATP7B associated with cisplatin resistance in human ovarian carcinoma cells. BMC Cancer 2008; 8: 175.

[111] Kotz S, Kullmann M, Crone B, Kalayda GV, Jaehde U, Metzger S. Combination of two-dimensional gel electrophoresis and a fluorescent carboxyfluorescein diacetate labeled cisplatin analogue allows the identification of intracellular cisplatin-protein adducts. Electrophoresis 2015: Epub ahead of print.

[112] Hendershot LM. The ER function BiP is a master regulator of ER function. Mt Sinai J Med 2004; 71: 289–297.

[113] Shin BK, Wang H, Yim AM, Le Naour F, Brichory F, Jang JH et al. Global profiling of the cell surface proteome of cancer cells uncovers an abundance of proteins with chaperone function. J Biol Chem 2003; 278: 7607–7616.

[114] Albanèse V, Frydman J. Where chaperones and nascent polypeptides meet. Nat Struct Biol 2002; 9: 716–718.

[115] Walter P, Ron D. The unfolded protein response: from stress pathway to homeostatic regulation. Science 2011; 334: 1081–1086.

[116] Tabas I, Ron D. Integrating the mechanisms of apoptosis induced by endoplasmic reticulum stress. Nat Cell Biol 2011; 13: 184–190.

[117] Lee AS. The ER chaperone and signaling regulator GRP78/BiP as a monitor of endoplasmic reticulum stress. Methods 2005; 35: 373–381.

[118] Roller C, Maddalo D. The molecular chaperone GRP78/BiP in the development of chemoresistance: mechanism and possible treatment. Front Pharmacol 2013; 4: 10.

[119] Harding HP, Zhang Y, Bertolotti A, Zeng H, Ron D. Perk is essential for translational regulation and cell survival during the unfolded protein response. Mol Cell 2000; 5: 897–904.

[120] Adams JM, Cory S. The Bcl-2 protein family: arbiters of cell survival. Science 1998; 281: 1322–1326.

[121] Hetz C. The unfolded protein response: controlling cell fate decisions under ER stress and beyond. Nat Rev Mol Cell Biol 2012; 13: 89–102.

[122] Schindler AJ, Schekman R. In vitro reconstitution of ER-stress induced ATF6 transport in COPII vesicles. Proc Natl Acad Sci USA 2009; 106: 17775–17780.

[123] Lin Y, Wang Z, Liu L, Chen L. Akt is the downstream target of GRP78 in mediating cisplatin resistance in ER stress-tolerant human lung cancer cells. Lung Cancer 2011; 71: 291–297.

[124] Ni M, Zhang Y, Lee AS. Beyond the endoplasmic reticulum: atypical GRP78 in cell viability, signalling and therapeutic targeting. Biochem J 2011; 434: 181–188.

[125] Franke TF, Kaplan DR, Cantley LC. PI3K: downstream AKTion blocks apoptosis. Cell 1997; 88: 435–437.

[126] Jessop CE, Watkins RH, Simmons JJ, Tasab M, Bulleid NJ. Protein disulphide isomerase family members show distinct substrate specificity: P5 is targeted to BiP client proteins. J Cell Sci 2009; 122: 4287–4295.

[127] Turano C, Coppari S, Altieri F, Ferraro A. Proteins of the PDI family: unpredicted non-ER locations and functions. J Cell Physiol 2002; 193: 154–163.

[128] Ferrari DM, Söling HD. The protein disulphide-isomerase family: unravelling a string of folds. Biochem J 1999; 339 (Pt 1): 1–10.

[129] Higa A, Chevet E. Redox signaling loops in the unfolded protein response. Cell Signal 2012; 24: 1548–1555.

[130] Coe H, Michalak M. ERp57, a multifunctional endoplasmic reticulum resident oxidoreductase. Int J Biochem Cell Biol 2010; 42: 796–799.

[131] Zimmermann T, Zeizinger M, Burda JV. Cisplatin interaction with cysteine and methionine, a theoretical DFT study. J Inorg Biochem 2005; 99: 2184–2196.

[132] Ali Khan H, Mutus B. Protein disulfide isomerase a multifunctional protein with multiple physiological roles. Front Chem 2014; 2: 70.

[133] Xu S, Sankar S, Neamati N. Protein disulfide isomerase: a promising target for cancer therapy. Drug Discov Today 2014; 19: 222–240.

[134] Shai R, Shi T, Kremen TJ, Horvath S, Liau LM, Cloughesy TF et al. Gene expression profiling identifies molecular subtypes of gliomas. Oncogene 2003; 22: 4918–4923.

[135] Welsh JB, Sapinoso LM, Su AI, Kern SG, Wang-Rodriguez J, Moskaluk CA et al. Analysis of gene expression identifies candidate markers and pharmacological targets in prostate cancer. Cancer Res 2001; 61: 5974–5978.

[136] Welsh JB, Zarrinkar PP, Sapinoso LM, Kern SG, Behling CA, Monk BJ et al. Analysis of gene expression profiles in normal and neoplastic ovarian tissue samples identifies candidate molecular markers of epithelial ovarian cancer. Proc Natl Acad Sci USA 2001; 98: 1176–1181.

[137] Bonome T, Levine DA, Shih J, Randonovich M, Pise-Masison CA, Bogomolniy F et al. A gene signature predicting for survival in suboptimally debulked patients with ovarian cancer. Cancer Res 2008; 68: 5478–5486.

[138] Chahed K, Kabbage M, Hamrita B, Guillier CL, Trimeche M, Remadi S et al. Detection of protein alterations in male breast cancer using two dimensional gel electrophoresis and mass spectrometry: the involvement of several pathways in tumorigenesis. Clin Chim Acta 2008; 388: 106–114.

[139] Chahed K, Kabbage M, Ehret-Sabatier L, Lemaitre-Guillier C, Remadi S, Hoebeke J et al. Expression of fibrinogen E-fragment and fibrin E-fragment is inhibited in the human infiltrating ductal carcinoma of the breast: the two-dimensional electrophoresis and MALDI-TOF-mass spectrometry analyses. Int J Oncol 2005; 27: 1425–1431.

[140] Xu S, Butkevich AN, Yamada R, Zhou Y, Debnath B, Duncan R et al. Discovery of an orally active small-molecule irreversible inhibitor of protein disulfide isomerase for ovarian cancer treatment. Proc Natl Acad Sci 2012; 109: 16348–16353.

[141] Turano C, Gaucci E, Grillo C, Chichiarelli S. ERp57/GRP58: a protein with multiple functions. Cell Mol Biol Lett 2011; 16: 539–563.

[142] Panaretakis T, Joza N, Modjtahedi N, Tesniere A, Vitale I, Durchschlag M et al. The co-translocation of ERp57 and calreticulin determines the immunogenicity of cell death. Cell Death Differ 2008; 15: 1499–1509.

[143] Russell SJ, Ruddock LW, Salo, Kirsi E H, Oliver JD, Roebuck QP, Llewellyn DH et al. The primary substrate binding site in the b' domain of ERp57 is adapted for endoplasmic reticulum lectin association. J Biol Chem 2004; 279: 18861–18869.

[144] Cicchillitti L, Di Michele M, Urbani A, Ferlini C, Donat MB, Scambia G et al. Comparative proteomic analysis of paclitaxel sensitive A2780 epithelial ovarian cancer cell line and its resistant counterpart A2780TC1 by 2D-DIGE: the role of ERp57. J Proteome Res 2009; 8: 1902–1912.

[145] Chay D, Cho H, Lim BJ, Kang ES, Oh YJ, Choi SM et al. ER-60 (PDIA3) is highly expressed in a newly established serous ovarian cancer cell line, YDOV-139. Int J Oncol 2010; 37: 399–412.

[146] Liao C, Wu T, Huang Y, Chang T, Wang C, Tsai M et al. Glucose-regulated protein 58 modulates cell invasiveness and serves as a prognostic marker for cervical cancer. Cancer Sci 2011; 102: 2255–2263.

[147] Boal AK, Rosenzweig AC. Crystal structures of cisplatin bound to a human copper chaperone. J Am Chem Soc 2009; 131: 14196–14197.

[148] Safaei R, Adams PL, Maktabi MH, Mathews RA, Howell SB. The CXXC motifs in the metal binding domains are required for ATP7B to mediate resistance to cisplatin. J Inorg Biochem 2012; 110: 8–17.

[149] Mueller H, Kassack MU, Wiese M. Comparison of the usefulness of the MTT, ATP, and calcein assays to predict the potency of cytotoxic agents in various human cancer cell lines. J Biomol Screen 2004; 9: 506–515.

[150] Alley MC, Scudiero DA, Monks A, Hursey ML, Czerwinski MJ, Fine DL et al. Feasibility of drug screening with panels of human tumor cell lines using a microculture tetrazolium assay. Cancer Res 1988; 48: 589–601.

[151] Barr MP, Gray SG, Hoffmann AC, Hilger RA, Thomale J, O'Flaherty JD et al. Generation and characterisation of cisplatin-resistant non-small cell lung cancer cell lines displaying a stem-like signature. PLoS ONE 2013; 8: e54193.

[152] Chou T. Theoretical basis, experimental design, and computerized simulation of synergism and antagonism in drug combination studies. Pharmacol Rev 2006; 58: 621–681.

[153] Chou TC, Talalay P. Quantitative analysis of dose-effect relationships: the combined effects of multiple drugs or enzyme inhibitors. Adv Enzyme Regul 1984; 22: 27–55.

[154] Motulsky H, Christopoulos A. Fitting models to biological data using linear and non-linear regression, Oxford University Press, New York, 2004.

[155] Zabel R, Kullmann M, Kalayda GV, Jaehde U, Weber G. Optimized sample preparation strategy for the analysis of low molecular mass adducts of a fluorescent cisplatin analogue in cancer cell lines by CE-dual-LIF. Electrophoresis 2015; 36: 509–517.

[156] Ackermann D, Wang W, Streipert B, Geib B, Grün L, König S. Comparative fluorescence two-dimensional gel electrophoresis using a gel strip sandwich

assembly for the simultaneous on-gel generation of a reference protein spot grid. Electrophoresis 2012; 33: 1406–1410.

[157] Cepeda V, Fuertes MA, Castilla J, Alonso C, Quevedo C, Pérez JM. Biochemical mechanisms of cisplatin cytotoxicity. Anticancer Agents Med Chem 2007; 7: 3–18.

[158] Zhuang F, Liu Y. Usefulness of the luciferase reporter system to test the efficacy of siRNA. Methods Mol Biol 2006; 342: 181–187.

[159] McManus MT, Sharp PA. Gene silencing in mammals by small interfering RNAs. Nat Rev Genet 2002; 3: 737–747.

[160] Peek AS, Behlke MA. Design of active small interfering RNAs. Curr Opin Mol Ther 2007; 9: 110–118.

[161] Schütze N. siRNA technology. Mol Cell Endocrinol 2004; 213: 115–119.

[162] Bonetta L. RNAi: Silencing never sounded better. Nat Methods 2004; 1: 79–85.

[163] Fire A, Xu S, Montgomery MK, Kostas SA, Driver SE, Mello CC. Potent and specific genetic interference by double-stranded RNA in Caenorhabditis elegans. Nature 1998; 391: 806–811.

[164] Davis ME, Zuckerman JE, Choi, Chung Hang J, Seligson D, Tolcher A, Alabi CA et al. Evidence of RNAi in humans from systemically administered siRNA via targeted nanoparticles. Nature 2010; 464: 1067–1070.

[165] Zhou Y, Zhang C, Liang W. Development of RNAi technology for targeted therapy - a track of siRNA based agents to RNAi therapeutics. J Control Release 2014; 193: 270–281.

[166] Kanasty R, Dorkin JR, Vegas A, Anderson D. Delivery materials for siRNA therapeutics. Nat Mater 2013; 12: 967–977.

[167] Goldberg MS. siRNA delivery for the treatment of ovarian cancer. Methods 2013; 63: 95–100.

[168] Fatemian T, Othman I, Chowdhury EH. Strategies and validation for siRNA-based therapeutics for the reversal of multi-drug resistance in cancer. Drug Discov Today 2014; 19: 71–78.

[169] Ren Y, Zhang Y. An update on RNA interference-mediated gene silencing in cancer therapy. Expert Opin Biol Ther 2014; 14: 1581–1592.

[170] Xu X, Xie K, Zhang X, Pridgen EM, Park GY, Cui DS et al. Enhancing tumor cell response to chemotherapy through nanoparticle-mediated codelivery of siRNA and cisplatin prodrug. Proc Natl Acad Sci USA 2013; 110: 18638–18643.

[171] Jiang CC, Mao ZG, Avery-Kiejda KA, Wade M, Hersey P, Zhang XD. Glucose-regulated protein 78 antagonizes cisplatin and adriamycin in human melanoma cells. Carcinogenesis 2009; 30: 197–204.

[172] Gray MJ, Mhawech-Fauceglia P, Yoo E, Yang W, Wu E, Lee AS et al. AKT inhibition mitigates GRP78 (glucose-regulated protein) expression and contribution to chemoresistance in endometrial cancers. Int J Cancer 2013; 133: 21–30.

[173] Lee E, Nichols P, Spicer D, Groshen S, Yu MC, Lee AS. GRP78 as a novel predictor of responsiveness to chemotherapy in breast cancer. Cancer Res 2006; 66: 7849–7853.

[174] Daneshmand S, Quek ML, Lin E, Lee C, Cote RJ, Hawes D et al. Glucose-regulated protein GRP78 is up-regulated in prostate cancer and correlates with recurrence and survival. Hum Pathol 2007; 38: 1547–1552.

[175] Lee AS. GRP78 induction in cancer: therapeutic and prognostic implications. Cancer Res 2007; 67: 3496–3499.

[176] Li J, Lee AS. Stress induction of GRP78/BiP and its role in cancer. Curr Mol Med 2006; 6: 45–54.

[177] Virrey JJ, Dong D, Stiles C, Patterson JB, Pen L, Ni M et al. Stress chaperone GRP78/BiP confers chemoresistance to tumor-associated endothelial cells. Mol Cancer Res 2008; 6: 1268–1275.

[178] Mhaidat NM, Alali FQ, Matalqah SM, Matalka II, Jaradat SA, Al-Sawalha NA et al. Inhibition of MEK sensitizes paclitaxel-induced apoptosis of human colorectal cancer cells by downregulation of GRP78. Anticancer Drugs 2009; 20: 601–606.

[179] Calì G, Insabato L, Conza D, Bifulco G, Parrillo L, Mirra P et al. GRP78 mediates cell growth and invasiveness in endometrial cancer. J Cell Physiol 2014; 229: 1417–1426.

[180] Ermakova SP, Kang BS, Choi BY, Choi HS, Schuster TF, Ma W et al. (-)-Epigallocatechin gallate overcomes resistance to etoposide-induced cell death by targeting the molecular chaperone glucose-regulated protein 78. Cancer Res 2006; 66: 9260–9269.

[181] Nakagawa H, Yamamoto D, Kiyozuka Y, Tsuta K, Uemura Y, Hioki K et al. Effects of genistein and synergistic action in combination with eicosapentaenoic acid on the growth of breast cancer cell lines. J Cancer Res Clin Oncol 2000; 126: 448–454.

[182] Martin S, Lamb HK, Brady C, Lefkove B, Bonner MY, Thompson P et al. Inducing apoptosis of cancer cells using small-molecule plant compounds that bind to GRP78. Br J Cancer 2013; 109: 433–443.

[183] Ahmad M, Hahn IF, Chatterjee S. GRP78 up-regulation leads to hypersensitization to cisplatin in A549 lung cancer cells. Anticancer Res 2014; 34: 3493–3500.

[184] Belfi CA, Chatterjee S, Gosky DM, Berger SJ, Berger NA. Increased sensitivity of human colon cancer cells to DNA cross-linking agents after GRP78 up-regulation. Biochem Biophys Res Commun 1999; 257: 361–368.

[185] Hägerlöf M, Hedman H, Elmroth SK. Platination of the siRNA sense-strand modulates both efficacy and selectivity in vitro. Biochem Biophys Res Commun 2007; 361: 14–19.

[186] Hedman HK, Kirpekar F, Elmroth SK. Platinum interference with siRNA non-seed regions fine-tunes silencing capacity. J Am Chem Soc 2011; 133: 11977–11984.

[187] Paranjpe S, Bowen WC, Tseng GC, Luo J, Orr A, Michalopoulos GK. RNA interference against hepatic epidermal growth factor receptor has suppressive effects on liver regeneration in rats. Am J Pathol 2010; 176: 2669–2681.

[188] Reiling JH, Olive AJ, Sanyal S, Carette JE, Brummelkamp TR, Ploegh HL et al. A CREB3-ARF4 signalling pathway mediates the response to Golgi stress and susceptibility to pathogens. Nat Cell Biol 2013; 15: 1473–1485.

[189] Hashida T, Kotake Y, Ohta S. Protein disulfide isomerase knockdown-induced cell death is cell-line-dependent and involves apoptosis in MCF-7 cells. J Toxicol Sci 2011; 36: 1–7.

[190] Sun S, Lee D, Ho AS, Pu JK, Zhang XQ, Lee NP et al. Inhibition of prolyl 4-hydroxylase, beta polypeptide (P4HB) attenuates temozolomide resistance in malignant glioma via the endoplasmic reticulum stress response (ERSR) pathways. Neuro-oncology 2013; 15: 562–577.

[191] Mandic A, Hansson J, Linder S, Shoshan MC. Cisplatin induces endoplasmic reticulum stress and nucleus-independent apoptotic signaling. J Biol Chem 2003; 278: 9100–9106.

[192] Chou T. Drug combination studies and their synergy quantification using the Chou-Talalay method. Cancer Res 2010; 70: 440–446.

[193] Hoffstrom BG, Kaplan A, Letso R, Schmid RS, Turmel GJ, Lo DC et al. Inhibitors of protein disulfide isomerase suppress apoptosis induced by misfolded proteins. Nat Chem Biol 2010; 6: 900–906.

[194] Khan MM, Simizu S, Lai NS, Kawatani M, Shimizu T, Osada H. Discovery of a small molecule PDI inhibitor that inhibits reduction of HIV-1 envelope glycoprotein gp120. ACS Chem Biol 2011; 6: 245–251.

[195] Ge J, Zhang C, Li L, Chong LM, Wu X, Hao P et al. Small molecule probe suitable for in situ profiling and inhibition of protein disulfide isomerase. ACS Chem Biol 2013; 8: 2577–2585.

[196] Eirich J, Braig S, Schyschka L, Servatius P, Hoffmann J, Hecht S et al. A small molecule inhibits protein disulfide isomerase and triggers the

chemosensitization of cancer cells. Angew Chem Int Ed Engl 2014; 53: 12960–12965.

[197] Kaplan A, Gaschler MM, Dunn DE, Colligan R, Brown LM, Palmer AG et al. Small molecule-induced oxidation of protein disulfide isomerase is neuroprotective. Proc Natl Acad Sci USA 2015; 112: E2245-52.

[198] Kozlov G, Maattanen P, Schrag JD, Pollock S, Cygler M, Nagar B et al. Crystal structure of the bb' domains of the protein disulfide isomerase ERp57. Structure 2006; 14: 1331–1339.

[199] Oliver JD, Roderick HL, Llewellyn DH, High S. ERp57 functions as a subunit of specific complexes formed with the ER lectins calreticulin and calnexin. Mol Biol Cell 1999; 10: 2573–2582.

[200] Zapun A, Darby NJ, Tessier DC, Michalak M, Bergeron JJ, Thomas DY. Enhanced catalysis of ribonuclease B folding by the interaction of calnexin or calreticulin with ERp57. J Biol Chem 1998; 273: 6009–6012.

[201] Coppari S, Altieri F, Ferraro A, Chichiarelli S, Eufemi M, Turano C. Nuclear localization and DNA interaction of protein disulfide isomerase ERp57 in mammalian cells. J Cell Biochem 2002; 85: 325–333.

[202] Su S, Adikesavan AK, Jaiswal AK. Si RNA inhibition of GRP58 associated with decrease in mitomycin C-induced DNA cross-linking and cytotoxicity. Chem Biol Interact 2006; 162: 81–87.

[203] Zhao G, Lu H, Li C. Proapoptotic activities of protein disulfide isomerase (PDI) and PDIA3 protein, a role of the Bcl-2 protein Bak. J Biol Chem 2015; 290: 8949–8963.

[204] Karala A, Ruddock LW. Bacitracin is not a specific inhibitor of protein disulfide isomerase. FEBS J 2010; 277: 2454–2462.

[205] Dickerhof N, Kleffmann T, Jack R, McCormick S. Bacitracin inhibits the reductive activity of protein disulfide isomerase by disulfide bond formation with free cysteines in the substrate-binding domain. FEBS J 2011; 278: 2034–2043.

[206] Xu D, Perez RE, Rezaiekhaligh MH, Bourdi M, Truog WE. Knockdown of ERp57 increases BiP/GRP78 induction and protects against hyperoxia and tunicamycin-induced apoptosis. Am J Physiol Lung Cell Mol Physiol 2009; 297: L44-51.

[207] Tufo G, Jones AW, Wang Z, Hamelin J, Tajeddine N, Esposti DD et al. The protein disulfide isomerases PDIA4 and PDIA6 mediate resistance to cisplatin-induced cell death in lung adenocarcinoma. Cell Death Differ 2014; 21: 685–695.

[208] Gatti L, Cassinelli G, Zaffaroni N, Lanzi C, Perego P. New mechanisms for old drugs: Insights into DNA-unrelated effects of platinum compounds and drug resistance determinants. Drug Resist Updat 2015; 20: 1–11.

[209] Segal E, Girault JP, Muzard G, Chottard G, Chottard JC, Le Pecq B. Structure determination of the adduct formed between the signal nucleotide diadenosine 5',5'''-P1,P4-tetraphosphate (Ap4A) and cis-[Pt(NH3)2Cl2]. Biopolymers 1984; 23: 1623–1635.

[210] Vartanian A, Alexandrov I, Prudowski I, McLennan A, Kisselev L. Ap4A induces apoptosis in human cultured cells. FEBS Lett 1999; 456: 175–180.

[211] Marriott AS, Copeland NA, Cunningham R, Wilkinson MC, McLennan AG, Jones NJ. Diadenosine 5', 5'''-P(1),P(4)-tetraphosphate (Ap4A) is synthesized in response to DNA damage and inhibits the initiation of DNA replication. DNA Repair (Amst) 2015; 33: 90–100.

[212] Krakowiak A, Pęcherzewska R, Kaczmarek R, Tomaszewska A, Nawrot B, Stec WJ. Evaluation of influence of Ap4A analogues on Fhit-positive HEK293T cells; cytotoxicity and ability to induce apoptosis. Bioorg Med Chem 2011; 19: 5053–5060.

[213] Chen HH, Kuo MT. Role of glutathione in the regulation of cisplatin resistance in cancer chemotherapy. Met Based Drugs 2010; 2010.

[214] Chen G, Hutter KJ, Zeller WJ. Positive correlation between cellular glutathione and acquired cisplatin resistance in human ovarian cancer cells. Cell Biol Toxicol 1995; 11: 273–281.

[215] Pratesi G, Dal Bo L, Paolicchi A, Tonarelli P, Tongiani R, Zunino F. The role of the glutathione-dependent system in tumor sensitivity to cisplatin: a study of human tumor xenografts. Ann Oncol 1995; 6: 283–289.

[216] Meijer C, Mulder NH, Timmer-Bosscha H, Sluiter WJ, Meersma GJ, de Vries, E. G. Relationship of cellular glutathione to the cytotoxicity and resistance of seven platinum compounds. Cancer Res 1992; 52: 6885–6889.

[217] Zhang K, Chew M, Yang EB, Wong KP, Mack P. Modulation of cisplatin cytotoxicity and cisplatin-induced DNA cross-links in HepG2 cells by regulation of glutathione-related mechanisms. Mol Pharmacol 2001; 59: 837–843.

[218] Andrews PA, Murphy MP, Howell SB. Differential sensitization of human ovarian carcinoma and mouse L1210 cells to cisplatin and melphalan by glutathione depletion. Mol Pharmacol 1986; 30: 643–650.

[219] Albers JW, Chaudhry V, Cavaletti G, Donehower RC. Interventions for preventing neuropathy caused by cisplatin and related compounds. Cochrane Database Syst Rev 2014; 3: CD005228.

[220] Kelley SL, Basu A, Teicher BA, Hacker MP, Hamer DH, Lazo JS. Overexpression of metallothionein confers resistance to anticancer drugs. Science 1988; 241: 1813–1815.

[221] Satoh M, Cherian MG, Imura N, Shimizu H. Modulation of resistance to anticancer drugs by inhibition of metallothionein synthesis. Cancer Res 1994; 54: 5255–5257.

[222] Liu J, Liu Y, Habeebu SS, Klaassen CD. Metallothionein (MT)-null mice are sensitive to cisplatin-induced hepatotoxicity. Toxicol Appl Pharmacol 1998; 149: 24–31.

[223] Satoh M, Shimada A, Zhang B, Tohyama C. Renal toxicity caused by cisplatinum in glutathione-depleted metallothionein-null mice. Biochem Pharmacol 2000; 60: 1729–1734.

[224] Csermely P, Schnaider T, Soti C, Prohászka Z, Nardai G. The 90-kDa molecular chaperone family: structure, function, and clinical applications. A comprehensive review. Pharmacol Ther 1998; 79: 129–168.

[225] Chatterjee M, Jain S, Stühmer T, Andrulis M, Ungethüm U, Kuban R et al. STAT3 and MAPK signaling maintain overexpression of heat shock proteins 90alpha and beta in multiple myeloma cells, which critically contribute to tumor-cell survival. Blood 2007; 109: 720–728.

[226] Ishida R, Takaoka Y, Yamamoto S, Miyazaki T, Otaka M, Watanabe S et al. Cisplatin differently affects amino terminal and carboxyl terminal domains of HSP90. FEBS Lett 2008; 582: 3879–3883.

[227] Richardson PG, Mitsiades CS, Laubach JP, Lonial S, Chanan-Khan AA, Anderson KC. Inhibition of heat shock protein 90 (HSP90) as a therapeutic strategy for the treatment of myeloma and other cancers. Br J Haematol 2011; 152: 367–379.

[228] Phalon C, Rao DD, Nemunaitis J. Potential use of RNA interference in cancer therapy. Expert Rev Mol Med 2010; 12: e26.

9   APPENDIX

Appendix A

HPLC method development

Chromatograms

Aqueous phase adjusted to pH 4.5
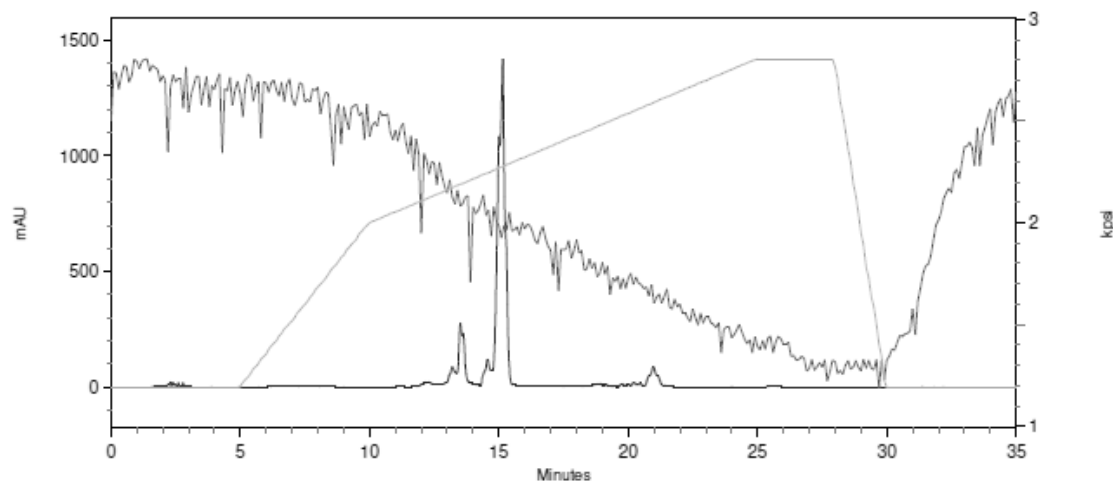
Aqueous phase adjusted to pH 5.5
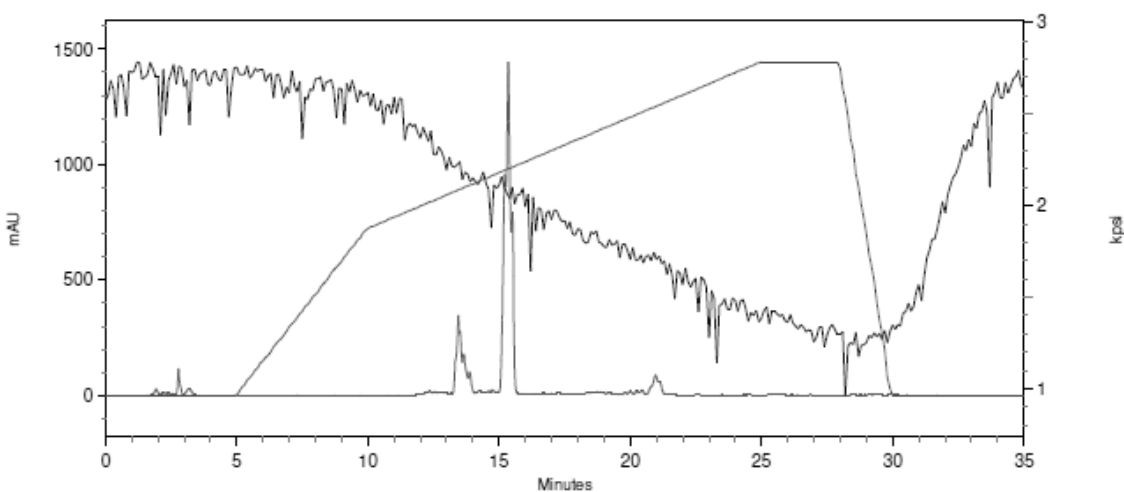
Aqueous phase adjusted to pH 6.5
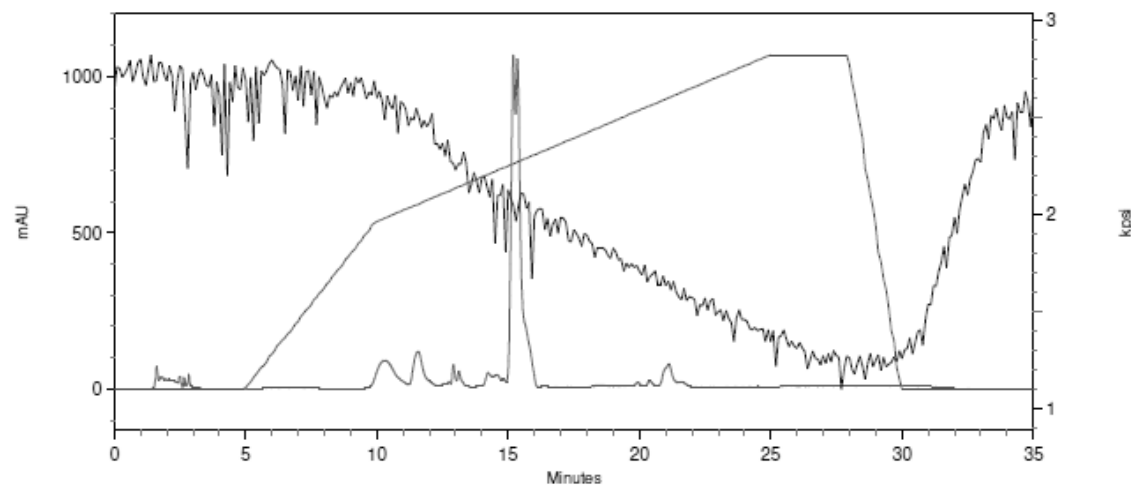
Aqueous phase adjusted to pH 7.5
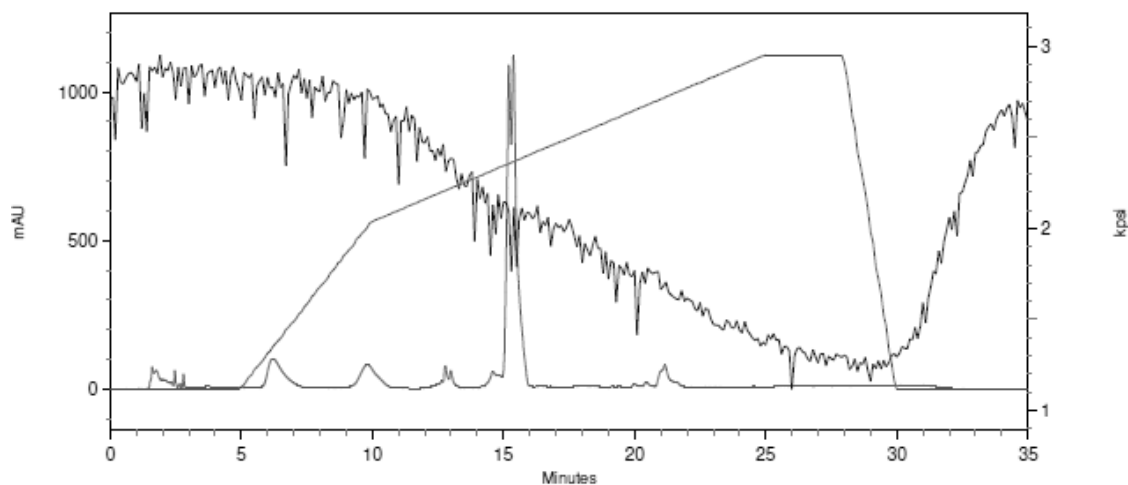
Aqueous phase adjusted to pH 8.0
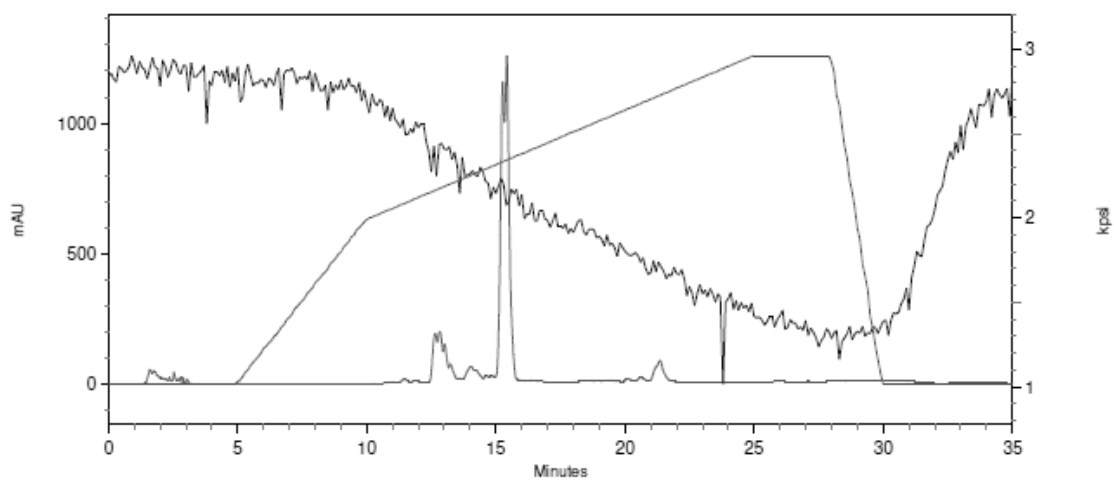
Appendix B

Influence of GRP78 knockdown

B1   SiRNA knockdown

GRP78 expression in A2780 and A2780cis cells with negative knockdown and PDIA1

knockdown in relation to cells without knockdown (results of individual testing)

	A2780 cells		A2780cis cells	
	negative knockdown	GRP78 knockdown	negative knockdown	GRP78 knockdown
	1.112	0.607	0.625	0.265
	0.767	0.214	0.487	0.152
	0.721	0.655	0.710	0.637
	1.033	0.494	0.958	0.486
		0.843		0.223
		0.706		0.448
Mean	0.908	0.587	0.695	0.369
SD	0.193	0.216	0.198	0.185
SEM	0.097	0.088	0.099	0.075

B2   Cytotoxicity of cisplatin

Individual pEC_{50} values for cisplatin cytotoxicity in A2780 and A2780cis cells without knockdown, with negative knockdown and with GRP78 knockdown (results of individual testing)

	A2780 cells		A2780cis cells	
	negative knockdown	GRP78 knockdown	negative knockdown	GRP78 knockdown
	5.301	5.121	4.769	4.601
	5.265	5.191	4.656	4.830
	5.529	5.409	4.868	4.704
	5.513	5.540	4.869	4.788
	5.299	5.424	4.914	4.715
	5.436	5.191	4.890	4.779
	5.301	5.364	4.717	4.661
			4.761	4.513
			4.561	4.601
Mean	5.378	5.320	4.778	4.699
SD	0.112	0.154	0.111	0.105
SEM	0.042	0.058	0.039	0.037

B3 Apoptosis induction

Percentage of late apoptotic, early apoptotic and viable A2780 cells without knockdown, with negative knockdown and with GRP78 knockdown without cisplatin treatment or with 10 µM cisplatin for 24 h (results of individual testing)

| | A2780 cells | | | | | |
| | Without cisplatin | | | With 10 µM cisplatin for 24 h | | |
	without knock-down	negative knock-down	GRP78 knock-down	without knock-down	negative knock-down	GRP78 knock-down
Late apoptotic cells	3.79	3.22	4.54	19.1	5.11	5.27
	1.96	4.94	11	7.03	11.2	12.1
	6.87	9.36	10.3	28.4	16.9	17.6
Mean	4.21	5.84	8.61	18.2	11.1	11.7
SD	2.48	3.17	3.55	10.7	5.90	6.18
SEM	1.43	1.83	2.05	6.19	3.40	3.57
Early apoptotic cells	3.43	5.57	7.36	11.7	10.1	10.1
	3.12	10.3	21.1	4.43	18.6	20.5
	3.90	1.25	6.2	11.2	7.81	11.7
Mean	3.48	5.71	11.6	9.11	12.2	14.1
SD	0.39	4.50	8.29	4.06	5.69	5.60
SEM	0.23	2.61	4.79	2.34	3.28	3.23
Viable cells	92.8	91.2	88.1	69.2	84.9	84.6
	94.2	84.8	67.9	88.5	70.2	67.4
	89.2	89.4	83.5	60.4	75.3	70.7
Mean	92.3	88.5	79.8	72.7	76.8	74.2
SD	2.87	3.33	10.6	14.4	7.41	9.15
SEM	1.66	1.92	6.11	8.31	4.28	5.28

Percentage of late apoptotic, early apoptotic and viable A2780cis cells without knockdown, with negative knockdown and with GRP78 knockdown without cisplatin treatment or with 10 µM cisplatin for 24 h (results of individual testing)

	A2780cis cells					
	Without cisplatin			With 10 µM cisplatin for 24 h		
	without knock-down	negative knock-down	GRP78 knock-down	without knock-down	negative knock-down	GRP78 knock-down
Late apoptotic cells	3.87	3.45	3.83	7.09	4.17	4.54
	3.83	6.49	5.45	10.40	6.67	3.98
	4.74	7.35	9.71	9.65	9.86	11.90
Mean	4.15	5.76	6.33	9.05	6.90	6.81
SD	0.51	2.05	3.04	1.74	2.85	4.42
SEM	0.29	1.18	1.75	1.00	1.65	2.55
Early apoptotic cells	0.99	2.10	2.28	1.62	1.73	3.32
	1.03	7.16	8.16	2.14	9.47	3.59
	0.89	1.73	2.48	1.92	3.89	3.27
Mean	0.97	3.66	4.31	1.89	5.03	3.39
SD	0.07	3.03	3.34	0.26	3.99	0.17
SEM	0.04	1.75	1.93	0.15	2.31	0.09
Viable cells	95.14	94.45	93.89	91.29	94.10	92.14
	95.14	86.35	86.39	87.46	83.86	92.43
	94.37	90.92	87.81	88.43	86.25	84.83
Mean	94.88	90.57	89.36	89.06	88.07	89.80
SD	0.45	4.06	3.98	1.99	5.36	4.31
SEM	0.26	2.35	2.30	1.15	3.09	2.49

Appendix C

Influence of PDIA1 knockdown

C1   SiRNA knockdown

PDIA1 expression in A2780 and A2780cis cells with negative knockdown and PDIA1

knockdown in relation to cells without knockdown (results of individual testing)

	A2780 cells		A2780cis cells	
	negative knockdown	PDIA1 knockdown	negative knockdown	PDIA1 knockdown
	1.50	0.33	1.00	0.50
	1.07	0.53	1.31	0.41
	0.56	0.47	1.34	0.47
	0.73	0.30	0.52	0.44
	0.61	0.63	1.00	0.53
	0.69	0.48	1.25	0.70
	1.25	0.51	1.01	0.29
	1.50	0.25	0.63	0.54
		0.40	1.06	0.62
		0.51	0.59	0.22
		0.53	1.00	0.50
			1.29	
			1.09	
Mean	0.989	0.449	1.01	0.474
SD	0.393	0.115	0.274	0.135
SEM	0.139	0.035	0.076	0.041

C2   Cytotoxicity of cisplatin

Individual pEC_{50} values for cisplatin cytotoxicity in A2780 and A2780cis cells without knockdown, with negative knockdown and with PDIA1 knockdown (results of individual testing)

	A2780 cells			A2780cis cells		
	without knockdown	negative knockdown	PDIA1 knockdown	without knockdown	negative knockdown	PDIA1 knockdown
	5.458	5.323	5.631	5.017	4.939	5.032
	5.377	5.216	5.394	4.876	4.849	4.973
	5.435	5.406	5.644	4.917	4.818	5.009
	5.266	5.450		4.802	4.747	
	5.234	5.409		4.843	4.889	
	5.439			4.864		
	5.357			4.844		
Mean	5.367	5.361	5.556	4.880	4.848	5.005
SD	0.0877	0.0932	0.1407	0.0697	0.0726	0.0297
SEM	0.0332	0.0417	0.0813	0.0264	0.0325	0.0172

C3   Apoptosis induction

Percentage of late apoptotic. early apoptotic and viable A2780 cells without knockdown, with negative knockdown and with PDIA1 knockdown without cisplatin treatment or with 10 µM cisplatin for 24 h (results of individual testing)

| | A2780 cells | | | | | |
| | Without cisplatin | | | With 10 µM cisplatin for 24 h | | |
	without knock-down	negative knock-down	PDIA1 knock-down	without knock-down	negative knock-down	PDIA1 knock-down
Late apoptotic cells	13.3	23.2	15.0	61.1	56.0	48.5
	5.05	13.3	14.7	60.1	39.2	37.5
	3.65	15.4	17.3	34.3	34.4	39.3
Mean	7.33	17.3	15.7	51.8	43.2	41.8
SD	5.21	5.22	1.42	15.2	11.3	5.90
SEM	3.01	3.01	0.82	8.77	6.55	3.41
Early apoptotic cells	2.28	6.5	4.68	6.58	22.1	15.8
	2.12	1.17	0.98	5.71	2.20	2.17
	2.29	6.4	6.65	0.48	12.9	11.7
Mean	2.23	4.69	4.10	4.26	12.4	9.89
SD	0.10	3.05	2.88	3.30	9.96	6.99
SEM	0.06	1.76	1.66	1.90	5.75	4.04
Viable cells	84.1	69.1	79.6	28.1	19.8	33.9
	92.7	81.6	80.7	31.6	52.4	56.1
	93.6	76.9	75.0	49.4	52.0	47.9
Mean	90.1	75.9	78.4	36.4	41.4	46.0
SD	5.24	6.31	3.02	11.4	18.7	11.2
SEM	3.03	3.65	1.75	6.59	10.8	6.48

Percentage of late apoptotic. early apoptotic and viable A2780cis cells without knockdown. with negative knockdown and with PDIA1 knockdown without cisplatin treatment or with 10 µM cisplatin for 24 h (results of individual testing)

	A2780cis cells					
	Without cisplatin			With 10 µM cisplatin for 24 h		
	without knock-down	negative knock-down	PDIA1 knock-down	without knock-down	negative knock-down	PDIA1 knock-down
Late apoptotic cells	4.64	8.09	7.09	13.5	11.0	22.5
	9.00	11.3	7.25	21.2	12.0	16.3
	13.5	23.7	22.1	20.9	16.7	25.6
Mean	9.05	14.4	12.2	18.5	13.2	21.5
SD	4.43	8.24	8.62	4.36	3.04	4.74
SEM	2.56	4.76	4.98	2.52	1.76	2.73
Early apoptotic cells	0.37	0.92	0.55	0.78	1.02	3.02
	2.36	2.15	1.08	2.77	2.00	4.18
	0.95	3.39	3.29	0.40	2.77	4.46
Mean	1.23	2.15	1.64	1.32	1.93	3.89
SD	1.02	1.24	1.45	1.27	0.88	0.76
SEM	0.59	0.71	0.84	0.73	0.51	0.44
Viable cells	94.9	90.5	92.2	85.5	87.6	75.1
	88.6	86.0	90.9	76.0	85.4	78.9
	80.7	71.7	73.7	73.3	80.0	69.4
Mean	88.1	82.7	85.6	78.3	84.3	74.5
SD	7.12	9.82	10.3	6.41	3.91	4.78
SEM	4.11	5.67	5.96	3.70	2.26	2.76

C4 DNA platination

DNA platination [pg platinum/ng DNA] after incubation with 100 µM cisplatin for 4 h in A2780 and A2780cis cells without knockdown, with negative knockdown and with PDIA1 knockdown (results of individual testing)

	A2780 cells			A2780cis cells		
	without knock-down	negative knock-down	PDIA1 knock-down	without knock-down	negative knock-down	PDIA1 knock-down
	201.4	249.3	169.8	49.1	129.8	103.8
	224.4	200.8	203.2	62.2	96.1	106.1
	239.7	190.1	215.2	67.1	94.6	172.4
	215.9	183.5	205.5		133.0	
Mean	220.3	205.9	198.4	59.4	113.4	127.4
SD	16.0	29.8	19.8	9.3	20.8	38.9
SEM	8.0	14.9	9.9	5.4	10.4	22.5

DNA platination [pg platinum/ng DNA] after incubation with 5 µM cisplatin for 24 h in A2780 and A2780cis cells without knockdown, with negative knockdown and with PDIA1 knockdown (results of individual testing)

	A2780 cells			A2780cis cells		
	without knock-down	negative knock-down	PDIA1 knock-down	without knock-down	negative knock-down	PDIA1 knock-down
	13.7	23.8	20.4	6.4	24.3	15.6
	13.9	19.1	25.3	11.6	21.3	12.1
	22.8	17.7	21.5	20.4	17.5	21.9
	19.4		20.6		28.0	
Mean	17.5	20.2	21.9	12.8	22.8	16.5
SD	4.4	3.2	2.3	7.1	4.5	5.0
SEM	2.2	1.9	1.1	4.1	2.2	2.9

Appendix D   Influence of co-treatment with PACMA31

D1   Cytotoxicity of PACMA31

Individual pEC_{50} and pEC_{10} values for PACMA31 cytotoxicity in A2780 and A2780cis cells (results of individual testing)

	A2780 cells		A2780cis cells	
	pEC_{50}	pEC_{10}	pEC_{50}	pEC_{10}
	6.320	6.452	6.085	6.620
	6.315	6.451	6.446	6.142
	6.400	6.580	6.369	6.450
	6.436	6.637	6.468	6.495
	6.502	6.596	6.491	6.544
	6.614	6.955	6.721	6.588
	6.748	7.001	6.570	6.864
	6.755	7.023	6.700	6.597
	6.700	6.986	6.587	6.915
	6.773	7.080	6.416	6.640
	6.292	6.474	6.075	6.465
	6.347	6.559	6.081	6.186
	6.383	6.635	6.061	6.137
	6.329	6.564	6.497	6.184
	6.188	6.312		6.582
		6.159		6.599
		6.175		6.475
		6.437		6.631
				6.378
Mean	6.47	6.62	6.40	6.50
SD	0.195	0.286	0.233	0.220
SEM	0.050	0.067	0.062	0.050

D2 Cytotoxicity of a combination of cisplatin and PACMA31

Individual pEC_{50} values for cisplatin cytotoxicity in A2780 and A2780cis cells without

and with co-treatment with 0.2 µM PACMA31 (results of individual testing)

	A2780 cells		A2780cis cells	
	Cisplatin	Cisplatin + PACMA31	Cisplatin	Cisplatin + PACMA31
	5.692	5.663	5.059	5.161
	5.809	5.678	5.160	5.157
	5.708	5.898	5.084	5.507
		5.777		5.599
		5.914		5.491
		5.917		5.521
Mean	5.737	5.798	5.102	5.406
SD	0.064	0.112	0.055	0.195
SEM	0.037	0.046	0.032	0.080

D3   Combination index (CI) of cisplatin and PACMA31

CI values determined EC_{50}. EC_{75}. EC_{90} and EC_{95} of the combination of cisplatin and PACMA31 in A2780 cells

	A2780 cells			
	EC_{50}	EC_{75}	EC_{90}	EC_{95}
	1.61	1.13	0.794	0.624
	1.50	1.06	0.740	0.582
	1.81	1.19	0.784	0.591
	1.67	1.12	0.756	0.578
	1.59	1.07	0.723	0.553
	1.43	1.09	0.871	0.777
	1.67	1.21	0.927	0.801
	0.86	0.817	0.786	0.770
	0.98	0.937	0.907	0.892
Mean	1.46	1.07	0.81	0.69
SD	0.325	0.124	0.074	0.124
SEM	0.108	0.041	0.025	0.041

CI values determined for EC_{50}. EC_{75}. EC_{90} and EC_{95} of the combination of cisplatin and PACMA31 in A2780cis cells

	A2780cis cells			
	EC_{50}	EC_{75}	EC_{90}	EC_{95}
	1.298	0.818	0.516	0.377
	1.175	0.737	0.463	0.337
	0.657	0.457	0.321	0.254
	1.389	0.986	0.708	0.568
	1.273	0.901	0.645	0.517
	0.620	0.624	0.632	0.639
	0.699	0.686	0.677	0.674
	0.822	0.803	0.785	0.773
	0.936	0.912	0.888	0.872
Mean	0.985	0.769	0.626	0.557
SD	0.302	0.164	0.172	0.206
SEM	0.101	0.055	0.057	0.069

Appendix E

Influence of PDIA3 knockdown

E1   SiRNA knockdown

PDIA3 expression in A2780 and A2780cis cells with negative knockdown and PDIA3

knockdown in relation to cells without knockdown (results of individual testing)

	A2780 cells		A2780cis cells	
	negative knockdown	PDIA3 knockdown	negative knockdown	PDIA3 knockdown
	0.470	1.006	0.870	0.350
	0.533	1.137	0.652	0.130
	0.209		1.224	0.014
Mean	1.072	0.404	0.915	0.165
SD	0.093	0.172	0.288	0.171
SEM	0.066	0.099	0.167	0.098

E2   Cytotoxicity of cisplatin

Individual pEC_{50} values for cisplatin cytotoxicity for A2780 and A2780cis cells without knockdown, with negative knockdown and with PDIA3 knockdown (results of individual testing)

	A2780 cells			A2780cis cells		
	without knock-down	negative knock-down	PDIA3 knock-down	without knock-down	negative knock-down	PDIA3 knock-down
	5.458	5.323	5.356	5.017	4.939	4.687
	5.377	5.216	5.514	4.876	4.849	4.796
	5.435	5.406	5.378	4.917	4.818	4.851
	5.266	5.450	5.288	4.802	4.747	4.782
	5.234	5.409	5.323	4.843	4.889	4.838
	5.439		5.462	4.864		4.814
	5.357			4.844		
Mean	5.367	5.361	5.387	4.880	4.848	4.795
SD	0.088	0.093	0.086	0.070	0.073	0.059
SEM	0.033	0.042	0.035	0.026	0.033	0.024

E3   Apoptosis induction

Percentage of late apoptotic, early apoptotic and viable A2780 cells without knockdown, with negative knockdown and with PDIA1 knockdown without cisplatin treatment or with 10 µM cisplatin for 24 h (results of individual testing)

	A2780 cells					
	Without cisplatin			With 10 µM cisplatin for 24 h		
	without knock-down	negative knock-down	PDIA1 knock-down	without knock-down	negative knock-down	PDIA1 knock-down
Late apoptotic cells	7.11	7.23	45.4	18.7	36.6	58.5
	7.72	54.0	53.2	22.5	49.8	61.8
	2.80	23.4	25.1	14.8	37.1	36.3
Mean	5.88	28.2	41.2	18.7	41.2	52.2
SD	2.68	23.8	14.5	3.85	7.48	13.9
SEM	1.55	13.7	8.38	2.22	4.32	8.01
Early apoptotic cells	2.29	1.09	5.72	6.56	6.38	6.52
	2.72	4.20	4.08	10.5	5.48	6.40
	1.97	3.89	5.41	7.99	7.42	8.64
Mean	2.33	3.06	5.07	8.35	6.43	7.19
SD	0.38	1.71	0.87	1.99	0.97	1.26
SEM	0.22	0.99	0.50	1.15	0.56	0.73
Viable cellls	90.5	91.5	46.1	74.3	56.3	32.1
	89.2	69.4	39.9	66.4	43.3	29.3
	95.1		67.2	76.7	53.2	53.5
Mean	91.6	80.5	51.1	72.5	50.9	38.3
SD	3.10	15.6	14.3	5.39	6.79	13.2
SEM	1.79	11.05	8.26	3.11	3.92	7.64

Percentage of late apoptotic, early apoptotic and viable A2780cis cells without knockdown, with negative knockdown and with PDIA3 knockdown without cisplatin treatment or with 10 µM cisplatin for 24 h (results of individual testing)

	A2780cis cells					
	Without cisplatin			With 10 µM cisplatin for 24 h		
	without knock-down	negative knock-down	PDIA3 knock-down	without knock-down	negative knock-down	PDIA3 knock-down
Late apoptotic cells	6.61	31.8	20.3	18.4	14.4	18.3
	15.1	17.2	31.8	28.1	30.5	39.7
	3.28	8.80	10.2	10.3	25.1	14.2
Mean	8.33	19.3	20.8	18.9	23.3	24.1
SD	6.09	11.6	10.8	8.91	8.19	13.7
SEM	3.52	6.72	6.24	5.15	4.73	7.91
Early apoptotic cells	0.51	4.51	1.67	1.86	1.71	1.36
	2.30	0.98	2.49	5.56	2.72	3.40
	0.62	0.76	1.97	1.90	1.74	2.69
Mean	1.14	2.08	2.04	3.11	2.06	2.48
SD	1.00	2.10	0.42	2.13	0.58	1.04
SEM	0.58	1.21	0.24	1.23	0.33	0.60
Viable cells	92.8	62.7	75.8	78.9	83.6	78.3
	82.2	81.7	65.3	64.6	66.4	56.3
	96.0	90.1	87.6	87.7	72.6	82.7
Mean	90.3	78.2	76.2	77.1	74.2	72.4
SD	7.22	14.0	11.2	11.7	8.71	14.1
SEM	4.17	8.10	6.44	6.73	5.03	8.17

E4   DNA platination

DNA platination [pg platinum/ng DNA] after incubation with 100 µM cisplatin for 4 h in A2780 and A2780cis cells without knockdown, with negative knockdown and with PDIA3 knockdown (results of individual testing)

	A2780 cells			A2780cis cells		
	without knock-down	negative knock-down	PDIA3 knock-down	without knock-down	negative knock-down	PDIA3 knock-down
	327.8	349.7	365.7	82.02	98.47	115.3
	362.2	319.9	363.5	125.4	188.7	237.3
	379.0	328.4	429.4	131.6	68.35	83.01
Mean	356.3	332.7	386.2	112.9	118.5	145.2
SD	26.1	15.3	37.4	27.0	62.6	81.4
SEM	15.1	8.9	21.6	15.6	36.2	46.9

DNA platination [pg platinum/ng DNA] after incubation with 5 µM cisplatin for 24 h in A2780 and A2780cis cells without knockdown, with negative knockdown and with PDIA3 knockdown (results of individual testing)

	A2780 cells			A2780cis cells		
	without knock-down	negative knock-down	PDIA3 knock-down	without knock-down	negative knock-down	PDIA3 knock-down
	10.34	29.40	47.55	19.38	17.54	26.33
	19.09	100.2	85.59	11.58	12.73	16.29
Mean	14.72	64.80	66.57	15.48	15.14	21.31
SD	6.187	50.06	26.90	5.515	3.401	7.099
SEM	4.375	35.40	19.02	3.900	2.405	5.020